

1996

# The problem of a rigid punch with friction on a graded elastic medium

Mehmet Ali Gèuler

*Lehigh University*

Follow this and additional works at: <http://preserve.lehigh.edu/etd>

---

## Recommended Citation

Gèuler, Mehmet Ali, "The problem of a rigid punch with friction on a graded elastic medium" (1996). *Theses and Dissertations*. Paper 422.

This Thesis is brought to you for free and open access by Lehigh Preserve. It has been accepted for inclusion in Theses and Dissertations by an authorized administrator of Lehigh Preserve. For more information, please contact [preserve@lehigh.edu](mailto:preserve@lehigh.edu).

Güler,  
Mehmet Ali

The Problem of a  
Rigid Punch with  
Friction on a  
Graded Elastic...

June 2, 1996

THE PROBLEM OF A RIGID PUNCH  
WITH FRICTION ON A GRADED  
ELASTIC MEDIUM

by  
Mehmet Ali Güler

A Thesis  
Presented to the Graduate and Research Committee  
of Lehigh University  
in Candidacy for the Degree of  
Master of Science  
in  
Mechanical Engineering

Lehigh University  
May 1996

This thesis is accepted in partial fulfillment of the requirements for the degree of  
Master of Science.

4/26/1996

---

(Date)

---

Prof. Fazıl Erdoğan  
(Thesis Advisor)

---

Prof. Robert P. Wei  
(Chairman of Department)

# Acknowledgments

First of all, I would like to express my deep thanks to Prof. Fazıl Erdoğan for his guidance and support during my graduate studies and of my thesis research.

I would like to also express my gratitude to Dr. Murat Öztürk for his assistance and consideration. I wish to thank also Ahmad Y. Banafa for his help for providing me with the essential materials in typing my thesis.

I want to especially mention the support and assistance of my family from back home during my graduate studies.

# Table of Contents

Acknowledgments	iii
Abstract	1
<b>1 Introduction</b>	<b>2</b>
1.1 Introduction . . . . .	2
1.2 Literature Survey . . . . .	3
1.3 The Organization . . . . .	5
<b>2 Formulation of the Problem</b>	<b>6</b>
<b>3 The Integral Equation and Its Solution</b>	<b>15</b>
3.1 Derivation of the Integral Equation . . . . .	15
3.2 The Fundamental Function . . . . .	18
3.3 Numerical Procedure . . . . .	19
<b>4 Results and Discussions</b>	<b>23</b>
4.1 The Flat Punch . . . . .	23
4.1.1 Solution for a Homogeneous Materials . . . . .	24
4.1.2 Solution for Graded Materials . . . . .	26
4.2 Triangular Punch . . . . .	41
4.2.1 Solution for Homogeneous Materials . . . . .	41
4.2.2 Solution for Graded Materials . . . . .	44
4.3 Semi Circular Punch . . . . .	63

4.3.1	Solution for Homogeneous Materials . . . . .	63
4.3.2	Solution for Graded Materials . . . . .	66
4.4	Cylindrical Punch . . . . .	85
4.4.1	Solution for Homogeneous Materials . . . . .	85
4.4.2	Solution for Graded Materials . . . . .	89
<b>5</b>	<b>Conclusions and Future Work</b>	<b>99</b>
	<b>Bibliography</b>	<b>101</b>
<b>A</b>	<b>Asymptotic Analysis of Kernels</b>	<b>105</b>
<b>B</b>	<b>Numerical Evaluation of Fredholm Kernels</b>	<b>112</b>
B.1	The Infinite Integral . . . . .	113
<b>C</b>	<b>Calculation of Logarithmic Kernels</b>	<b>117</b>
C.1	Calculation of the Logarithmic Kernel when $n = 0$ . . . . .	117
C.2	Calculation of the Logarithmic Kernel when $n > 0$ . . . . .	118
<b>Vita</b>		<b>122</b>

# List of Tables

4.1	Stress intensity factors for flat punch, $\theta_0 = -\frac{\pi}{\sin \pi\alpha}$ . . . . .	30
4.2	Stress intensity factors for triangular punch, $\theta_0 = \frac{2\pi\alpha}{\sin \pi\alpha}$ . . . . .	48
4.3	Stress intensity factors for triangular punch, $\theta_0 = \frac{2\pi\alpha}{\sin \pi\alpha}$ . . . . .	49
4.4	The first coefficient of the Jacobi series, $c_0$ for triangular punch . . .	50
4.5	The first coefficient of the Jacobi series, $c_0$ for triangular punch . . .	51
4.6	The first coefficient of the Jacobi series, $c_0$ for semi-circular punch .	70
4.7	The first coefficient of the Jacobi series, $c_0$ for semi-circular punch .	71
4.8	Stress intensity factors for semi-circular punch, $B(\alpha) = \frac{\pi(1+\alpha)}{2^{\alpha+1}\sin \pi\alpha}$ .	72
4.9	Stress intensity factors for semi-circular punch, $B(\alpha) = \frac{\pi(1+\alpha)}{2^{\alpha+1}\sin \pi\alpha}$ .	73



# List of Figures

3.1	Problem geometry . . . . .	16
4.1	Geometry of flat punch . . . . .	23
4.2	Stress distribution under a flat punch for various values of the material non-homogeneity parameter, $\gamma$ , when friction is not present, $\alpha = \beta = -0.5$ . . . . .	31
4.3	Stress distribution under a flat punch for various values of the material non-homogeneity parameter, $\gamma$ , in the presence of friction, $\eta = 0.1$ , $\alpha = -0.4909$ , $\beta = -0.5091$ . . . . .	32
4.4	Stress distribution under a flat punch for various values of the material non-homogeneity parameter, $\gamma$ , in the presence of friction, $\eta = 0.1$ , $\alpha = -0.4909$ , $\beta = -0.5091$ . . . . .	33
4.5	Stress distribution under a flat punch for various values of the material non-homogeneity parameter, $\gamma$ , in the presence of friction, $\eta = 0.3$ , $\alpha = -0.4728$ , $\beta = -0.5272$ . . . . .	34
4.6	Stress distribution under a flat punch for various values of the material non-homogeneity parameter, $\gamma$ , in the presence of friction, $\eta = 0.3$ , $\alpha = -0.4728$ , $\beta = -0.5272$ . . . . .	35
4.7	Stress distribution under a flat punch for various values of the material non-homogeneity parameter, $\gamma$ , in the presence of friction, $\eta = 0.5$ , $\alpha = -0.4548$ , $\beta = -0.5452$ . . . . .	36

4.8	Stress distribution under a flat punch for various values of the material non-homogeneity parameter, $\gamma$ , in the presence of friction, $\eta = 0.5$ $\alpha = -0.4548, \beta = -0.5452$ . . . . .	37
4.9	Variation of stress intensity factors with the non-homogeneity parameter, $k_1^*(a) = \frac{k_1(a)}{Pa^{\beta/\theta_0}}, k_1^*(-a) = \frac{k_1(-a)}{Pa^{\alpha/\theta_0}}$ . . . . .	38
4.10	Variation of stress intensity factors with the non-homogeneity parameter, $k_1^*(a) = \frac{k_1(a)}{Pa^{\beta/\theta_0}}, k_1^*(-a) = \frac{k_1(-a)}{Pa^{\alpha/\theta_0}}$ . . . . .	39
4.11	Variation of stress intensity factors with the non-homogeneity parameter, $k_1^*(a) = \frac{k_1(a)}{Pa^{\beta/\theta_0}}, k_1^*(-a) = \frac{k_1(-a)}{Pa^{\alpha/\theta_0}}$ . . . . .	40
4.12	Geometry of triangular punch . . . . .	41
4.13	Stress distribution under a triangular punch for various values of the material non-homogeneity parameter, $\gamma$ , when friction is not present, $\alpha = 0.5, \beta = -0.5$ . . . . .	52
4.14	Stress distribution under a triangular punch for various values of the material non-homogeneity parameter, $\gamma$ , in the presence of friction, $\eta = 0.1, \alpha = 0.5091, \beta = -0.5091$ . . . . .	53
4.15	Stress distribution under a triangular punch for various values of the material non-homogeneity parameter, $\gamma$ , in the presence of friction, $\eta = 0.3, \alpha = 0.5272, \beta = -0.5272$ . . . . .	54
4.16	Stress distribution under a triangular punch for various values of the material non-homogeneity parameter, $\gamma$ , in the presence of friction, $\eta = 0.5, \alpha = 0.5452, \beta = -0.5452$ . . . . .	55
4.17	Stress distribution under a triangular punch for various values of the material non-homogeneity parameter, $\gamma$ , in the presence of friction, $\eta = -0.1, \alpha = 0.4909, \beta = -0.4909$ . . . . .	56
4.18	Stress distribution under a triangular punch for various values of the material non-homogeneity parameter, $\gamma$ , in the presence of friction, $\eta = -0.3, \alpha = 0.4728, \beta = -0.4728$ . . . . .	57

4.19	Stress distribution under a triangular punch for various values of the material non-homogeneity parameter, $\gamma$ , in the presence of friction, $\eta = -0.5$ , $\alpha = 0.4548$ , $\beta = -0.4548$ . . . . .	58
4.20	Variation of stress intensity factor for the triangular punch with the non homogeneity parameter, $\gamma$ , $k_1^* = \frac{\theta_0}{2\alpha+1} \frac{k_1(0)}{Pb^{\alpha-1}}$ . . . . .	59
4.21	Variation of stress intensity factor for the triangular punch with the non homogeneity parameter $\gamma$ , $k_1^* = \frac{\theta_0}{2\alpha+1} \frac{k_1(0)}{Pb^{\alpha-1}}$ . . . . .	60
4.22	Variation of $c_0$ for the triangular punch with the non homogeneity parameter, $\gamma$ . . . . .	61
4.23	Variation of $c_0$ for the triangular punch with the non homogeneity parameter, $\gamma$ . . . . .	62
4.24	Geometry of semi-circular punch . . . . .	63
4.25	Stress distribution under a semi-circular punch for various values of the material non-homogeneity parameter, $\gamma$ , when friction is not present, $\alpha = 0.5$ , $\beta = -0.5$ . . . . .	74
4.26	Stress distribution under a semi-circular punch for various values of the material non-homogeneity parameter, $\gamma$ , in the presence of friction, $\eta = 0.1$ , $\alpha = 0.5091$ , $\beta = -0.5091$ . . . . .	75
4.27	Stress distribution under a semi-circular punch for various values of the material non-homogeneity parameter, $\gamma$ , in the presence of friction, $\eta = 0.3$ , $\alpha = 0.5272$ , $\beta = -0.5272$ . . . . .	76
4.28	Stress distribution under a semi-circular punch for various values of the material non-homogeneity parameter, $\gamma$ , in the presence of friction, $\eta = 0.5$ , $\alpha = 0.5452$ , $\beta = -0.5452$ . . . . .	77
4.29	Stress distribution under a semi-circular punch for various values of the material non-homogeneity parameter, $\gamma$ , in the presence of friction, $\eta = -0.1$ , $\alpha = 0.4909$ , $\beta = -0.4909$ . . . . .	78
4.30	Stress distribution under a semi-circular punch for various values of the material non-homogeneity parameter, $\gamma$ , in the presence of friction, $\eta = -0.3$ , $\alpha = 0.4728$ , $\beta = -0.4728$ . . . . .	79

4.31	Stress distribution under a semi-circular punch for various values of the material non-homogeneity parameter, $\gamma$ , in the presence of friction, $\eta = -0.5$ , $\alpha = 0.4548$ , $\beta = -0.4548$ . . . . .	80
4.32	Variation of $c_0$ for the semi-circular punch with the non homogeneity parameter, $\gamma$ . . . . .	81
4.33	Variation of $c_0$ for the semi-circular punch with the non homogeneity parameter, $\gamma$ . . . . .	82
4.34	Variation of stress intensity factor with the non homogeneity parameter, $\gamma$ , $k_1^*(0) = \frac{\pi(1+\alpha)}{2^{\alpha+1}\sin\pi\alpha} \frac{k_1(0)}{Pb^{\alpha-1}}$ . . . . .	83
4.35	Variation of stress intensity factor with the non homogeneity parameter, $\gamma$ , $k_1^*(0) = \frac{\pi(1+\alpha)}{2^{\alpha+1}\sin\pi\alpha} \frac{k_1(0)}{Pb^{\alpha-1}}$ . . . . .	84
4.36	Geometry of cylindrical punch . . . . .	85
4.37	Stress distribution under a cylindrical punch for various values of the material non-homogeneity parameter, $\gamma$ , when friction is not present, $\alpha = 0.5$ , $\beta = 0.5$ . . . . .	93
4.38	Stress distribution under a cylindrical punch for various values of the material non-homogeneity parameter, $\gamma$ , in the presence of friction, $\eta = 0.1$ , $\alpha = 0.5091$ , $\beta = 0.4909$ . . . . .	94
4.39	Stress distribution under a cylindrical punch for various values of the material non-homogeneity parameter, $\gamma$ , in the presence of friction, $\eta = 0.3$ , $\alpha = 0.5272$ , $\beta = 0.4728$ . . . . .	95
4.40	Stress distribution under a cylindrical punch for various values of the material non-homogeneity parameter, $\gamma$ , in the presence of friction, $\eta = 0.5$ , $\alpha = 0.5452$ , $\beta = 0.4548$ . . . . .	96
4.41	Variation of the end points of the contact region for a cylindrical punch on a homogeneous medium with respect to the coefficient of friction, $\eta$ , $a^* = \frac{a}{R} \left( \frac{P}{\mu R} \right)^{1/2}$ , $b^* = \frac{b}{R} \left( \frac{P}{\mu R} \right)^{1/2}$ . . . . .	97
4.42	Variation of the end points of the contact region for a cylindrical punch with respect to nonhomogeneity parameter, $\gamma$ for various values of the coefficient of friction, $\eta$ , $a^* = \frac{a}{R} \left( \frac{P}{\mu R} \right)^{1/2}$ , $b^* = \frac{b}{R} \left( \frac{P}{\mu R} \right)^{1/2}$ . . . . .	98

# Abstract

In this study, the contact problem for a graded elastic medium in the presence of friction is considered. The problem has a great variety of important structural applications such as case hardened materials, gears, cams, machine tools, foundations, pavements in roads and runways, rolling mills, and ball and roller bearings. The objective of this study is to determine the contact stresses and, whenever applicable, the stress intensity factors.

The specific problem studied in this thesis is that of a nonhomogeneous half-space loaded through a rigid punch. Different punch profiles such as flat, triangular, semi-circular and cylindrical are used to simulate the load transfer in practical applications. The variable shear modulus of the medium is represented by an exponential function. The problem is assumed to be linear elastic and Poisson's ratio is assumed to be constant. The theoretical part of the study includes Fourier transforms of the governing equations and boundary conditions. The resulting integral equation is solved numerically. The pressure profiles under the punch and the load required for given punch size are evaluated and presented. The results are compared with frictionless punch results for a semi-infinite medium. The effect of the non-homogeneity parameter and coefficient of friction on the contact stresses is studied in detail.

When friction is present, there appears to be a critical value of the nonhomogeneity parameter beyond which the technique used in this study has some convergence problems and some other method needs to be developed for solving the problem. The results, however, give valuable insight into the mechanics of the problem.

# Chapter 1

## Introduction

### 1.1 Introduction

The main cause of failure in mechanical structures is fracture and fatigue. Crack initiation and propagation take place essentially in areas of high stresses or in areas where friction and wear are present. In contact zones in a variety of load transmission components quasi-static loads can lead to friction and to high stresses which results in erosion and fatigue of the surfaces. It is thus necessary, in order to design these elements, to predict the magnitude of contact stresses.

The contact problem in solid mechanics involving an elastic layer or an elastic half space, has been widely studied since it has applications to a great variety of structural components (such as connecting-rods, bolted connections, shrink fits, rolling mills, turbine blade roots, ball and roller bearings, foundations, pavements in roads and runways, and other structures consisting of layered media).

We can categorize the contact problems into two broad sections, namely frictionless and with friction.

In the first type forces of friction between the contacting solids are neglected which simplifies the problem significantly. This assumption is in most cases justified for contact problems which arises in well-lubricated components. Usually, there is a lubricant layer between machine parts in contact, which means that the friction

force between bodies are quite small.

In the second type, forces of friction are not small, therefore we can not neglect the effect of friction. Here two cases can arise. In the first case, one elastic body moves with respect to the other, and the movement is so slow that dynamic effect can be neglected. This is the case in this study. In the second case no displacement of the punch as a whole with respect to the elastic body takes place. However when  $\sigma_{xy} < \mu\sigma_{yy}$  a rigid linkage, and when  $\sigma_{xy} > \mu\sigma_{yy}$  a relative displacement would take place between the contacting solids.

In this study, dynamic effects are neglected and it is assumed that forces of friction obey Coulomb's law which states that

$$\sigma_{xy} = \mu\sigma_{yy}$$

where  $\mu$  is the coefficient of friction.

The primary aim of this study is to determine the stresses on the contact surface. The variation of these stresses with material properties and geometrical parameters is studied. Four different punch profiles namely, flat, triangular, semicircular and cylindrical are used as examples.

Usually the size of the contact area is small in comparison with the radius of curvature of the bodies in contact; therefore it is assumed that one of the bodies can be replaced by an elastic semi-infinite space. One of the major advantages of graded material is shielding the base material from the adverse thermal and chemical environments. Additional potential benefits arise from the enhanced resistance to crack initiation and growth.

In this study, it is further assumed that material is isotropic, the Poisson's ratio is constant, and the shear modulus is an exponential function. For the different punch profiles the response of the non-homogeneous graded materials will be investigated.

## 1.2 Literature Survey

The problem of determining the stress distribution in a semi-infinite elastic solid under the compressive action of a rigid body was first considered by Boussinesq.

Hence problems of this kind are referred to as *Boussinesq problems*. The general description of the problem may be found, for example, in [1]-[2]. Harding and Sneddon [3] obtained the general solution of the Boussinesq problem for an axisymmetric punch. By the use of this general solution, Sneddon reconsidered the Boussinesq problem of a flat-ended cylinder [4] and rigid cone [3]. Solutions to many plane as well as axisymmetric problems can be found in the work done by Galin [5]. A general solution of such problems using integral transforms was given by Sneddon [6].

The general method of solving frictionless plane contact problems was given by Muskhelishvili [7]. An extensive survey for the contact problems solved by the method of integral transforms may be found in the book by Uflyand [8].

In subsequent studies a layer between the punch and the substrate was introduced. A systematic treatment of this kind of problems can be found in [9]-[11]. Recently, Kasmalkar solved the axisymmetric contact problem for a layer bonded to substrate for different indenter geometries [12].

Ratwani and Erdoğan [13] have considered the plane contact problem for an elastic layer lying frictionlessly on an elastic half space. Civelek and Erdoğan [14] have solved the problem in axisymmetric case.

Frictional phenomena have to be considered when the tangential part of the motion is important in the response of two or more bodies coming into contact during static or dynamic load transfer. Most of the formulation relies on the law of Coulomb. However, in some cases local micro-mechanical phenomena within the contact interface has to be taken into account. An extensive overview may be found in [15]. For the physical background of the frictional phenomena reader is referred to [16].

For frictional contact problems of linear elasticity, most of the solutions given are approximate solutions, obtained by using either finite element method or a more specific variational formulation. The finite element method has been used by many investigators to study contact problems. Chan and Tuba [17], Tsuta and Yamaji [18] and Ohte [19] studied contact problems for plane and axisymmetric problems. An ideal type of Coulomb friction has been included. Lindeman [20] has used the



finite element method to study shrink fit problems.

Contact problems of a rigid punch on a non-homogeneous medium were solved approximately for small values of the non-homogeneity parameter [21]-[25]. Bakırtas [26] considered the frictionless elastostatic problem of a rigid punch on an elastic half plane. This is similar to the present study if there is no friction. He has also given solutions of certain elasticity problems for a medium with varying modulus of elasticity [27].

### 1.3 The Organization

The statement of the problem and the description of the geometric and material parameters used in this study are given in Chapter 2. It includes formulation of the problem by using the governing differential equations and the boundary conditions.

Solution and the derivation of the integral equation are given in Chapter 3 where a numerical procedure implemented in this study is also described.

In Chapter 4, the problem is solved for various punch profiles. It includes solutions for both homogeneous and graded materials. The results are plotted and, discussion and comparison of special cases with previously published results are made.

Chapter 5 contains the conclusions of the study and suggestions for further research in the field.

## Chapter 2

### Formulation of the Problem

Consider the punch problem for a non-homogeneous medium. The non-homogeneity of the medium is assumed to be such that its shear modulus is approximated by

$$\mu(y) = \mu_0 e^{\gamma y}.$$

For the plane contact problem under consideration the Hooke's law can be written as

$$\sigma_{xx}(x, y) = \frac{\mu_0 e^{\gamma y}}{\kappa - 1} \left[ (\kappa + 1) \frac{\partial u}{\partial x} + (3 - \kappa) \frac{\partial v}{\partial y} \right], \quad (2.1)$$

$$\sigma_{yy}(x, y) = \frac{\mu_0 e^{\gamma y}}{\kappa - 1} \left[ (3 - \kappa) \frac{\partial u}{\partial x} + (\kappa + 1) \frac{\partial v}{\partial y} \right], \quad (2.2)$$

$$\sigma_{xy}(x, y) = \mu_0 e^{\gamma y} \left[ \frac{\partial u}{\partial y} + \frac{\partial v}{\partial x} \right], \quad (2.3)$$

where  $\kappa = 3 - 4\nu$  for plane strain and  $\kappa = (3 - \nu)/(1 + \nu)$  for the generalized plane stress conditions.

In the absence of body forces, equations of equilibrium which are the governing equations can be written as

$$\frac{\partial \sigma_{xx}}{\partial x} + \frac{\partial \sigma_{xy}}{\partial y} = 0, \quad (2.4)$$

$$\frac{\partial \sigma_{xy}}{\partial x} + \frac{\partial \sigma_{yy}}{\partial y} = 0. \quad (2.5)$$

Substituting stresses found from equations (2.1), (2.2) and (2.3) into equations of equilibrium (2.4), (2.5) we obtain the Naviers equations as follows

$$(\kappa + 1)\frac{\partial^2 u}{\partial x^2} + (\kappa - 1)\frac{\partial^2 u}{\partial y^2} + 2\frac{\partial^2 v}{\partial x \partial y} + \gamma(\kappa - 1)\frac{\partial u}{\partial y} + \gamma(\kappa - 1)\frac{\partial v}{\partial x} = 0, \quad (2.6)$$

$$(\kappa + 1)\frac{\partial^2 v}{\partial y^2} + (\kappa - 1)\frac{\partial^2 v}{\partial x^2} + 2\frac{\partial^2 u}{\partial x \partial y} + \gamma(3 - \kappa)\frac{\partial u}{\partial x} + \gamma(\kappa + 1)\frac{\partial v}{\partial y} = 0. \quad (2.7)$$

To solve the Navier's equations we define the Fourier transforms of the two displacement components,  $u(x, y)$  and  $v(x, y)$ , as

$$F(\alpha, y) = \int_{-\infty}^{\infty} u(x, y) e^{-i\alpha x} dx, \quad (2.8)$$

$$G(\alpha, y) = \int_{-\infty}^{\infty} v(x, y) e^{-i\alpha x} dx. \quad (2.9)$$

The functions  $u(x, y)$  and  $v(x, y)$  are given by the following inverse transforms;

$$u(x, y) = \frac{1}{2\pi} \int_{-\infty}^{\infty} F(\alpha, y) e^{i\alpha x} d\alpha, \quad (2.10)$$

$$v(x, y) = \frac{1}{2\pi} \int_{-\infty}^{\infty} G(\alpha, y) e^{i\alpha x} d\alpha. \quad (2.11)$$

Substituting (2.10) and (2.11) into (2.6) and (2.7) yields the following system of differential equations with constant coefficients.

$$\begin{aligned} (\kappa - 1)\frac{d^2 F}{dy^2} + \gamma(\kappa - 1)\frac{dF}{dy} - (\kappa + 1)\alpha^2 F \\ + 2i\alpha\frac{dG}{dy} + i\alpha\gamma(\kappa - 1)G = 0, \end{aligned} \quad (2.12)$$

$$\begin{aligned} (\kappa + 1)\frac{d^2 G}{dy^2} + \gamma(\kappa + 1)\frac{dG}{dy} - (\kappa - 1)\alpha^2 G \\ + 2i\alpha\frac{dF}{dy} + i\alpha\gamma(3 - \kappa)F = 0. \end{aligned} \quad (2.13)$$

Assuming a solution of the form

$$F(\alpha, y) = C(\alpha) e^{ny}, \quad (2.14)$$

$$G(\alpha, y) = D(\alpha) e^{ny}, \quad (2.15)$$

we obtain the solution of (2.12) and (2.13) as

$$F(\alpha, y) = \sum_{j=1}^4 C_j(\alpha) e^{n_j y}, \quad (2.16)$$

$$G(\alpha, y) = \sum_{j=1}^4 D_j(\alpha) e^{n_j y}, \quad (2.17)$$

where  $n_j$ , ( $j = 1, \dots, 4$ ) satisfies the following characteristic equation

$$(n^2 - \alpha^2 + \gamma n)^2 + \delta^2 \alpha^2 \gamma^2 = 0, \quad (2.18)$$

with

$$\delta^2 = \frac{3 - \kappa}{\kappa + 1}.$$

The roots of the characteristic equation are given by

$$n_1 = \frac{1}{2} \left( -\gamma + \sqrt{\gamma^2 + 4(\alpha^2 + i\alpha\gamma\delta)} \right), \quad (2.19)$$

$$n_2 = \frac{1}{2} \left( -\gamma - \sqrt{\gamma^2 + 4(\alpha^2 + i\alpha\gamma\delta)} \right), \quad (2.20)$$

$$n_3 = \frac{1}{2} \left( -\gamma + \sqrt{\gamma^2 + 4(\alpha^2 - i\alpha\gamma\delta)} \right), \quad (2.21)$$

$$n_4 = \frac{1}{2} \left( -\gamma - \sqrt{\gamma^2 + 4(\alpha^2 - i\alpha\gamma\delta)} \right). \quad (2.22)$$

The functions  $C_j(\alpha)$  and  $D_j(\alpha)$  ( $j = 1 \dots 4$ ) are unknown functions and are not independent. The relationship between them can be found by substituting (2.16) and (2.17) into (2.13)

$$C_j(\alpha) = A_j(\alpha) D_j(\alpha), \quad j = 1, 2 \quad (2.23)$$

$$C_j(\alpha) = -\bar{A}_j(\alpha) D_j(\alpha), \quad j = 3, 4 \quad (2.24)$$

where

$$A_j(\alpha) = \frac{2i\alpha - (\kappa + 1)\delta\gamma}{2n_j + \gamma(3 - \kappa)}. \quad (2.25)$$

Since both  $u$  and  $v$  vanish as  $x^2 + y^2 \rightarrow \infty$ , the admissible roots are  $n_2$  and  $\widehat{n_4}$ , i.e.,  $\Re(n_j) < 0$  for  $j = 2, 4$  and in the solution given by (2.16) and (2.17),  $D_1$  and  $D_3$  must be set to zero. Thus (2.16) and (2.17) reduce to

$$F(\alpha, y) = A_2(\alpha) D_2(\alpha) e^{n_2 y} - \bar{A}_2(\alpha) D_4(\alpha) e^{n_4 y}, \quad (2.26)$$

$$G(\alpha, y) = D_2(\alpha) e^{n_2 y} + D_4(\alpha) e^{n_4 y}. \quad (2.27)$$

Defining the Fourier transforms of the tractions on the boundary as

$$P(\alpha) = \int_{-\infty}^{\infty} \sigma_{yy}(t, 0) e^{-i\alpha t} dt, \quad (2.28)$$

$$Q(\alpha) = \int_{-\infty}^{\infty} \sigma_{xy}(t, 0) e^{-i\alpha t} dt. \quad (2.29)$$

we obtain two equations to determine  $D_2$  and  $D_4$

$$(\kappa + 1) \left( \frac{d}{dy} G(\alpha, 0) + i\alpha(3 - \kappa) F(\alpha, 0) \right) = \frac{\kappa - 1}{\mu_0} P(\alpha), \quad (2.30)$$

$$\frac{d}{dy} F(\alpha, 0) + i\alpha G(\alpha, 0) = \frac{1}{\mu_0} Q(\alpha). \quad (2.31)$$

After substituting from (2.26) and (2.27) into (2.30) and (2.31) we obtain

$$D_2(\alpha) = \frac{1}{\mu_0 \Delta_0} [-(\kappa - 1) P(\alpha) \bar{Z}_2 - \bar{Z}_1 Q(\alpha)], \quad (2.32)$$

$$D_4(\alpha) = \frac{1}{\mu_0 \Delta_0} [Z_1 Q(\alpha) - (\kappa - 1) Z_2 P(\alpha)], \quad (2.33)$$

where,  $Z_1$  and  $Z_2$  are given in Appendix A and

$$\Delta_0 = -(Z_1 \bar{Z}_2 + \bar{Z}_1 Z_2). \quad (2.34)$$

So far, we have found all the constants ( $D_2, D_4$ ) to determine  $u(x, y)$  and  $v(x, y)$  in the Fourier domain in (2.26) and (2.27). Since displacement vector is specified on the part of the boundary  $y = 0$  and the traction vector is specified on the remainder, our problem is a mixed boundary value problem. Input to the problem is the  $y$  component of the displacement vector and the unknowns are  $\sigma_{xy}(x, 0)$  and  $\sigma_{yy}(x, 0)$ .

Thus writing the derivatives of (2.10) and (2.11) with respect to  $x$  gives

$$\frac{\partial}{\partial x} v(x, y) = \frac{1}{2\pi} \int_{-\infty}^{\infty} i\alpha G(\alpha, y) e^{i\alpha x} d\alpha, \quad (2.35)$$

$$\frac{\partial}{\partial x} u(x, y) = \frac{1}{2\pi} \int_{-\infty}^{\infty} i\alpha F(\alpha, y) e^{i\alpha x} d\alpha, \quad (2.36)$$

Substituting (2.26) and (2.27) into (2.35) and (2.36) and using (2.28) and (2.29), we obtain

$$2\pi\mu_0 \frac{\partial}{\partial x} v(x, y) = \int_{-\infty}^{\infty} K_{11}(x, y, t) \sigma_{yy}(t, y) dt + \int_{-\infty}^{\infty} K_{12}(x, y, t) \sigma_{xy}(t, y) dt. \quad (2.37)$$

$$2\pi\mu_0 \frac{\partial}{\partial x} u(x, y) = \int_{-\infty}^{\infty} K_{21}(x, y, t) \sigma_{yy}(t, y) dt + \int_{-\infty}^{\infty} K_{22}(x, y, t) \sigma_{xy}(t, y) dt. \quad (2.38)$$

where

$$K_{11}(x, y, t) = \int_{-\infty}^{\infty} H_{11}(\alpha, y) e^{-i\alpha(t-x)} d\alpha, \quad (2.39)$$

$$K_{21}(x, y, t) = \int_{-\infty}^{\infty} H_{21}(\alpha, y) e^{-i\alpha(t-x)} d\alpha, \quad (2.40)$$

$$K_{12}(x, y, t) = \int_{-\infty}^{\infty} H_{12}(\alpha, y) e^{-i\alpha(t-x)} d\alpha, \quad (2.41)$$

$$K_{22}(x, y, t) = \int_{-\infty}^{\infty} H_{22}(\alpha, y) e^{-i\alpha(t-x)} d\alpha, \quad (2.42)$$

$$H_{11}(\alpha, y) = \frac{-i\alpha(\kappa-1)}{\Delta_0(\alpha)} \left( \bar{Z}_2(\alpha) e^{n_2 y} + Z_2(\alpha) e^{n_4 y} \right), \quad (2.43)$$

$$H_{21}(\alpha, y) = \frac{-i\alpha(\kappa-1)}{\Delta_0(\alpha)} \left( A_2 \bar{Z}_2(\alpha) e^{n_2 y} - \bar{A}_2 Z_2(\alpha) e^{n_4 y} \right), \quad (2.44)$$

$$H_{12}(\alpha, y) = \frac{i\alpha}{\Delta_0(\alpha)} \left( -\bar{Z}_1(\alpha) e^{n_2 y} + Z_1(\alpha) e^{n_4 y} \right), \quad (2.45)$$

$$H_{22}(\alpha, y) = \frac{i\alpha}{\Delta_0(\alpha)} \left( -A_2 \bar{Z}_1(\alpha) e^{n_2 y} - \bar{A}_2 Z_1(\alpha) e^{n_4 y} \right). \quad (2.46)$$

The singularities in the kernels come from the asymptotic behavior of the integrands. The asymptotic analysis has to be made in order to extract the singularity as  $\alpha \rightarrow \infty$ . The details of asymptotic expansion of the kernels  $K_{11}(x, y, t)$ ,  $K_{12}(x, y, t)$ ,  $K_{21}(x, y, t)$  and  $K_{22}(x, y, t)$  are given in Appendix (A). For  $\alpha \rightarrow \infty$  the asymptotic behavior of  $H_{11}(\alpha, y)$ ,  $H_{12}(\alpha, y)$ ,  $H_{21}(\alpha, y)$  and  $H_{22}(\alpha, y)$  are as follows:

$$H_{11}(\alpha, y) = i \frac{\alpha}{|\alpha|} e^{-\alpha y} \left( -\frac{\kappa+1}{4} + \frac{(5+\kappa)}{8} \frac{\gamma}{\alpha} + O\left(\frac{1}{\alpha^2}\right) \right), \quad (2.47)$$

$$H_{21}(\alpha, y) = e^{-\alpha y} \left( \frac{\kappa-1}{4} + \frac{(\kappa+1)}{8} \frac{\gamma}{\alpha} + O\left(\frac{1}{\alpha^2}\right) \right), \quad (2.48)$$

$$H_{12}(\alpha, y) = e^{-\alpha y} \left( -\frac{\kappa-1}{4} + \frac{(\kappa+1)}{8} \frac{\gamma}{\alpha} + O\left(\frac{1}{\alpha^2}\right) \right), \quad (2.49)$$

$$H_{22}(\alpha, y) = i \frac{\alpha}{|\alpha|} e^{-\alpha y} \left( -\frac{\kappa+1}{4} + \frac{(\kappa+1)\gamma}{8\alpha} + O\left(\frac{1}{\alpha^2}\right) \right). \quad (2.50)$$

We may now write  $K_{11}$ ,  $K_{21}$ ,  $K_{12}$ ,  $K_{22}$  as

$$K_{11}(x, y, t) = \int_{-\infty}^{+\infty} \left( H_{11}(\alpha, y) + i \frac{\kappa+1}{4} \frac{\alpha}{|\alpha|} e^{-|\alpha|y} \right) e^{-i\alpha(t-x)} d\alpha + K_{11\infty}, \quad (2.51)$$

$$K_{21}(x, y, t) = \int_{-\infty}^{+\infty} \left( H_{21}(\alpha, y) - \frac{\kappa-1}{4} e^{-|\alpha|y} \right) e^{-i\alpha(t-x)} d\alpha + K_{21\infty}, \quad (2.52)$$

$$K_{12}(x, y, t) = \int_{-\infty}^{+\infty} \left( H_{12}(\alpha, y) + \frac{\kappa-1}{4} e^{-|\alpha|y} \right) e^{-i\alpha(t-x)} d\alpha + K_{12\infty}, \quad (2.53)$$

$$K_{22}(x, y, t) = \int_{-\infty}^{+\infty} \left( H_{22}(\alpha, y) + i \frac{\kappa+1}{4} \frac{\alpha}{|\alpha|} e^{-|\alpha|y} \right) e^{-i\alpha(t-x)} d\alpha + K_{22\infty}, \quad (2.54)$$

where

$$K_{11\infty}(x, y, t) = -i \frac{\kappa+1}{4} \int_{-\infty}^{\infty} \frac{\alpha}{|\alpha|} e^{-|\alpha|y} e^{-i\alpha(t-x)} d\alpha, \quad (2.55)$$

$$K_{21\infty}(x, y, t) = \frac{\kappa-1}{4} \int_{-\infty}^{\infty} e^{-|\alpha|y} e^{-i\alpha(t-x)} d\alpha, \quad (2.56)$$

$$K_{12\infty}(x, y, t) = -\frac{\kappa-1}{4} \int_{-\infty}^{\infty} e^{-|\alpha|y} e^{-i\alpha(t-x)} d\alpha, \quad (2.57)$$

$$K_{22\infty}(x, y, t) = -i \frac{\kappa+1}{4} \int_{-\infty}^{\infty} \frac{\alpha}{|\alpha|} e^{-|\alpha|y} e^{-i\alpha(t-x)} d\alpha. \quad (2.58)$$

The first integrals in (2.51)-(2.54) are bounded and, when substituted into (2.37) and (2.38) limit can be put under the integral sign. Thus, it may easily be shown that

$$K_{11\infty}(x, y, t) = -\frac{\kappa+1}{2} \frac{t-x}{(t-x)^2 + y^2}, \quad (2.59)$$

$$K_{21\infty}(x, y, t) = \frac{\kappa-1}{2} \frac{y}{(t-x)^2 + y^2}, \quad (2.60)$$

$$K_{12\infty}(x, y, t) = -\frac{\kappa-1}{2} \frac{y}{(t-x)^2 + y^2}, \quad (2.61)$$

$$K_{22\infty}(x, y, t) = -\frac{\kappa+1}{2} \frac{t-x}{(t-x)^2 + y^2}. \quad (2.62)$$

By substituting now  $y = 0$  in equations (2.51)-(2.54) and noting that

$$\lim_{y \rightarrow 0} \frac{y}{(t-x)^2 + y^2} = \pi \delta(t-x), \quad (2.63)$$

we obtain

$$\begin{aligned}
\frac{4\mu_0}{\kappa+1} \frac{\partial}{\partial x} v(x, 0) &= \frac{2}{\pi(\kappa+1)} \int_{-\infty}^{\infty} \sigma_{yy}(t, 0) I_{11}(t, x) dt \\
&+ \frac{2}{\pi(\kappa+1)} \int_{-\infty}^{\infty} \sigma_{xy}(t, 0) I_{12}(t, x) dt \\
&- \frac{1}{\pi} \int_{-\infty}^{\infty} \frac{\sigma_{yy}(t, 0) dt}{(t-x)} - \lambda \sigma_{xy}(x, 0), \tag{2.64}
\end{aligned}$$

$$\begin{aligned}
\frac{4\mu_0}{\kappa+1} \frac{\partial}{\partial x} u(x, 0) &= \frac{2}{\pi(\kappa+1)} \int_{-\infty}^{\infty} \sigma_{yy}(t, 0) I_{21}(t, x) dt \\
&+ \frac{2}{\pi(\kappa+1)} \int_{-\infty}^{\infty} \sigma_{xy}(t, 0) I_{22}(t, x) dt \\
&- \frac{1}{\pi} \int_{-\infty}^{\infty} \frac{\sigma_{xy}(t, 0) dt}{(t-x)} + \lambda \sigma_{yy}(x, 0), \tag{2.65}
\end{aligned}$$

where

$$I_{11}(t, x) = \int_{-\infty}^{\infty} \left( H_{11}(\alpha, 0) + i \frac{\kappa+1}{4} \frac{\alpha}{|\alpha|} \right) e^{-i\alpha(t-x)} d\alpha, \tag{2.66}$$

$$I_{21}(t, x) = \int_{-\infty}^{+\infty} \left( H_{21}(\alpha, 0) - \frac{\kappa-1}{4} \right) e^{-i\alpha(t-x)} d\alpha, \tag{2.67}$$

$$I_{12}(t, x) = \int_{-\infty}^{\infty} \left( H_{12}(\alpha, 0) + \frac{\kappa-1}{4} \right) e^{-i\alpha(t-x)} d\alpha, \tag{2.68}$$

$$I_{22}(t, x) = \int_{-\infty}^{+\infty} \left( H_{22}(\alpha, 0) + i \frac{\kappa+1}{4} \frac{\alpha}{|\alpha|} \right) e^{-i\alpha(t-x)} d\alpha, \tag{2.69}$$

$$\lambda = \frac{\kappa-1}{\kappa+1}. \tag{2.70}$$

Further refinements can be made by analyzing the kernels  $I_{11}(t, x), I_{21}(t, x), I_{12}(t, x)$  and  $I_{22}(t, x)$  in equation (2.64) and (2.65). Observing that

$$\begin{aligned}
I_{11} &= 2 \int_0^{\infty} \Re \left[ \left( \frac{-i\alpha(\kappa-1)}{\Delta_0} (\bar{Z}_2 + Z_2) + i \frac{\kappa+1}{4} \frac{\alpha}{|\alpha|} \right) e^{-i\alpha(t-x)} \right] d\alpha, \\
&= 2 \int_0^{\infty} \left( -\frac{\alpha(\kappa-1)}{\Delta_0} (\bar{Z}_2 + Z_2) + \frac{\kappa+1}{4} \frac{\alpha}{|\alpha|} \right) \sin \alpha(t-x), \tag{2.71}
\end{aligned}$$



$$\begin{aligned}
I_{21} &= 2 \int_0^\infty \Re \left[ \left( \frac{-i\alpha(\kappa-1)}{\Delta_0} (A_2 \bar{Z}_2 - \bar{A}_2 Z_2) + i \frac{\kappa+1}{4} \frac{\alpha}{|\alpha|} \right) e^{-i\alpha(t-x)} \right] d\alpha, \\
&= 2 \int_0^\infty \left( -\frac{\alpha(\kappa-1)}{\Delta_0} (A_2 \bar{Z}_2 - \bar{A}_2 Z_2) + \frac{\kappa+1}{4} \frac{\alpha}{|\alpha|} \right) \sin \alpha(t-x), \quad (2.72)
\end{aligned}$$

$$\begin{aligned}
I_{12} &= 2 \int_0^\infty \Re \left[ \left( \frac{i\alpha}{\Delta_0} (-\bar{Z}_1 + Z_1) + \frac{\kappa-1}{4} \right) e^{-i\alpha(t-x)} \right] d\alpha, \\
&= 2 \int_0^\infty \left[ \left( \frac{i\alpha}{\Delta_0} (-\bar{Z}_1 + Z_1) + \frac{\kappa-1}{4} \right) \cos \alpha(t-x) \right] d\alpha, \quad (2.73)
\end{aligned}$$

$$\begin{aligned}
I_{22} &= 2 \int_0^\infty \Re \left[ \left( \frac{i\alpha}{\Delta_0} (-A_2 \bar{Z}_1 - \bar{A}_2 Z_1) - \frac{\kappa-1}{4} \right) e^{-i\alpha(t-x)} \right] d\alpha, \\
&= 2 \int_0^\infty \left[ \left( \frac{i\alpha}{\Delta_0} (-A_2 \bar{Z}_1 - \bar{A}_2 Z_1) - \frac{\kappa-1}{4} \right) \cos \alpha(t-x) \right] d\alpha, \quad (2.74)
\end{aligned}$$

we can write (2.64) and (2.65) as;

$$\begin{aligned}
&-\lambda \sigma_{xy}(x, 0) - \frac{1}{\pi} \int_{-\infty}^\infty \frac{\sigma_{yy}(t, 0)}{(t-x)} dt \\
&+ \int_{-\infty}^\infty \sigma_{yy}(t, 0) J_{11}(t, x) dt + \int_{-\infty}^\infty \sigma_{xy}(t, 0) J_{12}(t, x) dt = f(x), \quad (2.75)
\end{aligned}$$

$$\begin{aligned}
&\lambda \sigma_{yy}(x, 0) - \frac{1}{\pi} \int_{-\infty}^\infty \frac{\sigma_{xy}(t, 0)}{(t-x)} dt \\
&+ \int_{-\infty}^\infty \sigma_{yy}(t, 0) J_{21}(t, x) dt + \int_{-\infty}^\infty \sigma_{xy}(t, 0) J_{22}(t, x) dt = g(x), \quad (2.76)
\end{aligned}$$

where

$$f(x) = \frac{4\mu_0}{\kappa+1} \frac{\partial}{\partial x} v(x, 0), \quad (2.77)$$

$$g(x) = \frac{4\mu_0}{\kappa+1} \frac{\partial}{\partial x} u(x, 0), \quad (2.78)$$

$$J_{11}(t, x) = \frac{4}{\pi(\kappa+1)} \int_0^\infty \Phi_{11}(\alpha) \sin \alpha(t-x) d\alpha, \quad (2.79)$$

$$J_{21}(t, x) = \frac{4}{\pi(\kappa+1)} \int_0^\infty \Phi_{21}(\alpha) \sin \alpha(t-x) d\alpha, \quad (2.80)$$

$$J_{12}(t, x) = \frac{4}{\pi(\kappa+1)} \int_0^\infty \Phi_{12}(\alpha) \cos \alpha(t-x) d\alpha, \quad (2.81)$$

$$J_{22}(t, x) = \frac{4}{\pi(\kappa+1)} \int_0^\infty \Phi_{22}(\alpha) \cos \alpha(t-x) d\alpha, \quad (2.82)$$

$$\Phi_{11}(\alpha) = -\frac{\alpha(\kappa-1)}{\Delta_0(\alpha)} \left[ \bar{Z}_2(\alpha) + Z_2(\alpha) \right] + \frac{\kappa+1}{4} \frac{\alpha}{|\alpha|}, \quad (2.83)$$

$$\Phi_{21}(\alpha) = -\frac{\alpha(\kappa-1)}{\Delta_0(\alpha)} \left[ A_2 \bar{Z}_2(\alpha) - \bar{A}_2 Z_2(\alpha) \right] + \frac{\kappa+1}{4} \frac{\alpha}{|\alpha|}, \quad (2.84)$$

$$\Phi_{12}(\alpha) = \frac{i\alpha}{\Delta_0(\alpha)} \left[ -\bar{Z}_1(\alpha) + Z_1(\alpha) \right] + \frac{\kappa-1}{4}, \quad (2.85)$$

$$\Phi_{22}(\alpha) = \frac{i\alpha}{\Delta_0(\alpha)} \left[ -A_2 \bar{Z}_1(\alpha) - \bar{A}_2 Z_1(\alpha) \right] - \frac{\kappa-1}{4}. \quad (2.86)$$

## Chapter 3

# The Integral Equation and Its Solution

### 3.1 Derivation of the Integral Equation

If the direction of the forces  $P$  and  $Q$  are taken to be as in Fig. 3.1, boundary conditions become

$$\sigma_{yy}(x, 0) = \begin{cases} -p(x) & c < x < d, \\ 0 & x < c, \quad x > d. \end{cases} \quad (3.1)$$

$$\sigma_{xy}(x, 0) = \begin{cases} -q(x) & c < x < d, \\ 0 & x < c, \quad x > d. \end{cases} \quad (3.2)$$

Shear stress at the surface of the medium is related to the normal stress by coefficient of friction  $\eta$  as follows:

$$\sigma_{xy}(x, 0) = \eta \sigma_{yy}(x, 0), \quad (3.3)$$

$$q(x) = \eta p(x). \quad (3.4)$$

Substituting (3.1) through (3.4) into eq (2.75) we have

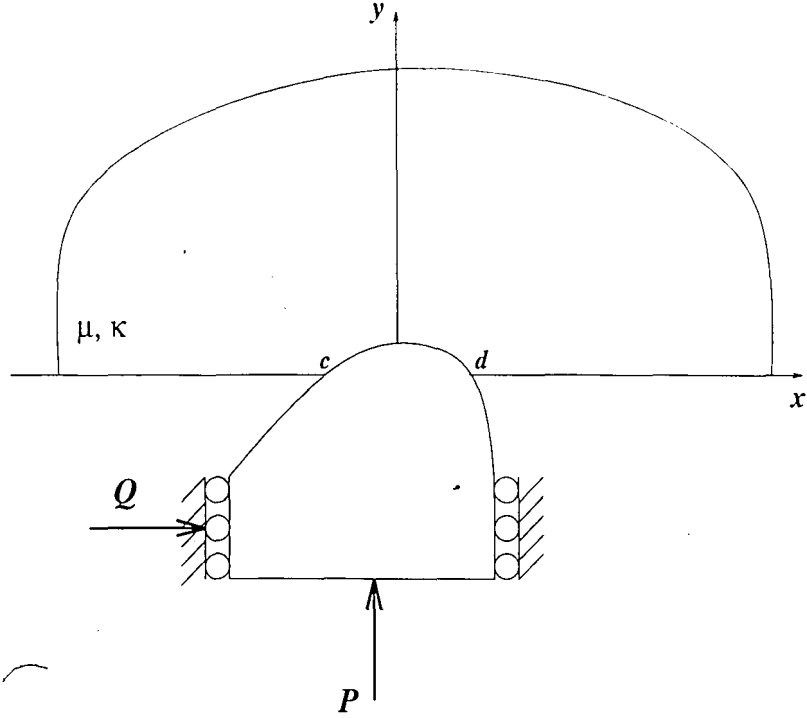


Figure 3.1: Problem geometry

$$\omega p(x) + \frac{1}{\pi} \int_c^d \frac{p(t)dt}{(t-x)} - \int_c^d p(t)J_1(t,x)dt - \eta \int_c^d p(t)J_2(t,x)dt = f(x), \quad c < x < d. \quad (3.5)$$

where

$$\omega = \frac{\kappa - 1}{\kappa + 1} \eta. \quad (3.6)$$

In the singular integral equation (3.5) the contact pressure  $p(x)$  is always unknown. But,  $c$  and  $d$  depends on the shape of the punch profile and is found by applying the equilibrium and, if needed, consistency conditions. The equilibrium of the punch requires that the total pressure on the contact area should be equal to the total load applied to the punch. This can be expressed as

$$\int_c^d p(t)dt = P. \quad (3.7)$$

where  $P$  is the known compressive force per unit depth in  $y$  direction, applied to the punch away from the contact region.

To solve the singular integral equation we first normalize the interval  $(c, d)$  to  $(-1, 1)$ . This can be done by defining the new variables

$$x = \frac{d-c}{2}r + \frac{d+c}{2}, \quad (3.8)$$

$$t = \frac{d-c}{2}s + \frac{d+c}{2}, \quad (3.9)$$

$$p(x) = \phi(r), \quad (3.10)$$

$$J_1(t, x) = \frac{2}{d-c} J_1^*(s, r), \quad (3.11)$$

$$J_2(t, x) = \frac{2}{d-c} J_2^*(s, r), \quad (3.12)$$

$$f(x) = f^*(r), \quad (3.13)$$

$$\alpha = \frac{2}{d-c} \zeta, \quad (3.14)$$

$$\Phi_1(\alpha) = \Phi_1^*(\zeta), \quad (3.15)$$

$$\Phi_2(\alpha) = \Phi_2^*(\zeta), \quad (3.16)$$

$$\gamma = \frac{2}{d-c} \gamma^*. \quad (3.17)$$

The singular integral equation (3.5) then becomes

$$\begin{aligned} \omega \phi(r) + \frac{1}{\pi} \int_{-1}^1 \frac{\phi(s) ds}{(s-r)} \\ - \int_{-1}^1 \left[ J_1^*(s, r) + \eta \int_{-1}^1 J_2^*(s, r) \right] \phi(s) ds = f^*(r), \quad -1 < r < 1. \end{aligned} \quad (3.18)$$

where

$$J_1^*(s, r) = \frac{4}{\pi(\kappa+1)} \int_0^\infty \Phi_1^*(\zeta) \sin \zeta(s-r) d\zeta, \quad (3.19)$$

$$J_2^*(s, r) = \frac{4}{\pi(\kappa+1)} \int_0^\infty \Phi_2^*(\zeta) \cos \zeta(s-r) d\zeta, \quad (3.20)$$

$$\Phi_1^*(\zeta) = -\frac{\zeta(\kappa-1)}{\Delta_0(\zeta)} [\bar{Z}_2(\zeta) + Z_2(\zeta)] + \frac{\kappa+1}{4} \frac{\zeta}{|\zeta|}, \quad (3.21)$$

$$\Phi_2^*(\zeta) = \frac{i\zeta}{\Delta_0(\zeta)} [Z_1(\zeta) - \bar{Z}_1(\zeta)] + \frac{\kappa-1}{4}. \quad (3.22)$$

## 3.2 The Fundamental Function

The dominant part of the singular integral equation of the second kind (3.18) is of the form

$$A\phi(r) + \frac{B}{\pi} \int_{-1}^1 \frac{\phi(s)}{s-r} ds = f^*(r), \quad -1 < r < 1. \quad (3.23)$$

where the bounded function  $f^*(r)$  contains part of the integral equation with the Fredholm kernels. Defining

$$F(z) = \frac{1}{\pi} \int_{-1}^1 \frac{\phi(s)}{s-z} ds. \quad (3.24)$$

and using the following general Plemelj formulas

$$F^+(r) - F^-(r) = \begin{cases} 2i\phi(r) & -1 < r < 1, \\ 0 & r < -1, r > 1, \end{cases} \quad (3.25)$$

$$F^+(r) + F^-(r) = \begin{cases} \frac{2}{\pi} \int_{-1}^1 \frac{\phi(s)}{s-r} ds & -1 < r < 1, \\ 4iF(r) & r < -1, r > 1, \end{cases} \quad (3.26)$$

we may reduce (3.23) to the following Riemann-Hilbert problem for the sectionally holomorphic function  $F(z)$ :

$$F^+(r) - \frac{A-iB}{A+iB} F^-(r) = \frac{2if^*(r)}{A+iB}. \quad (3.27)$$

considering the corresponding homogeneous equation

$$X^+(r) - \frac{A-iB}{A+iB} X^-(r) = 0. \quad (3.28)$$

we obtain the fundamental solution  $X(z)$  and the fundamental function  $w(x)$  of (3.23) as [28]

$$X(z) = (z-1)^\alpha (z+1)^\beta, \quad (3.29)$$

$$w(r) = (1-r)^\alpha (r+1)^\beta. \quad (3.30)$$

where

$$\alpha = \frac{1}{2\pi i} \log \frac{A-iB}{A+iB} + N, \quad (3.31)$$

$$\beta = -\frac{1}{2\pi i} \log \frac{A-iB}{A+iB} + M, \quad (3.32)$$

$$-1 < \Re(\alpha) < 1, \quad -1 < \Re(\beta) < 1.$$

where  $N$  and  $M$  are arbitrary (positive, zero, or negative) integers. The index of the integral equation is defined by

$$\kappa_0 = -(\alpha + \beta) = -(N + M). \quad (3.33)$$

$\alpha$  and  $\beta$  can also be written as

$$\alpha = -\frac{1}{\pi}\theta + N, \quad (3.34)$$

$$\beta = \frac{1}{\pi}\theta + M, \quad (3.35)$$

$$\theta = \arctan \frac{B}{A}. \quad (3.36)$$

From (3.5) and (3.23) we observe that in the punch problem with friction  $A = \omega = \eta(\kappa - 1)/(\kappa + 1)$  and  $B = 1$ . Therefore, the powers of stress singularity  $\alpha$  and  $\beta$  will depend only on the coefficient of friction  $\eta$  and the value of the Poisson's ratio on the surface of the elastic half space. In this study the Poisson's ratio is assumed to be constant, consequently  $\alpha$  and  $\beta$  would be independent of the non-homogeneity parameter  $\gamma$ .

### 3.3 Numerical Procedure

We have derived the singular integral equation for the punch problem. The integral equation has a Cauchy kernel and two Fredholm kernels. The solution of the singular integral equation is generally obtained either through function theoretical technique as given by Muskhelishvili [28] or through numerical methods [29] and [30]. In this study the method of using orthogonal polynomials with the unknown functions represented by Jacobi polynomials, associated with the weight function  $w(t)$  and described in [31] is used.

The singular integral equation does not have a closed form solution. Hence a numerical method has to be used. In this study Jacobi polynomials are used to reduce the singular integral equation to an infinite system of linear algebraic equations.

Once the fundamental function,  $w(s)$  of the integral equation is determined, the solution of (3.18) may be expressed as

$$\phi(s) = g(s)w(s), \quad -1 < s < 1. \quad (3.37)$$

where  $g(s)$  is a bounded continuous function and can always be represented by an infinite series. Observing that  $w(s)$  is the weight function of the Jacobi Polynomials, one may write

$$\phi(s) = \sum_0^{\infty} c_n w(s) P_n^{(\alpha, \beta)}(t), \quad (3.38)$$

where  $c_n$ , ( $n = 0, 1, \dots$ ) are undetermined constants.

Before substituting (3.38) into (3.18) note that for  $\kappa = (-1, 0, 1)$  (see Tricomi [32], Szegő [33])

$$\begin{aligned} \frac{1}{\pi} \int_{-1}^1 \frac{w(t) P_n^{(\alpha, \beta)}(t)}{t - x} dt &= \cot \pi \alpha w(x) P_n^{(\alpha, \beta)}(x) \\ &\quad - \frac{2^{\alpha+\beta} \Gamma(\alpha) \Gamma(n + \beta + 1)}{\pi \Gamma(n + \alpha + \beta + 1)} F\left(n + 1, -n - \alpha - \beta, 1 - \alpha, \frac{1 - x}{2}\right), \\ -1 < x < 1, \quad \Re(\alpha) > -1, \quad \Re(\beta) > -1, \\ \alpha + \beta &= -\kappa, \quad \Re(\alpha) \neq (0, 1, \dots). \end{aligned} \quad (3.39)$$

By observing that

$$P_{n-\kappa}^{(-\alpha, -\beta)}(x) = \frac{\Gamma(n - \kappa - \alpha + 1)}{\Gamma(n - \kappa + 1) \Gamma(1 - \alpha)} F\left(n + 1, -n + \kappa, 1 - \alpha, \frac{1 - x}{2}\right), \quad (3.40)$$

and substituting  $\kappa = -(\alpha + \beta)$  in (3.40) yields

$$F\left(n + 1, -n + \kappa, 1 - \alpha, \frac{1 - x}{2}\right) = \frac{\Gamma(n + \alpha + \beta + 1) \Gamma(1 - \alpha)}{\Gamma(n + \beta + 1)} P_{n-\kappa}^{(-\alpha, -\beta)}(x). \quad (3.41)$$

By substituting now (3.41) back into (3.39), we obtain

$$\frac{1}{\pi} \int_{-1}^1 \frac{w(t) P_n^{(\alpha, \beta)}(t)}{t - x} dt = \frac{\cos \pi \alpha}{\sin \pi \alpha} w(x) P_n^{(\alpha, \beta)}(x) - 2^{-\kappa} \frac{\Gamma(\alpha) \Gamma(1 - \alpha)}{\pi} P_{n-\kappa}^{(-\alpha, -\beta)}(x) \quad (3.42)$$

$-1 < x < 1$

Note also that

$$\frac{\Gamma(\alpha) \Gamma(1 - \alpha)}{\pi} = \frac{1}{\sin \pi \alpha}. \quad (3.43)$$



Equation (3.39) further reduces to

$$AP_n^{(\alpha, \beta)}(r)w(r) + \frac{B}{\pi} \int_{-1}^1 \frac{P_n^{(\alpha, \beta)}(s)w(s)}{(s-r)} ds = -2^{-\kappa_0} \frac{B}{\sin \pi \alpha} P_{n-\kappa_0}^{(-\alpha, -\beta)}(r),$$

$$-1 < r < 1, \quad \Re(\alpha) > -1, \quad \Re(\beta) > -1, \quad \Re(\alpha) \neq (0, 1, \dots). \quad (3.44)$$

By substituting (3.38) into (3.18) and making use of (3.44), we find

$$\sum_0^\infty c_n \left[ \frac{-2^{-\kappa_0}}{\sin \pi \alpha} P_{n-\kappa_0}^{(-\alpha, -\beta)}(r) + h_n^1(r) + h_n^2(r) \right] = f^*(r), \quad -1 < r < 1. \quad (3.45)$$

where

$$h_n^1(r) = \int_{-1}^1 J_1^*(s, r) P_n^{(\alpha, \beta)}(s) w(s) ds, \quad (3.46)$$

$$h_n^2(r) = \int_{-1}^1 J_2^*(s, r) P_n^{(\alpha, \beta)}(s) w(s) ds. \quad (3.47)$$

The functional equation (3.45) can be reduced to a system of algebraic equations in  $c_n$  through a suitable collocation technique. In the numerical solution of (3.45), higher accuracy is obtained when the density of the collocation points is increased near the ends by choosing the collocation points  $(r_i, \quad i = 0, 1, \dots, N)$  as the roots of the Jacobi polynomials depending on the index of the problem. Also using the orthogonality relations (see [34]) of the Jacobi Polynomials given below

$$\int_{-1}^1 P_n^{(\alpha, \beta)}(t) P_k^{(\alpha, \beta)}(t) w(t) dt = \begin{cases} 0 & n \neq k, \\ \theta_k(\alpha, \beta) & n = k, \end{cases} \quad (3.48)$$

where

$$\theta_k(\alpha, \beta) = \frac{2^{\alpha+\beta+1} \Gamma(k+\alpha+1) \Gamma(k+\beta+1)}{(2k+\alpha+\beta+1) k! \Gamma(\alpha+\beta+2)}, \quad (3.49)$$

$$\theta_0(\alpha, \beta) = \frac{2^{\alpha+\beta+1} \Gamma(\alpha+1) \Gamma(\beta+1)}{\Gamma(\alpha+\beta+2)}, \quad (3.50)$$

we can also reduce the functional equation (3.45) into an infinite system of algebraic equations in  $c_n$  by expanding both sides into series of Jacobi polynomials

$P_k^{(-\alpha, -\beta)}(r)$  ( $k = 0, 1, \dots$ ), and comparing the respective coefficients. Truncating the series gives

$$-\frac{2^{-\kappa_0}}{\sin \pi \alpha} \theta_k(-\alpha, -\beta) c_{k+\kappa_0} + \sum_{n=0}^N (d_{nk}^1 + d_{nk}^2) c_n = F_k^*, \quad (k = 0, 1, \dots, N). \quad (3.51)$$

where

$$d_{nk}^1 = \int_{-1}^1 P_k^{(-\alpha, -\beta)}(r) w(-\alpha, -\beta, r) h_n^1(r) dr, \quad (3.52)$$

$$d_{nk}^2 = \int_{-1}^1 P_k^{(-\alpha, -\beta)}(r) w(-\alpha, -\beta, r) h_n^2(r) dr, \quad (3.53)$$

$$F_k^* = \int_{-1}^1 P_k^{(-\alpha, -\beta)}(r) w(-\alpha, -\beta, r) f^*(r) dr, \quad (3.54)$$

$$w(-\alpha, -\beta, r) = (1-r)^{-\alpha} (1+r)^{-\beta} = w^{-1}(r). \quad (3.55)$$

# Chapter 4

## Results and Discussions

### 4.1 The Flat Punch

The problem for a flat punch is described in Fig. 4.1 where the punch profile is given by

$$v(x, 0) = C. \quad (4.1)$$

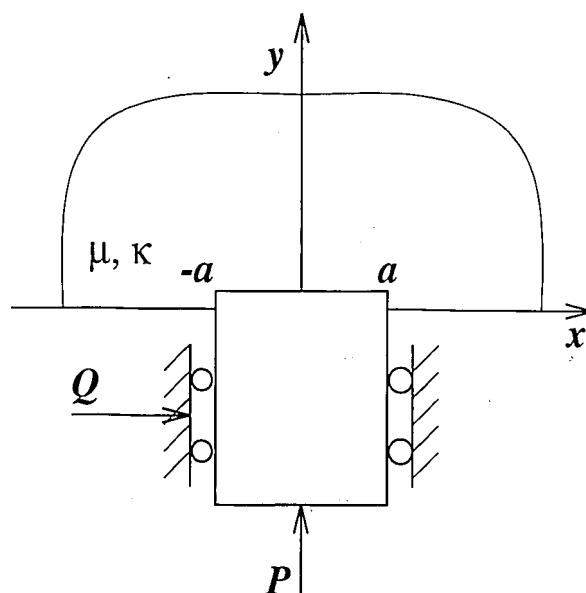


Figure 4.1: Geometry of flat punch

Differentiating (4.1) with respect to  $x$ , the input function  $f(x)$  in equation (3.5)

for the flat punch becomes

$$f(x) = \frac{4\mu}{\kappa + 1} \frac{\partial}{\partial x} v(x, 0) = 0. \quad (4.2)$$

#### 4.1.1 Solution for a Homogeneous Materials

For a homogeneous material,  $\gamma = 0$ , equation (2.75) reduces to

$$\lambda \sigma_{xy}(x, 0) - \frac{1}{\pi} \int_{-\infty}^{\infty} \frac{\sigma_{yy}(t, 0) dt}{(t - x)} = \frac{4\mu_0}{\kappa + 1} \frac{\partial}{\partial x} v(x, 0), \quad (4.3)$$

where

$$\lambda = \frac{\kappa - 1}{\kappa + 1}.$$

By substituting

$$\sigma_{yy}(x, 0) = -p(x), \quad \sigma_{xy}(x, 0) = -\eta p(x), \quad -a < x < a, \quad (4.4)$$

$$\sigma_{yy}(x, 0) = \sigma_{xy}(x, 0) = 0, \quad x < -a, \quad x > a. \quad (4.5)$$

equation (4.3) becomes

$$Ap(x) + \frac{1}{\pi} \int_{-a}^a \frac{p(t) dt}{(t - x)} = \frac{4\mu_0}{\kappa + 1} \frac{\partial}{\partial x} v(x, 0), \quad -a < x < a, \quad (4.6)$$

where

$$A = \eta \frac{\kappa - 1}{\kappa + 1}. \quad (4.7)$$

The equilibrium equation is given as

$$\int_{-a}^a p(t) dt = P. \quad (4.8)$$

In order to solve the integral equation the limits have to be normalized. Now setting  $d = a$ , and  $c = -a$ , equations (3.8) to (3.12) become

$$t = as, \quad -1 < s < 1, \quad (4.9)$$

$$x = ar, \quad -1 < r < 1, \quad (4.10)$$

$$\sigma_0 = \frac{P}{2a}. \quad (4.11)$$

Also letting

$$p(t) = 2\sigma_0\phi(s) \quad (4.12)$$

from (4.6) and (4.8) one obtains

$$A\phi(r) + \frac{1}{\pi} \int_{-1}^1 \frac{\phi(s)ds}{s-r} = 0, \quad -1 < r < 1, \quad (4.13)$$

$$\int_{-1}^1 \phi(s)ds = 1. \quad (4.14)$$

Since  $p(x)$  has integrable singularities at  $x = a$ , and at  $x = -a$ , from the physics of the problem we must require that  $\alpha$  and  $\beta$  must be negative. Therefore,  $N = 0$  and  $M = -1$  in equation (3.34) and (3.35). The index of the problem is found to be from equation (3.33)

$$\kappa_0 = -(N + M) = -(0 - 1) = 1. \quad (4.15)$$

By observing that  $A = \eta(\kappa - 1)/(\kappa + 1)$  and  $B = 1$ , from (3.34)-(3.36) the powers of singularity  $\alpha$  and  $\beta$  may be obtained as

$$\alpha = -\frac{\theta}{\pi}, \quad (4.16)$$

$$\beta = \frac{\theta}{\pi} - 1, \quad (4.17)$$

$$\theta = \arctan \frac{\kappa + 1}{\eta(\kappa - 1)}. \quad (4.18)$$

Now assuming a solution of the form (3.37), the solution of (4.13) is given by equation (3.45), which becomes

$$\sum_1^N c_n \left[ -2^{-1} \frac{1}{\sin \pi \alpha} P_{n-1}^{(-\alpha, -\beta)}(r) \right] = 0. \quad (4.19)$$

substituting  $\phi(s)$  into equation 4.14 and using orthogonality of Jacobi Polynomials given by equation (3.49), the only nonzero coefficient  $c_0$  can be found as

$$c_0 \theta_0 = P_0^{(\alpha, \beta)}(r) = 1. \quad (4.20)$$

where in this case ( $\alpha + \beta = -1$ ),  $\theta_0$  becomes

$$\theta_0 = -\frac{\pi}{\sin \pi \alpha}. \quad (4.21)$$

Therefore the solution is

$$\begin{aligned} p(r) &= 2\sigma_0\phi(r), \\ &= \frac{P}{a\theta_0} (1-r)^\alpha (1+r)^\beta. \end{aligned} \quad (4.22)$$

From equation (4.4)

$$\begin{aligned} \sigma_{yy}(x, 0) &= -\frac{P}{a\theta_0} \left(1 - \frac{x}{a}\right)^\alpha \left(1 + \frac{x}{a}\right)^\beta \\ &= -\frac{P}{\theta_0} (a-x)^\alpha (x+a)^\beta. \end{aligned} \quad (4.23)$$

or in normalized form

$$\frac{\sigma_{yy}(x, 0)}{P/2a} = -\frac{2}{\theta_0} \left(1 - \frac{x}{a}\right)^\alpha \left(1 + \frac{x}{a}\right)^\beta. \quad (4.24)$$

This result agrees with the solution given in [31]

### Stress intensity factors for the homogeneous medium

The stress intensity factors for a punch with sharp corners are defined by

$$k_1(a) = \lim_{x \rightarrow a} \frac{p(x)}{2^\beta (a-x)^\alpha} = \frac{Pa^\beta}{\theta_0}. \quad (4.25)$$

$$k_1(-a) = \lim_{x \rightarrow -a} \frac{p(x)}{2^\alpha (x+a)^\beta} = \frac{Pa^\alpha}{\theta_0}. \quad (4.26)$$

For the homogeneous case i.e.,  $\alpha = \beta = -1/2$ , referring to equation (4.18),  $\theta_0$  becomes  $\pi$  and equations (4.25) and (4.26) reduce to

$$k_1(a) = k_1(-a) = \frac{P}{\pi\sqrt{a}}. \quad (4.27)$$

which is the well known result.

### 4.1.2 Solution for Graded Materials

Consider the punch problem for the non-homogeneous medium shown in Figure(4.1).

Let  $\mu$  be the shear modulus varying exponentially in  $y$  direction ,

$$\mu(y) = \mu_0 e^{\gamma y}, \quad (4.28)$$

where  $\gamma$  is the non-homogeneity parameter and has the dimension of  $L^{-1}$ .

Using equations (4.4) and (4.5) equation (2.75) becomes

$$Ap(x) + \frac{1}{\pi} \int_{-a}^a \frac{p(t)dt}{(t-x)} - \int_{-a}^a (J_1(t, x) + \eta J_2(t, x)) p(t)dt = f(x), \quad -a < x < a. \quad (4.29)$$

where

$$f(x) = \frac{4\mu_0}{\kappa + 1} \frac{\partial}{\partial x} v(x, 0) = 0, \quad (4.30)$$

and  $A$  is given in equation (4.7). Using equations (4.9)-(4.12) and defining

$$\gamma^* = a\gamma, \quad (4.31)$$

$$J_1(t, x) = J_1^*(s, r), \quad (4.32)$$

$$J_2(t, x) = J_2^*(s, r). \quad (4.33)$$

one obtains

$$A\phi(r) + \frac{1}{\pi} \int_{-1}^1 \frac{\phi(s)ds}{s-r} - \int_{-1}^1 (J_1^*(s, r) + \eta J_2^*(s, r)) \phi(s)ds = 0, \quad (4.34)$$

$$\int_{-1}^1 \phi(s)ds = 1. \quad (4.35)$$

Using the same procedure as in homogeneous case, the index  $\kappa_0$  becomes 1. Assuming a solution of the form (3.37) equation (4.34) becomes

$$\sum_1^N c_n \left[ -2^{-1} \frac{1}{\sin \pi \alpha} P_{n-1}^{(-\alpha, -\beta)}(r) + h_n^1(r) + h_n^2(r) \right] = 0. \quad (4.36)$$

Equation (4.36) provides  $N$  equations for  $N + 1$  unknown constants  $c_0, \dots, c_N$ . The additional equation for a unique solution is provided by the equilibrium condition given (4.35), which becomes

$$\sum_0^\infty c_n \int_{-1}^1 w(s) P_n^{(\alpha, \beta)}(s) dr = 1. \quad (4.37)$$

Using the orthogonality condition, we obtain the following  $N + 1$  equations

$$c_0 \theta_0 = 1, \quad (4.38)$$

$$\sum_0^N c_n F_n(r_i) = 0, \quad i = 1, \dots, N. \quad (4.39)$$

In 4.39  $r_i$  ( $i = 1, \dots, N$ ) are obtained by setting

$$P_{n-1}^{(\alpha+1, \beta+1)}(r_i) = 0, \quad i = 1, \dots, N, \quad (4.40)$$

$$F_n(r_i) = -2^{-1} \frac{1}{\sin \pi \alpha} P_{n-1}^{(-\alpha, -\beta)}(r_i) + h_n^1(r_i) + h_n^2(r_i). \quad (4.41)$$

where  $h_n^1(r_i)$  and  $h_n^2(r_i)$  are given by equations (3.46) and (3.46). Therefore, from (4.12) we obtain

$$\begin{aligned} p(r) &= 2\sigma_0 \phi(r), \\ &= \frac{P}{a} (1-r)^\alpha (1+r)^\beta \sum_0^N c_n P_n^{(\alpha, \beta)}(r). \end{aligned} \quad (4.42)$$

Contact stresses can be found from (4.4) as

$$\sigma_{yy}(x, 0) = -p(x) \quad (4.43)$$

$$= -\frac{P}{a} \left(1 - \frac{x}{a}\right)^\alpha \left(1 + \frac{x}{a}\right)^\beta \sum_0^N c_n P_n^{(\alpha, \beta)}\left(\frac{x}{a}\right) \quad (4.44)$$

$$= -P(a-x)^\alpha (x+a)^\beta \sum_0^N c_n P_n^{(\alpha, \beta)}\left(\frac{x}{a}\right). \quad (4.45)$$

or in normalized form

$$\frac{\sigma_{yy}(x, 0)}{P/2a} = -2 \left(1 - \frac{x}{a}\right)^\alpha \left(1 + \frac{x}{a}\right)^\beta \sum_0^N c_n P_n^{(\alpha, \beta)}\left(\frac{x}{a}\right). \quad (4.46)$$

Fig. 4.2 gives the stress distribution under a flat punch for various values of the non-dimensional material non-homogeneity parameter,  $\gamma a$ , in the case of no friction. The stress distribution is unbounded at the ends of the punch. When the non-homogeneity parameter is very small (e.g.  $\gamma a = 0.1$ ), the solution reduces to the homogeneous solution and when it tends to infinity medium behaves as a rigid medium and pressure profile becomes  $\sigma_{yy}(x, 0) = P/2a$ .

Figures 4.3 to 4.8 give the stress distribution under a flat punch for various values of the material non-homogeneity parameter,  $\gamma$ , in the case of friction. Friction coefficients are taken to be  $\eta = 0.1, 0.3, 0.5$ . The stress distribution is not symmetric as observed in the frictionless case. The stress concentration near the edge  $x = -a$



is greater than that near  $x = a$ . As  $\eta$  increases the shape of the stress distribution curve becomes more slanted. In Fig.4.8 when  $\gamma a = 2$  stress become zero around  $x/a = 0.2$ , meaning that for  $\gamma a > 2$  separation will occur in the contact region. Again, note that the powers of stress singularity are independent of  $\gamma$  and are given by (4.16)-(4.18). The calculated values for  $\alpha$  and  $\beta$  corresponding to the results shown in Figures 4.3-4.8 are given in Table 4.1

### Stress intensity factors

Mode I stress intensity factors at the ends of the punch are defined as

$$k_1(a) = \lim_{x \rightarrow a} \frac{p(x)}{2^\beta (a-x)^\alpha} = P a^\beta \sum_0^N c_n P_n^{(\alpha, \beta)}(1), \quad (4.47)$$

$$k_1(-a) = \lim_{x \rightarrow -a} \frac{p(x)}{2^\alpha (x+a)^\beta} = P a^\alpha \sum_0^N c_n P_n^{(\alpha, \beta)}(-1), \quad (4.48)$$

giving the non-dimensional stress intensity factors as

$$\begin{aligned} k_1^*(a) &= \frac{\theta_0}{P a^\beta} k_1(a) = \theta_0 \sum_0^N c_n P_n^{(\alpha, \beta)}(1), \\ &= \frac{1}{c_0} \sum_0^N c_n P_n^{(\alpha, \beta)}(1), \\ k_1^*(-a) &= \frac{\theta_0}{P a^\alpha} k_1(a) = \theta_0 \sum_0^N c_n P_n^{(\alpha, \beta)}(-1), \\ &= \frac{1}{c_0} \sum_0^N c_n P_n^{(\alpha, \beta)}(-1). \end{aligned}$$

Table 4.1 gives the normalized stress intensity factors at the ends of the flat punch by assuming  $\nu = 0.3$ . The first column is for the case of frictionless punch. Note that as  $\gamma a$  increases stress intensity factor decreases and is the same for both ends of the punch. For the case of friction, it can be seen that,  $k_1^*(-a)$  decreases up to a certain value of  $\gamma a$  and then increases as  $\gamma a$  is increased, whereas  $k_1^*(a)$  decreases monotonously with increasing  $\gamma a$ .

Variation of the stress intensity factor for various values of the friction coefficient is given in figures 4.9 to 4.11. In the frictionless case, stress intensity factors at the

two ends are the same. It is seen that as  $\gamma a$  increases material becomes stiffer and stress intensity factors decrease.

Table 4.1: Stress intensity factors for flat punch,  $\theta_0 = -\frac{\pi}{\sin \pi \alpha}$

	$\eta = 0.0$	$\eta = 0.1$		$\eta = 0.3$		$\eta = 0.5$	
	$\alpha = -0.5$ $\beta = -0.5$	$\alpha = -0.4909$ $\beta = -0.5091$		$\alpha = -0.4728$ $\beta = -0.5272$		$\alpha = -0.4548$ $\beta = -0.5452$	
$\gamma a$	$\frac{k_1(a)}{Pa^{\beta/\theta_0}}$	$\frac{k_1(-a)}{Pa^{\alpha/\theta_0}}$	$\frac{k_1(a)}{Pa^{\beta/\theta_0}}$	$\frac{k_1(-a)}{Pa^{\alpha/\theta_0}}$	$\frac{k_1(a)}{Pa^{\beta/\theta_0}}$	$\frac{k_1(-a)}{Pa^{\alpha/\theta_0}}$	$\frac{k_1(a)}{Pa^{\beta/\theta_0}}$
0.0	1.0000	1.0000	1.0000	1.0000	1.0000	1.0000	1.0000
0.1	0.9351	0.9347	0.9356	0.9350	0.9380	0.9360	0.9351
0.4	0.8028	0.8236	0.7826	0.8695	0.7487	0.9175	0.8028
0.7	0.7144	0.7692	0.6637	0.8918	0.5834	1.0205	0.7144
1.0	0.6492	0.7484	0.5629	0.9771	0.4439	1.2151	0.6492
2.0	0.5142	0.8376	0.3064	1.6000	0.2365	2.2178	0.5142
2.5	0.4715	0.9540	0.2207	2.0031	0.2704	2.7204	0.4715
3.0	0.4378	1.1082	0.1676	2.3899	0.3339	3.1767	0.4378

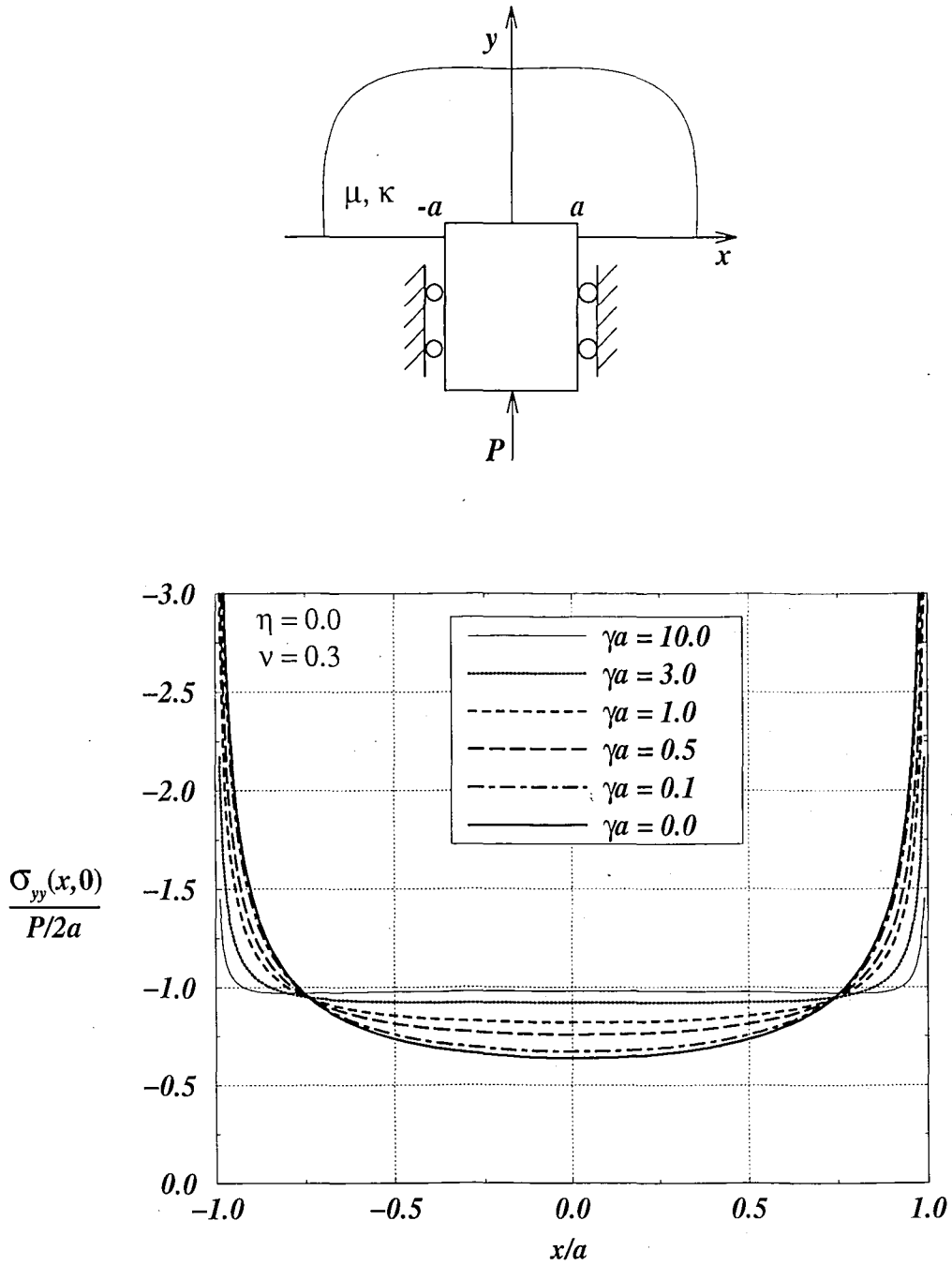


Figure 4.2: Stress distribution under a flat punch for various values of the material non-homogeneity parameter,  $\gamma$ , when friction is not present,  $\alpha = \beta = -0.5$ .

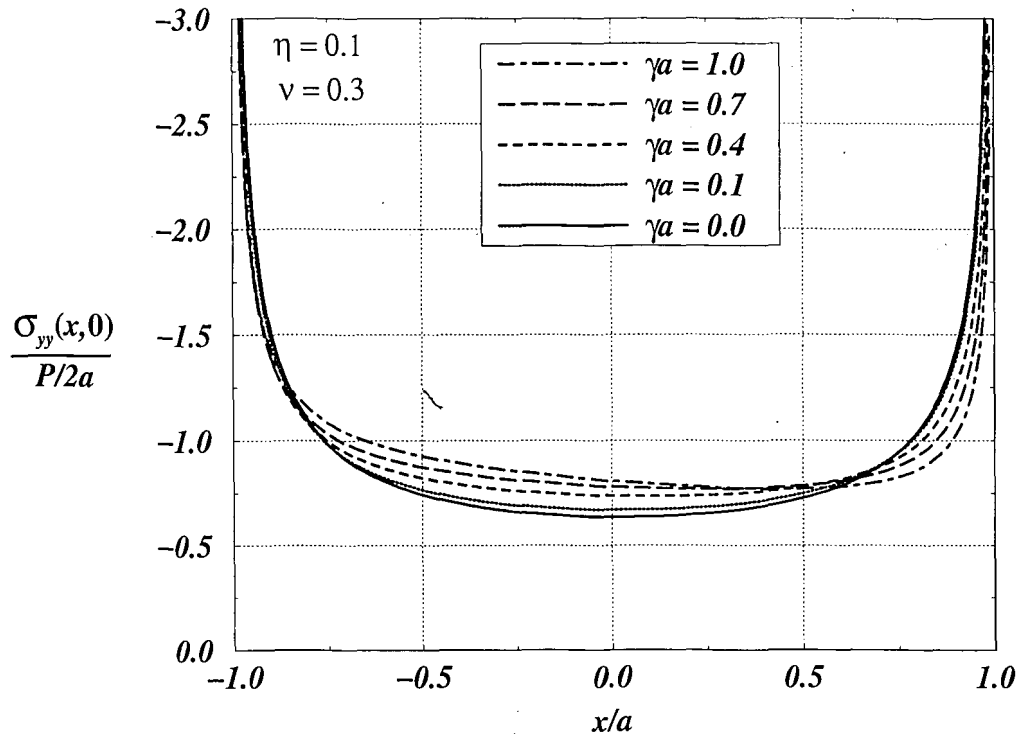
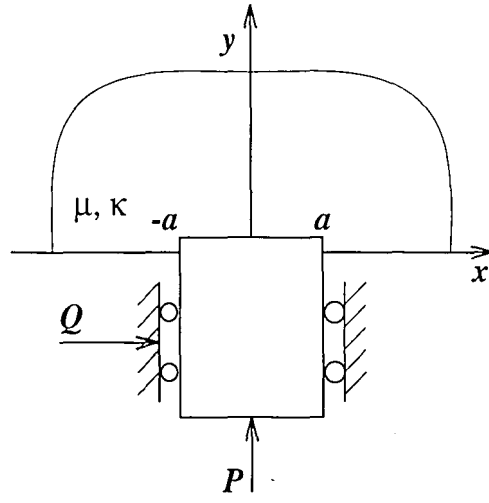


Figure 4.3: Stress distribution under a flat punch for various values of the material non-homogeneity parameter,  $\gamma$ , in the presence of friction,  $\eta = 0.1$ ,  $\alpha = -0.4909$ ,  $\beta = -0.5091$ .

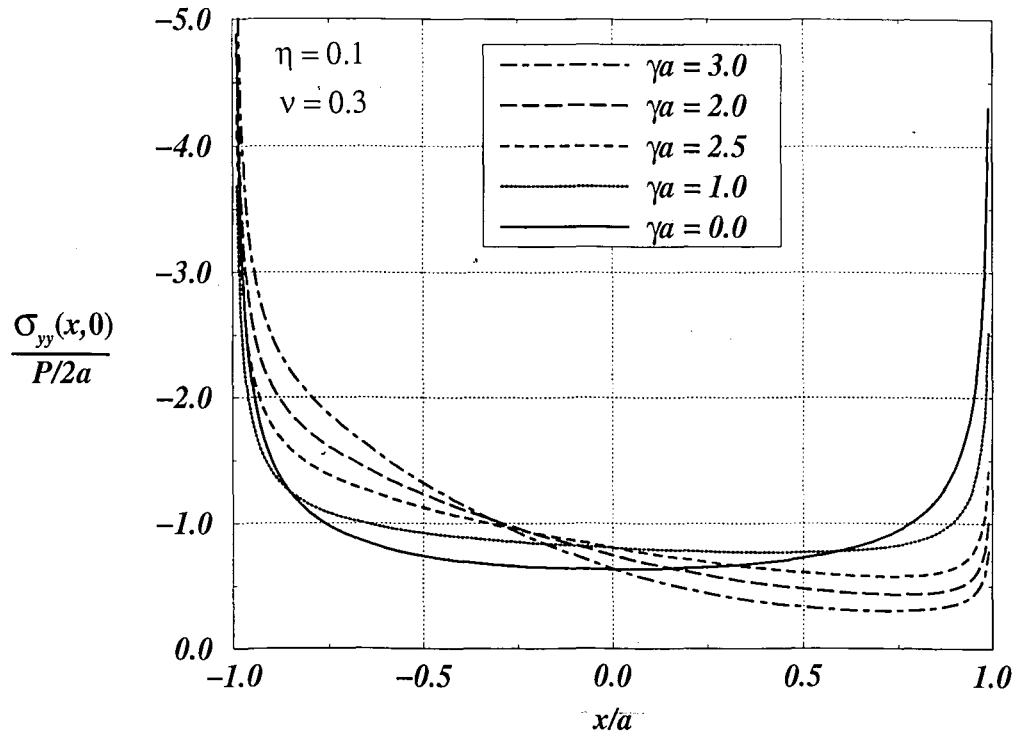
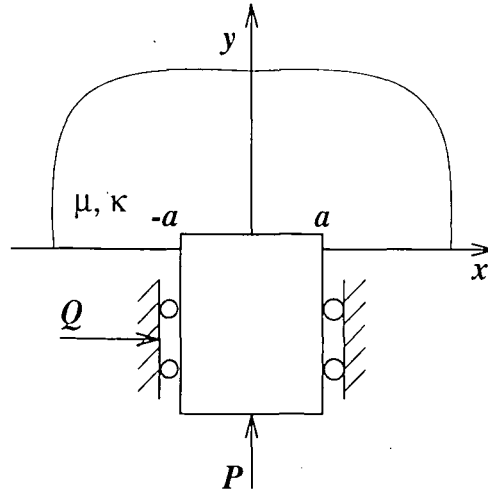


Figure 4.4: Stress distribution under a flat punch for various values of the material non-homogeneity parameter,  $\gamma$ , in the presence of friction,  $\eta = 0.1$ ,  $\alpha = -0.4909$ ,  $\beta = -0.5091$ .

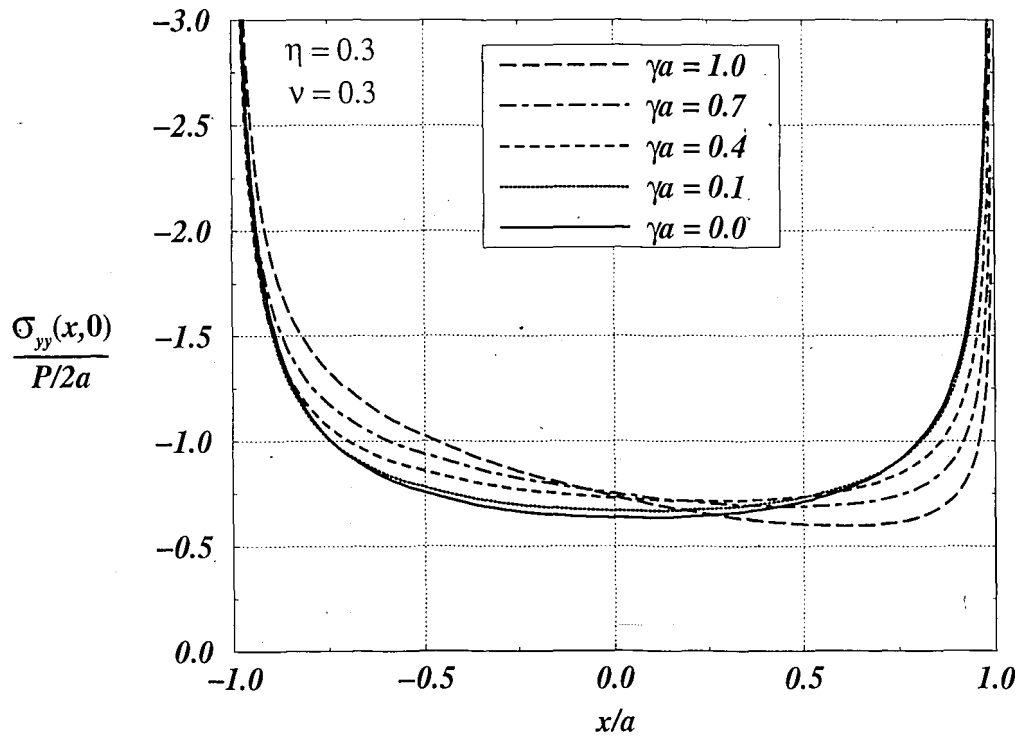
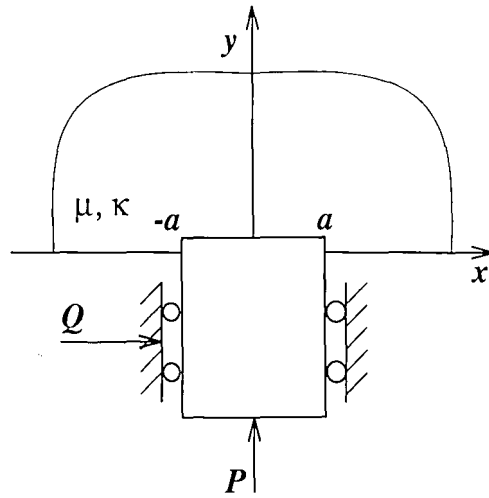


Figure 4.5: Stress distribution under a flat punch for various values of the material non-homogeneity parameter,  $\gamma$ , in the presence of friction,  $\eta = 0.3$ ,  $\alpha = -0.4728$ ,  $\beta = -0.5272$ .

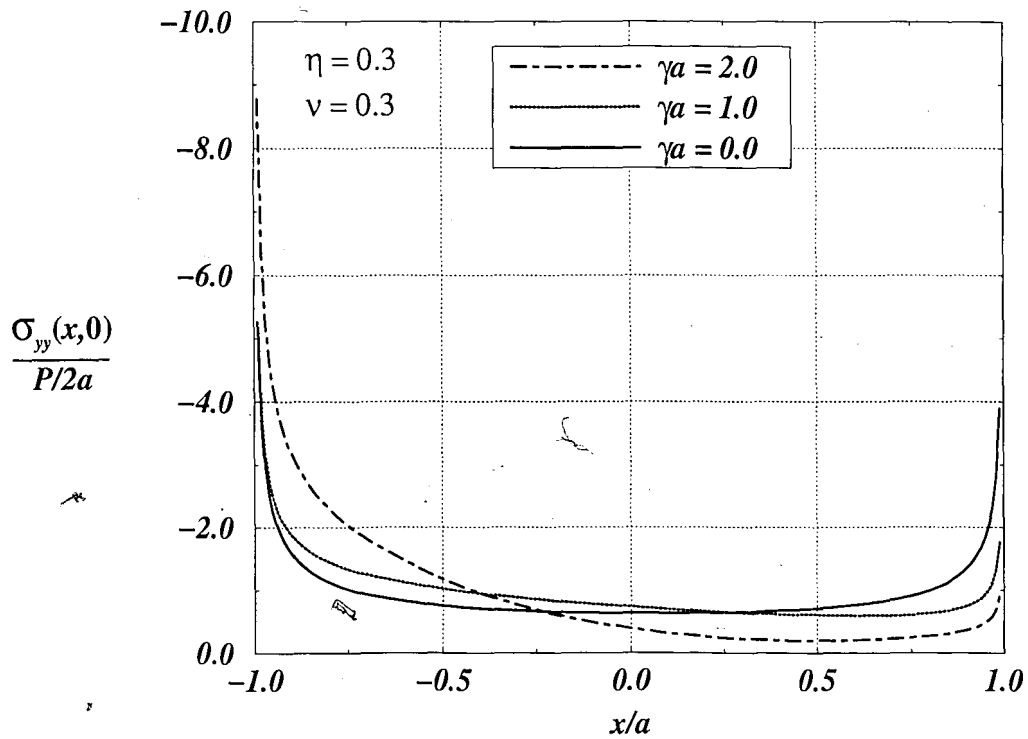
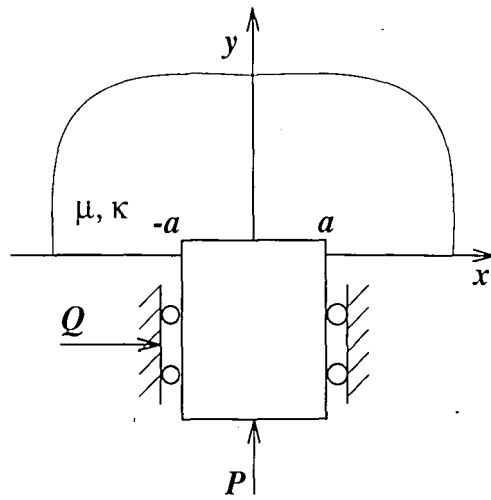


Figure 4.6: Stress distribution under a flat punch for various values of the material non-homogeneity parameter,  $\gamma$ , in the presence of friction,  $\eta = 0.3$ ,  $\alpha = -0.4728$ ,  $\beta = -0.5272$ .

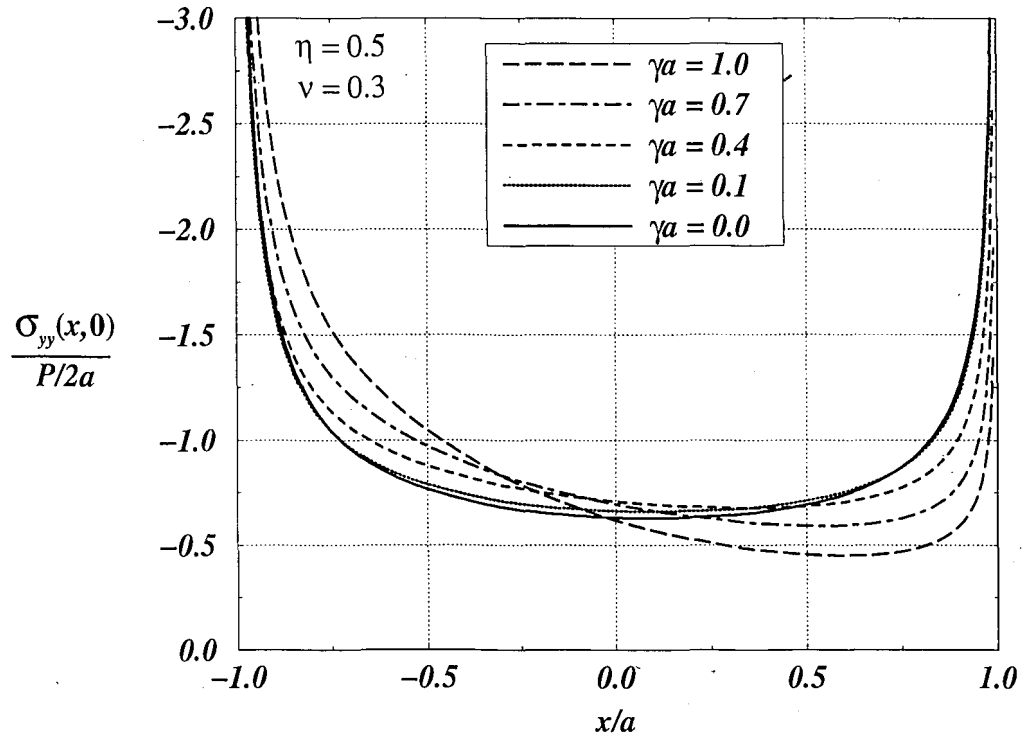
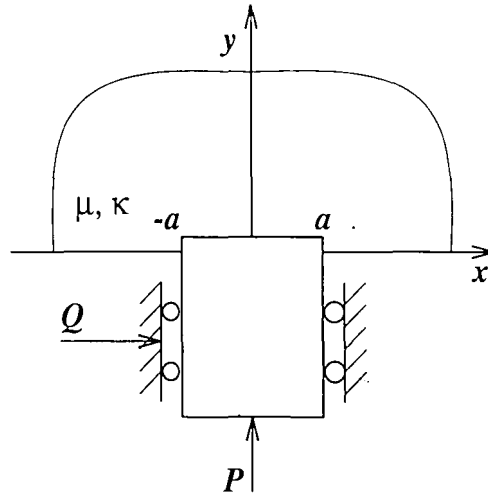


Figure 4.7: Stress distribution under a flat punch for various values of the material non-homogeneity parameter,  $\gamma$ , in the presence of friction,  $\eta = 0.5$ ,  $\alpha = -0.4548$ ,  $\beta = -0.5452$ .



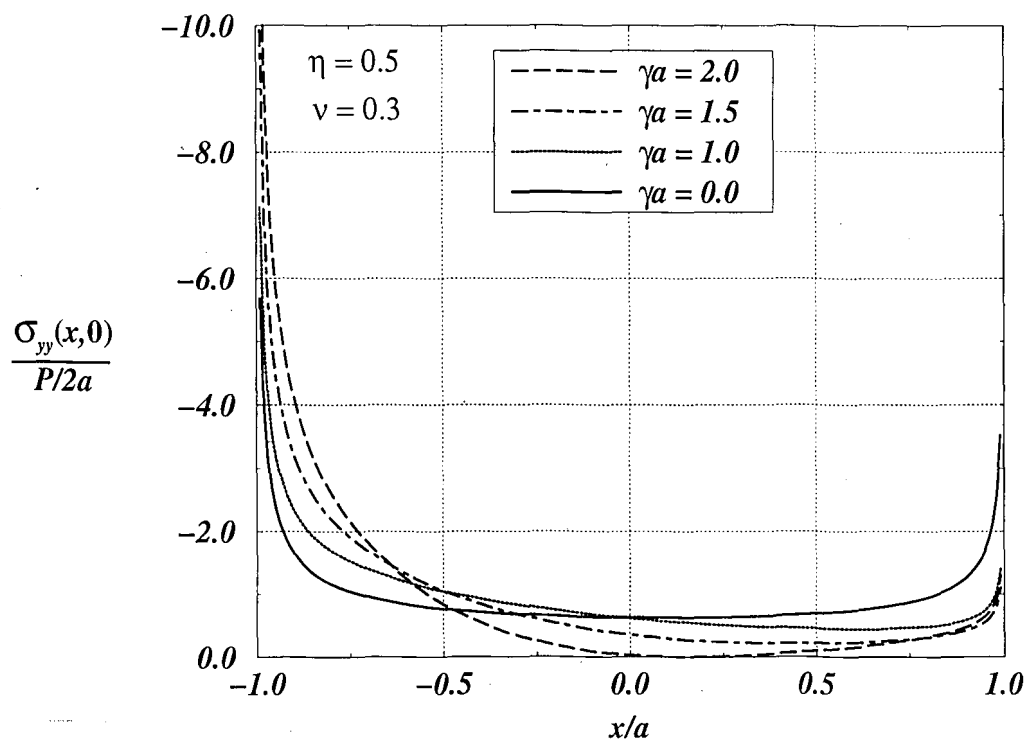
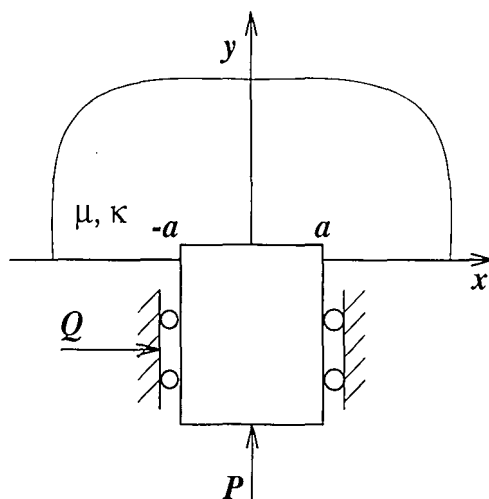


Figure 4.8: Stress distribution under a flat punch for various values of the material non-homogeneity parameter,  $\gamma$ , in the presence of friction,  $\eta = 0.5$   $\alpha = -0.4548$ ,  $\beta = -0.5452$ .

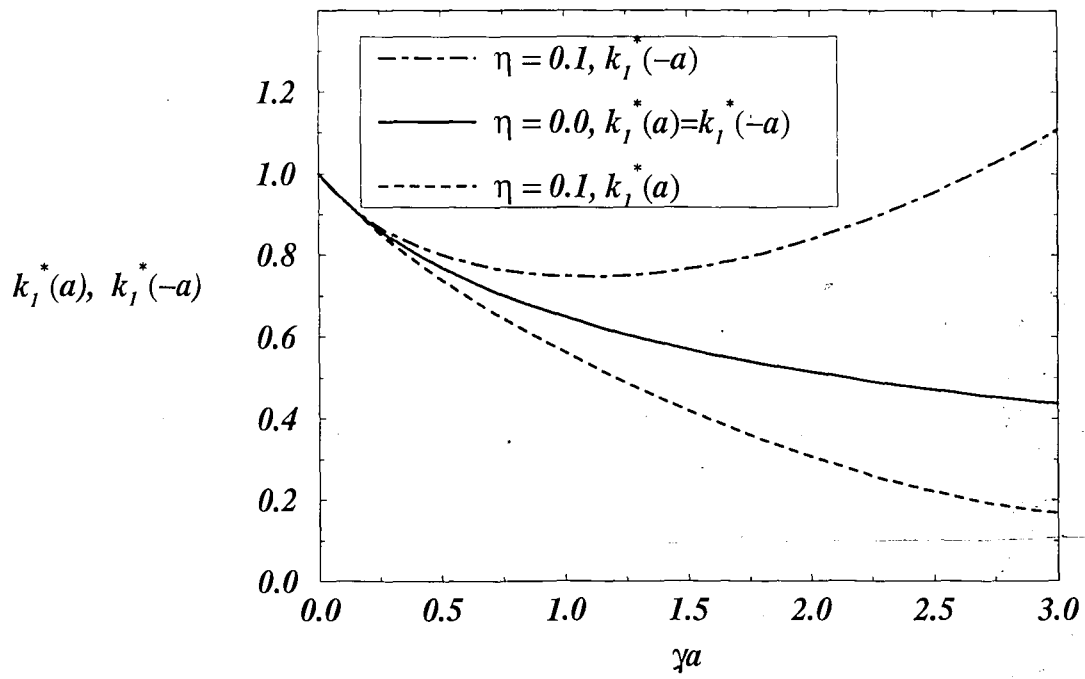


Figure 4.9: Variation of stress intensity factors with the non-homogeneity parameter,

$$k_1^*(a) = \frac{k_1(a)}{Pa^\beta/\theta_0}, \quad k_1^*(-a) = \frac{k_1(-a)}{Pa^\alpha/\theta_0}$$

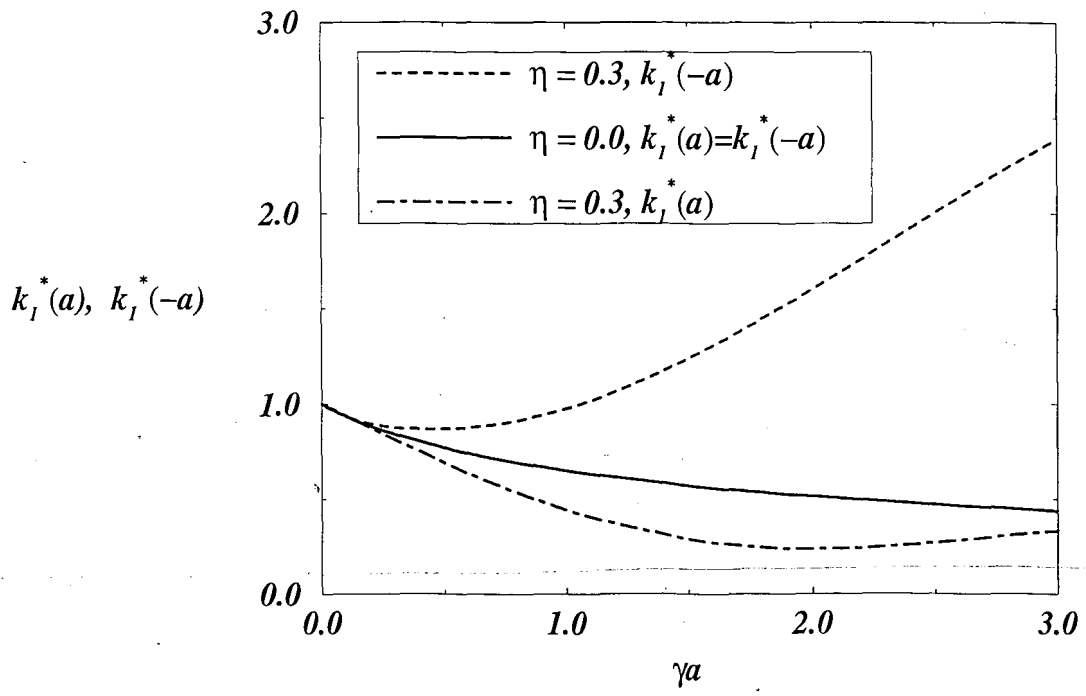


Figure 4.10: Variation of stress intensity factors with the non-homogeneity parameter,  $k_I^*(a) = \frac{k_1(a)}{Pa^\beta/\theta_0}$ ,  $k_I^*(-a) = \frac{k_1(-a)}{Pa^\alpha/\theta_0}$

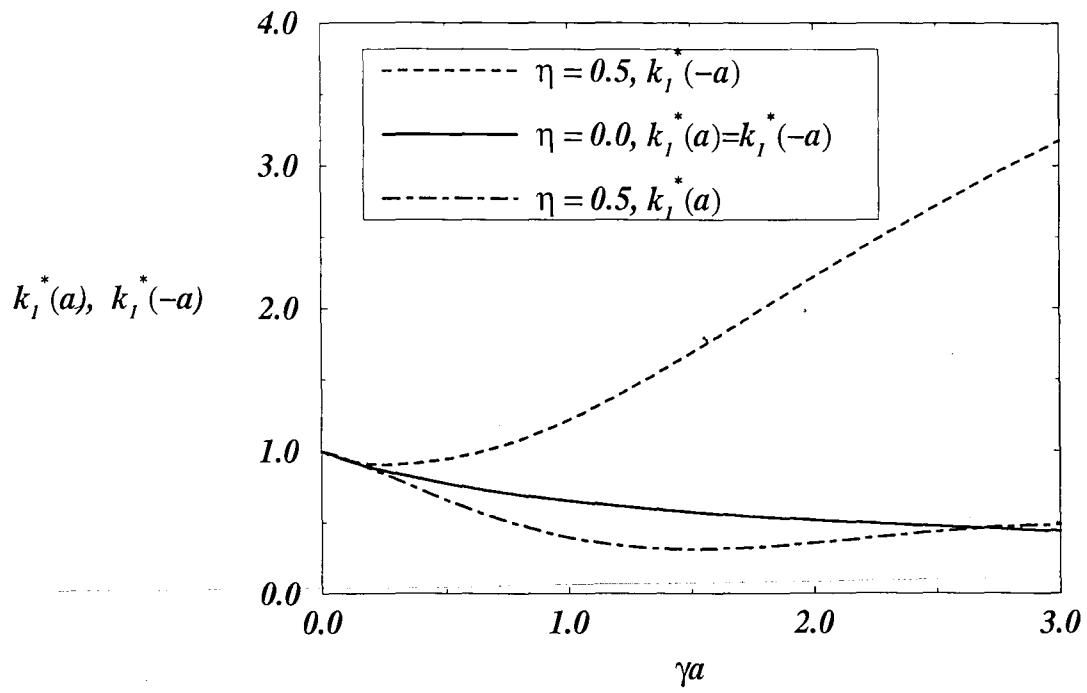


Figure 4.11: Variation of stress intensity factors with the non-homogeneity parameter,  $k_I^*(a) = \frac{k_1(a)}{Pa^\beta/\theta_0}$ ,  $k_I^*(-a) = \frac{k_1(-a)}{Pa^\alpha/\theta_0}$

## 4.2 Triangular Punch

For a triangular punch shown in Fig. (4.12), the punch profile is given as

$$v(x, 0) = -mx + C. \quad (4.49)$$

Differentiating (4.49) with respect to  $x$ , the input function  $f(x)$  in equation (3.5) for the triangular punch becomes

$$f(x) = \frac{4\mu}{\kappa + 1} \frac{\partial}{\partial x} v(x, 0) = -m. \quad (4.50)$$

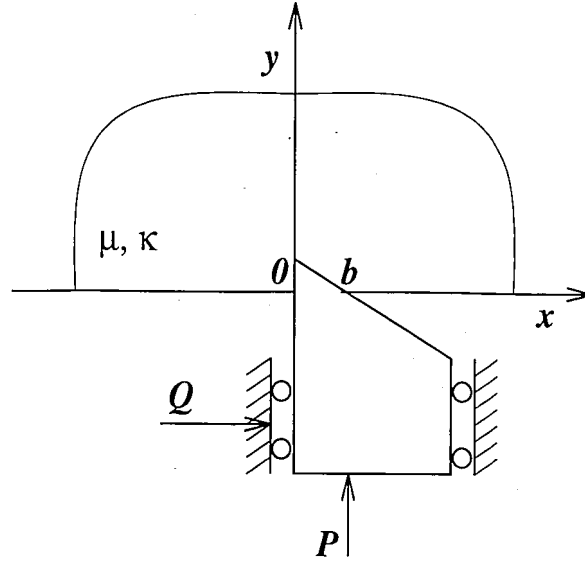


Figure 4.12: Geometry of triangular punch

### 4.2.1 Solution for Homogeneous Materials

The integral equation given in equation (4.3) is still valid. Thus by letting

$$\sigma_{yy}(x, 0) = -p(x), \quad \sigma_{xy}(x, 0) = -\eta p(x), \quad 0 < x < b, \quad (4.51)$$

$$\sigma_{yy}(x, 0) = \sigma_{xy}(x, 0) = 0, \quad x < 0, \quad x > b. \quad (4.52)$$

equation (4.3) becomes

$$Ap(x) + \frac{1}{\pi} \int_0^b \frac{p(t)dt}{(t-x)} = \frac{4\mu_0}{\kappa+1} \frac{\partial}{\partial x} v(x,0), \quad 0 < x < b. \quad (4.53)$$

Also, equilibrium equation may be expressed as

$$\int_0^b p(t)dt = P. \quad (4.54)$$

In order to solve the integral equation the limits of integration have to be normalized.

Now setting  $d = b$ , and  $c = 0$ , equations (3.8) to (3.12) becomes

$$t = \frac{b}{2}(s+1), \quad -1 < s < 1, \quad (4.55)$$

$$x = \frac{b}{2}(r+1), \quad -1 < r < 1, \quad (4.56)$$

$$\sigma_0 = \frac{P}{b}. \quad (4.57)$$

Again substituting

$$p(t) = 2\sigma_0\phi(s). \quad (4.58)$$

one obtains

$$A\phi(r) + \frac{1}{\pi} \int_{-1}^1 \frac{\phi(s)ds}{s-r} = -\frac{2\mu_0}{\kappa+1} \frac{m}{\sigma_0}, \quad -1 < r < 1, \quad (4.59)$$

$$\int_{-1}^1 \phi(s)ds = 1. \quad (4.60)$$

Since  $p(x)$  has an integrable singularity at  $x = 0$ , and is bounded at  $x = b$ , from the physics of the problem we must require that  $\alpha$  be positive and  $\beta$  be negative.

Therefore, from equation (3.33) the index of the problem becomes

$$\kappa_0 = -(N+M) = -(1-1) = 0. \quad (4.61)$$

Now assuming a solution of the form

$$\phi(s) = \frac{2\mu_0}{\kappa+1} \frac{m}{\sigma_0} \sum_0^\infty c_n w(s) P_n^{(\alpha,\beta)}(t), \quad (4.62)$$

solution of (4.59) becomes

$$\sum_0^N c_n \left[ -\frac{1}{\sin \pi \alpha} P_n^{(-\alpha,-\beta)}(r) \right] = -1. \quad (4.63)$$

By expanding the right hand side of (4.63) into a series of Jacobi polynomials, it can be shown that  $c_0$  is the only nonzero coefficient which becomes

$$c_0 = \sin \pi \alpha.$$

Thus, by substituting  $\phi(s)$  into equation (4.60) and using orthogonality of Jacobi Polynomials given by equation (3.49), the unknown  $b$  can be found from

$$\frac{2\mu_0}{\kappa+1} \frac{m}{\sigma_0} c_0 \theta_0 = P_0^{(\alpha,\beta)}(r) = 1, \quad (4.64)$$

where, in this case  $\alpha + \beta = 0$ , and  $\theta_0$  is given by

$$\theta_0 = \frac{2\pi\alpha}{\sin \pi\alpha}, \quad (4.65)$$

$$c_0 \theta_0 = 2\pi\alpha. \quad (4.66)$$

Substituting  $\sigma_0$  from (4.57) into (4.64), we find

$$b = \frac{\kappa+1}{4\mu_0 m \pi \alpha} P. \quad (4.67)$$

Also, from (4.64) and (4.66) we have

$$\frac{2\mu_0}{\kappa+1} \frac{m}{\sigma_0} = \frac{1}{c_0 \theta_0} = \frac{1}{2\pi\alpha}. \quad (4.68)$$

Observing that  $\beta = -\alpha$ , the solution is found to be

$$\begin{aligned} p(x) &= 2\sigma_0 \phi(x), \\ &= \frac{2P}{b\theta_0} \left( \frac{b-x}{x} \right)^\alpha. \end{aligned} \quad (4.69)$$

Then from equation (4.4) it follows that

$$\sigma_{yy}(x, 0) = -\frac{2P}{b\theta_0} \left( \frac{b-x}{x} \right)^\alpha, \quad (4.70)$$

or in normalized form

$$\frac{\sigma_{yy}(x, 0)}{P/b} = -\frac{2}{\theta_0} \left( \frac{b-x}{x} \right)^\alpha. \quad (4.71)$$

## Stress intensity factor for the homogeneous medium

The stress intensity factor is defined by

$$k_1(0) = \lim_{x \rightarrow 0} 2^\alpha x^\alpha p(x) = \frac{2^{\alpha+1}}{\theta_0} P b^{\alpha-1}. \quad (4.72)$$

For the homogeneous case  $\alpha = 1/2$  and (4.72) becomes

$$k_1(0) = 2\sqrt{2} \frac{P}{\pi\sqrt{b}}. \quad (4.73)$$

### 4.2.2 Solution for Graded Materials

Consider the punch problem shown in Fig. (4.12) for a non-homogeneous medium. Let  $\mu$  be the shear modulus varying exponentially in  $y$  direction. Using equations (4.4) and (4.5) equation (2.75) becomes

$$Ap(x) + \frac{1}{\pi} \int_0^b \frac{p(t)dt}{(t-x)} - \int_0^b (J_1(t, x) + \eta J_2(t, x)) p(t)dt = f(x), \quad 0 < x < b \quad (4.74)$$

where

$$f(x) = \frac{4\mu_0}{\kappa+1} \frac{\partial}{\partial x} v(x, 0) = -\frac{4\mu_0}{\kappa+1} m. \quad (4.75)$$

Using equations (4.9) and (4.12) and defining

$$\gamma^* = \frac{b}{2} \gamma, \quad (4.76)$$

$$J_1(t, x) = J_1^*(s, r), \quad (4.77)$$

$$J_2(t, x) = J_2^*(s, r), \quad (4.78)$$

we obtain

$$A\phi(r) + \frac{1}{\pi} \int_{-1}^1 \frac{\phi(s)ds}{s-r} - \int_{-1}^1 (J_1^*(s, r) + \eta J_2^*(s, r)) \phi(s)ds = -\frac{4\mu_0}{\kappa+1} m, \quad (4.79)$$

$$\int_{-1}^1 \phi(s)ds = 1. \quad (4.80)$$



As in the homogeneous half space, in this case too,  $\kappa_0$  becomes 0. Assuming a solution of the form (4.62), equation (4.79) becomes

$$\sum_0^N c_n \left[ -\frac{1}{\sin \pi \alpha} P_n^{(-\alpha, -\beta)}(r) + h_n^1(r) + h_n^2(r) \right] = -1. \quad (4.81)$$

By using a method of collocation, equation (4.81) provides  $N+1$  equations for  $N+1$  unknown constants,  $c_0, \dots, c_N$  as follows:

$$\sum_0^N c_n F_n(r_i) = -1, \quad i = 1, \dots, N+1, \quad (4.82)$$

$$F_n(r_i) = -2^{-1} \frac{1}{\sin \pi \alpha} P_n^{(-\alpha, -\beta)}(r_i) + h_n^1(r_i) + h_n^2(r_i), \quad (4.83)$$

where  $r_i$  ( $i = 1, \dots, N+1$ ) are defined by

$$P_n^{(\alpha-1, \beta+1)}(r_i) = 0. \quad (4.84)$$

Substituting  $\phi(s)$  into equation (4.80) and using orthogonality of Jacobi Polynomials given by equation (3.49), the unknown  $b$  can be found as

$$b = \frac{\kappa + 1}{2\mu_0 m c_0 \theta_0} P. \quad (4.85)$$

Normalizing (4.85) we have

$$b^* = \frac{\mu_0 m}{P} b = \frac{\kappa + 1}{2c_0 \theta_0}.$$

The solution then becomes

$$\begin{aligned} p(r) &= 2\sigma_0 \phi(r) \\ &= \frac{2P}{bc_0 \theta_0} \left( \frac{1-r}{1+r} \right)^\alpha \sum_0^N c_n P_n^{(\alpha, \beta)}(r). \end{aligned} \quad (4.86)$$

From equation (4.4) it follows that

$$\sigma_{yy}(x, 0) = -\frac{2P}{bc_0 \theta_0} \left( \frac{b-x}{x} \right)^\alpha \sum_0^N c_n P_n^{(\alpha, \beta)}(2x/b - 1). \quad (4.87)$$

or in normalized form

$$\frac{\sigma_{yy}(x, 0)}{P/b} = -\frac{2}{c_0\theta_0} \left(\frac{b-x}{x}\right)^\alpha \sum_0^N c_n P_n^{(\alpha, \beta)}(2x/b - 1). \quad (4.88)$$

Referring to (3.5), (3.6), (3.23) and (3.34)-(3.36) for the triangular punch shown in Fig.4.12, the powers  $\alpha$  and  $\beta$  of the stress singularity may be expressed as follows:

$$\eta = 0 : \quad \alpha = 0.5, \quad \beta = -0.5, \quad (4.89)$$

$$\eta > 0 : \quad \alpha = 1 - \frac{\theta}{\pi}, \quad \beta = \frac{\theta}{\pi} - 1, \quad \theta = \arctan \frac{\kappa + 1}{\eta(\kappa - 1)} > 0 \quad (4.90)$$

$$\eta < 0 : \quad \alpha = -\frac{\theta}{\pi}, \quad \beta = \frac{\theta}{\pi}, \quad \theta = \arctan \frac{\kappa + 1}{\eta(\kappa - 1)} < 0, \quad (4.91)$$

where  $\eta > 0$  and  $\eta < 0$  corresponds to the directions of tangential force  $Q$  shown in Figures 4.14-4.16 and Figures 4.17-4.19, respectively. Again, note that  $\alpha$  and  $\beta$  are associated respectively with the end points  $x = d$  and  $x = c$  shown in 3.1 or  $x = b$  and  $x = 0$  shown in Fig.4.12. The calculated values of  $\alpha$  and  $\beta$  for the friction coefficients considered are given in Table 4.1.

Fig. 4.13 gives the stress distribution under a triangular punch for various values of the material non-homogeneity parameter,  $\gamma$ , for the case of no friction. The stress is bounded at  $x = b$  and is zero. On the other hand, it is unbounded at the sharp edge at  $x = 0$ . When the non-homogeneity parameter is very small, the solution for non-homogeneous medium reduces to the homogeneous solution. All of the curves intersect at a point near the sharp edge and change trend. Figures 4.14 to 4.19 gives the stress distribution under a triangular punch for various values of the material non-homogeneity parameter,  $\gamma$  and for various values of the friction coefficient.

### Stress intensity factor

Mode  $I$  stress intensity factor at the sharp end  $x = 0$  of the punch is defined as

$$k_1(0) = \lim_{x \rightarrow 0} 2^\alpha x^\alpha p(x) = \frac{2^{\alpha+1} P b^{\alpha-1}}{c_0 \theta_0} \sum_0^N c_n P_n^{(\alpha, \beta)}(-1). \quad (4.92)$$

The normalized stress intensity factor may then be expressed as follows:

$$k_1^*(0) = \frac{\theta_0}{2^{\alpha+1}} \frac{k_1(0)}{P b^{\alpha-1}} = \frac{1}{c_0} \sum_0^N c_n P_n^{(\alpha, \beta)}(-1)$$

Tables 4.2 and 4.3 give the normalized stress intensity factors at the sharp end of the triangular punch according to the direction of application of the force  $Q$  by assuming  $\nu = 0.3$ . Note that for  $\gamma \rightarrow 0$ , as expected, the stress intensity factor ratios reduce to those of a homogeneous medium. These data are plotted in Figures 4.20 and 4.21. The interesting result to note here is that although in the absence of friction stress intensity factor decreases with increasing  $\gamma$ , in the presence of friction stress intensity factor increases. Furthermore, the trend of the curves changes as the direction of the application of the force  $Q$  is reversed.

Since the non-dimensional stress intensity factor is a function of the first coefficient,  $c_0$  in the Jacobi series expansion, we need to investigate the behavior of  $c_0$  which is a function of  $\gamma$  and  $\eta$ . Variation of  $c_0$  with respect to  $\gamma$  and  $\eta$  are tabulated in Tables 4.4 and 4.5. For frictionless case  $c_0$  linearly increases with increasing  $\gamma b$ . On the other hand  $c_0$  decreases, for frictional case, with increasing  $\gamma b$ .

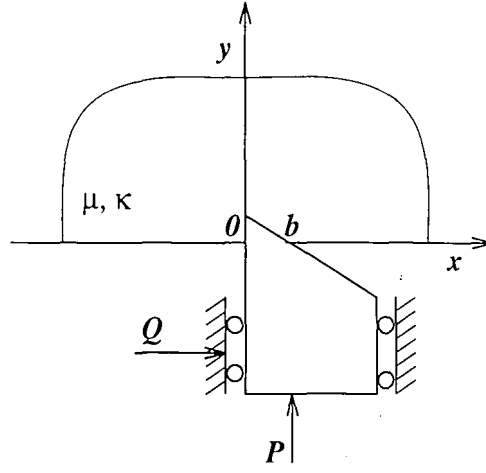


Table 4.2: Stress intensity factors for triangular punch,  $\theta_0 = \frac{2\pi\alpha}{\sin \pi\alpha}$

	$\eta = 0.0$	$\eta = 0.1$	$\eta = 0.3$	$\eta = 0.5$
	$\alpha = +0.5$ $\beta = -0.5$	$\alpha = +0.5091$ $\beta = -0.5091$	$\alpha = +0.5272$ $\beta = -0.5272$	$\alpha = +0.5452$ $\beta = -0.5452$
$\gamma$	$\frac{\theta_0}{2\alpha+1} \frac{k_1(0)}{Pb^{\alpha-1}}$	$\frac{\theta_0}{2\alpha+1} \frac{k_1(0)}{Pb^{\alpha-1}}$	$\frac{\theta_0}{2\alpha+1} \frac{k_1(0)}{Pb^{\alpha-1}}$	$\frac{\theta_0}{2\alpha+1} \frac{k_1(0)}{Pb^{\alpha-1}}$
0.0	1.0000	1.0000	1.0000	1.0000
0.2	0.9350	1.0166	1.0225	1.0286
0.4	0.8834	1.0508	1.0637	1.0775
0.6	0.8400	1.0974	1.1193	1.1427
0.8	0.8024	1.1544	1.1874	1.2231
1.0	0.7694	1.2206	1.2673	1.3185
1.2	0.7401	1.2951	1.3589	1.4295
1.4	0.7138	1.3775	1.4622	1.5570

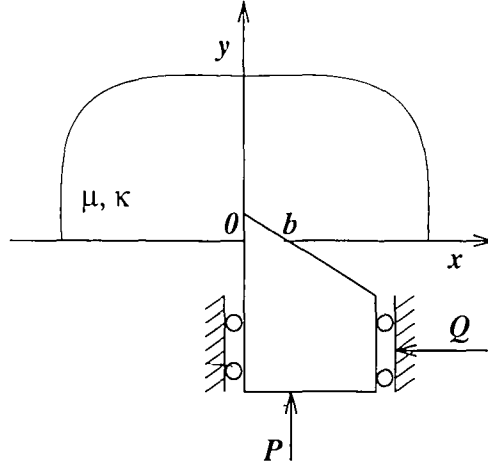


Table 4.3: Stress intensity factors for triangular punch,  $\theta_0 = \frac{2\pi\alpha}{\sin \pi\alpha}$

	$\eta = 0.0$	$\eta = -0.1$	$\eta = -0.3$	$\eta = -0.5$
	$\alpha = +0.5$ $\beta = -0.5$	$\alpha = +0.4909$ $\beta = -0.4909$	$\alpha = +0.4728$ $\beta = -0.4728$	$\alpha = +0.4548$ $\beta = -0.4548$
$\gamma$	$\frac{\theta_0}{2^{\alpha+1}} \frac{k_1(0)}{Pb^{\alpha-1}}$	$\frac{\theta_0}{2^{\alpha+1}} \frac{k_1(0)}{Pb^{\alpha-1}}$	$\frac{\theta_0}{2^{\alpha+1}} \frac{k_1(0)}{Pb^{\alpha-1}}$	$\frac{\theta_0}{2^{\alpha+1}} \frac{k_1(0)}{Pb^{\alpha-1}}$
0.0	1.0000	1.0000	1.0000	1.0000
0.2	0.9350	1.0112	1.0063	1.0019
0.4	0.8834	1.0389	1.0282	1.0188
0.6	0.8340	1.0776	1.0600	1.0448
0.8	0.8024	1.1249	1.0991	1.0773
1.0	0.7694	1.1792	1.1438	1.1143
1.2	0.7401	1.2395	1.1927	1.1546
1.4	0.7138	1.3048	1.2449	1.1970

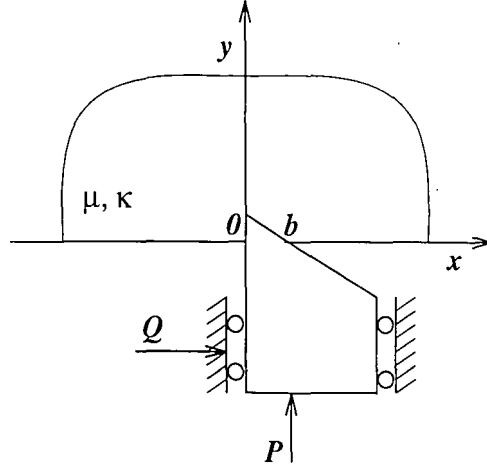


Table 4.4: The first coefficient of the Jacobi series ,  $c_0$  for triangular punch

	$\eta = 0.0$	$\eta = 0.1$	$\eta = 0.3$	$\eta = 0.5$
	$\alpha = +0.5$ $\beta = -0.5$	$\alpha = +0.5091$ $\beta = -0.5091$	$\alpha = +0.5272$ $\beta = -0.5272$	$\alpha = +0.5452$ $\beta = -0.5452$
$\gamma$	$c_0$	$c_0$	$c_0$	$c_0$
0.0	1.0000	0.9996	0.9963	0.9899
0.2	1.1444	0.9652	0.9440	0.9189
0.4	1.2828	0.9123	0.8856	0.8546
0.6	1.4197	0.8529	0.8238	0.7900
0.8	1.5565	0.7931	0.7628	0.7274
1.0	1.6937	0.7362	0.7049	0.6682
1.2	1.8316	0.6833	0.6511	0.6130
1.4	1.9703	0.6350	0.6016	0.5620

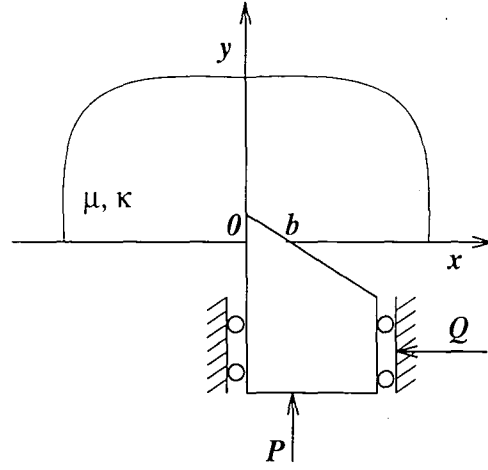


Table 4.5: The first coefficient of the Jacobi series ,  $c_0$  for triangular punch

	$\eta = 0.0$	$\eta = -0.1$	$\eta = -0.3$	$\eta = -0.5$
	$\alpha = +0.5$ $\beta = -0.5$	$\alpha = +0.4909$ $\beta = -.4909$	$\alpha = +0.4728$ $\beta = -0.4728$	$\alpha = +0.4548$ $\beta = -0.4548$
$\gamma$	$c_0$	$c_0$	$c_0$	$c_0$
0.0	1.0000	.9996	.9963	.9899
0.2	1.1444	.9819	.9940	1.0013
0.4	1.2828	.9341	.9507	.9619
0.6	1.4197	.8766	.8946	.9067
0.8	1.5565	.8176	.8357	.8475
1.0	1.6937	.7610	.7789	.7899
1.2	1.8316	.7085	.7260	.7363
1.4	1.9703	.6606	.6780	.6876

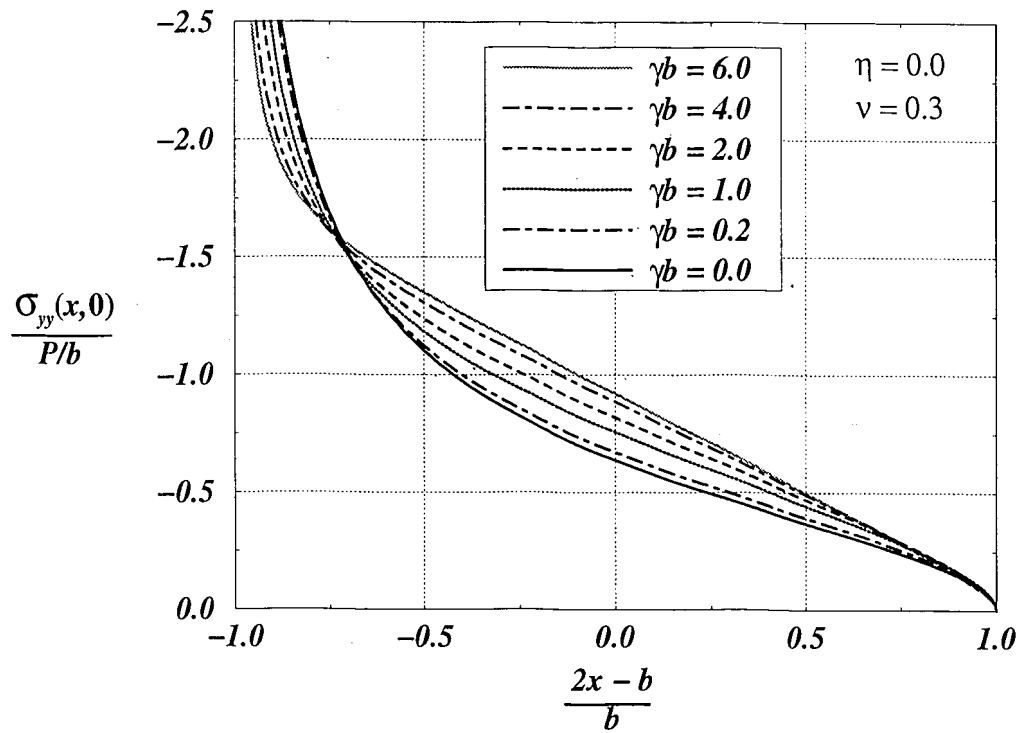
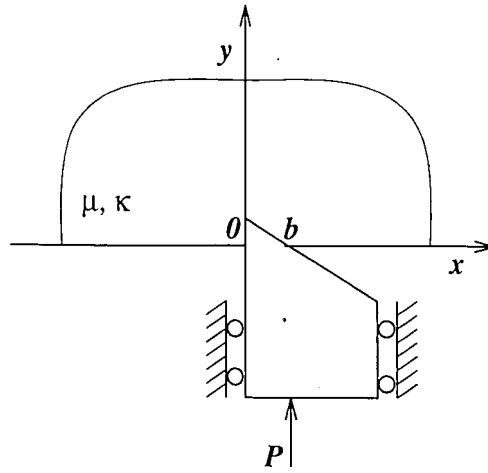


Figure 4.13: Stress distribution under a triangular punch for various values of the material non-homogeneity parameter,  $\gamma$ , when friction is not present,  $\alpha = 0.5$ ,  $\beta = -0.5$



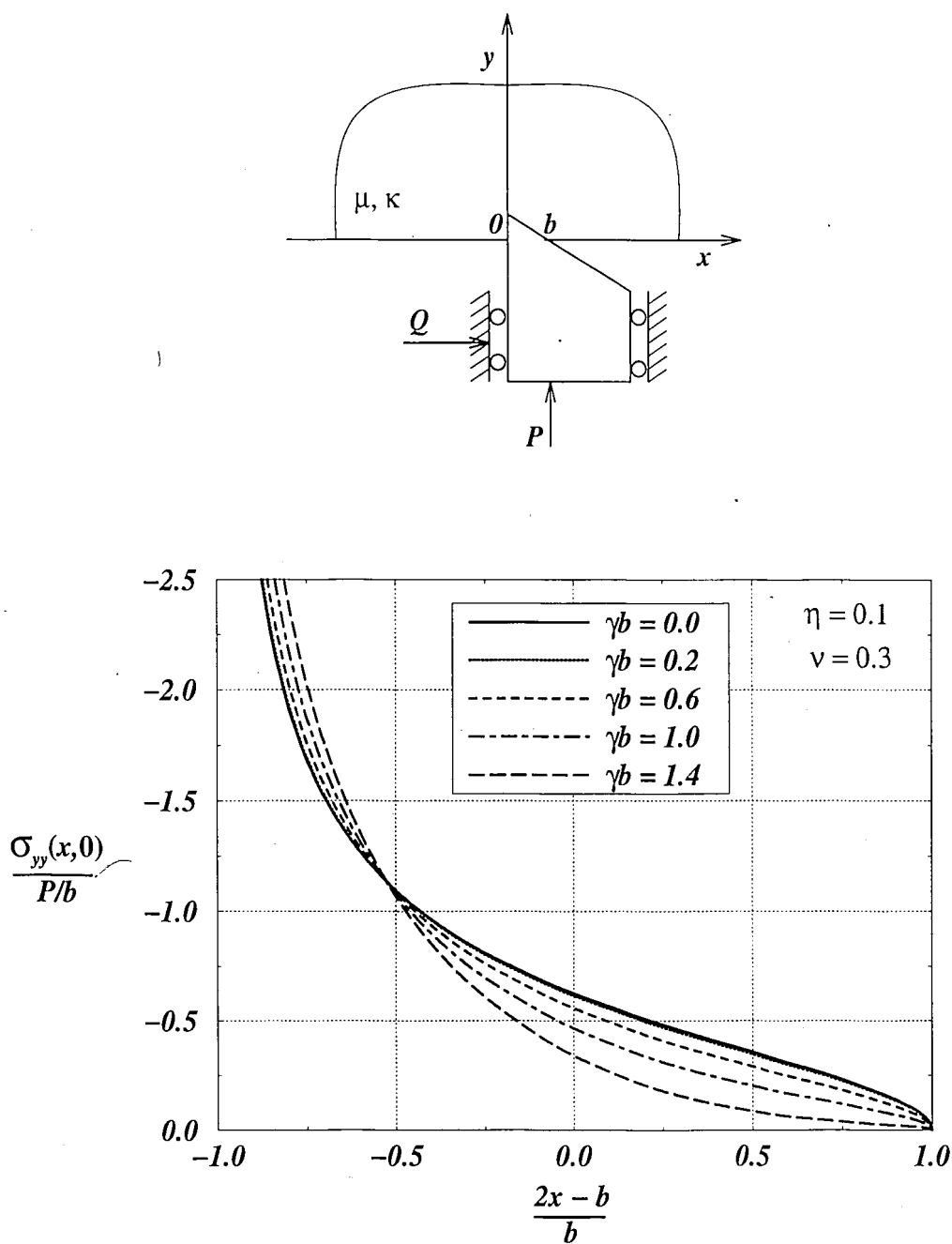


Figure 4.14: Stress distribution under a triangular punch for various values of the material non-homogeneity parameter,  $\gamma$ , in the presence of friction,  $\eta = 0.1$ ,  $\alpha = 0.5091$ ,  $\beta = -0.5091$ .

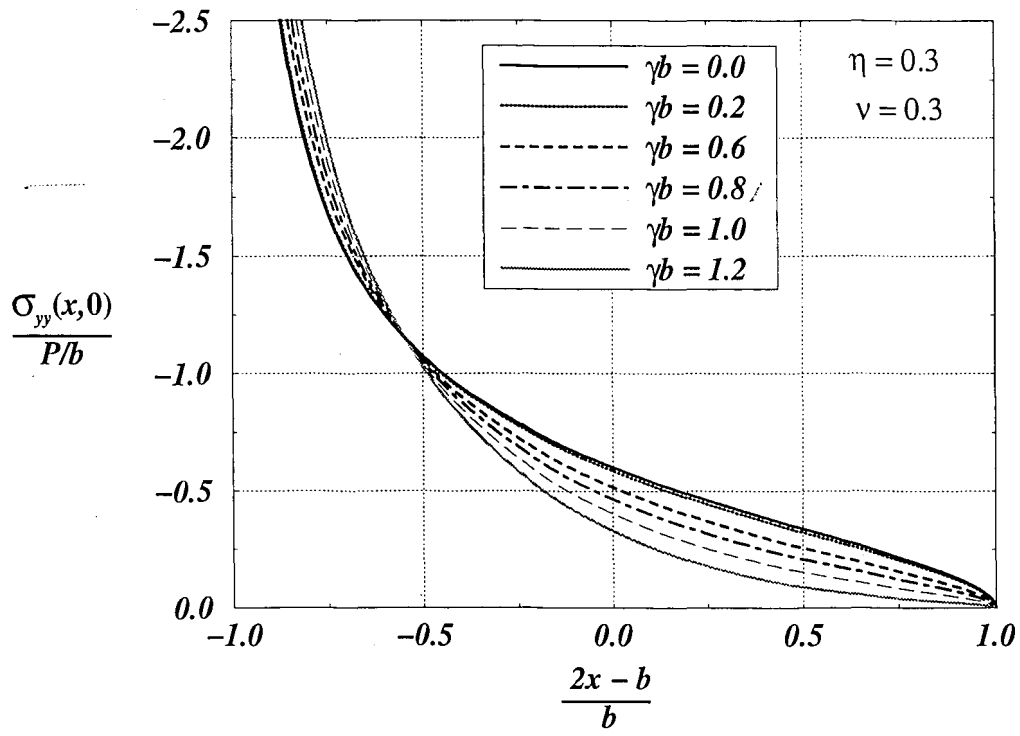
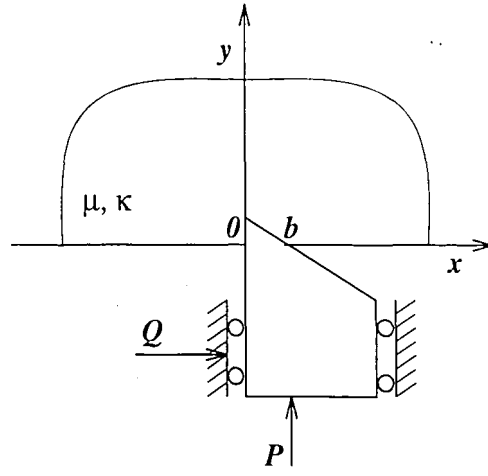


Figure 4.15: Stress distribution under a triangular punch for various values of the material non-homogeneity parameter,  $\gamma$ , in the presence of friction,  $\eta = 0.3$ ,  $\alpha = 0.5272$ ,  $\beta = -0.5272$ .

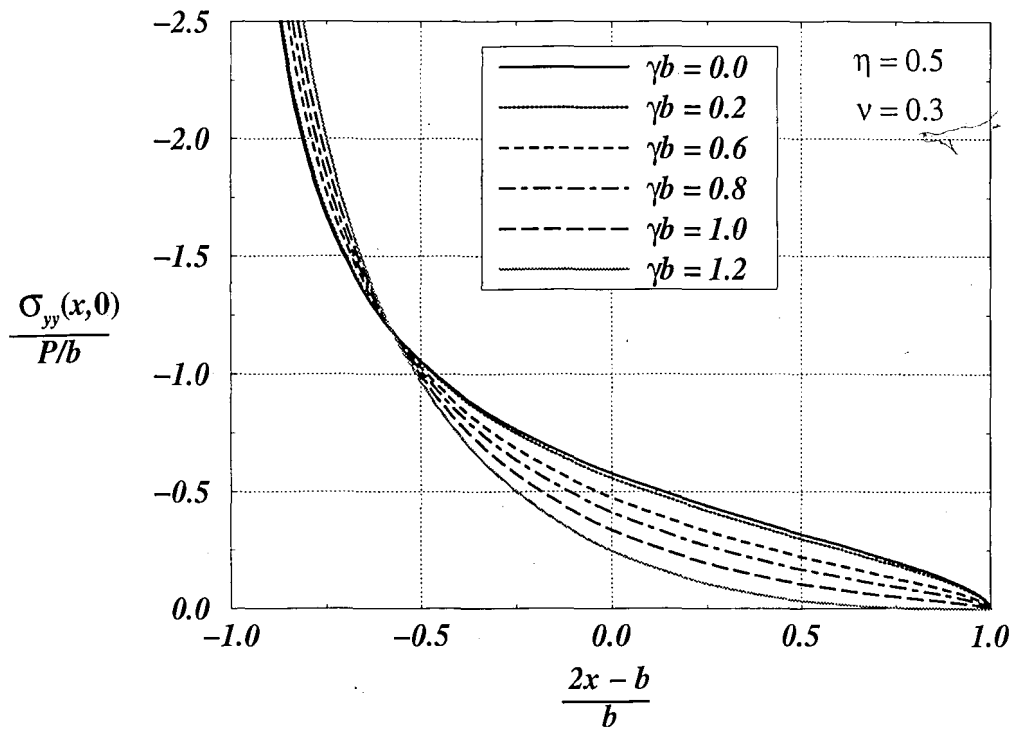
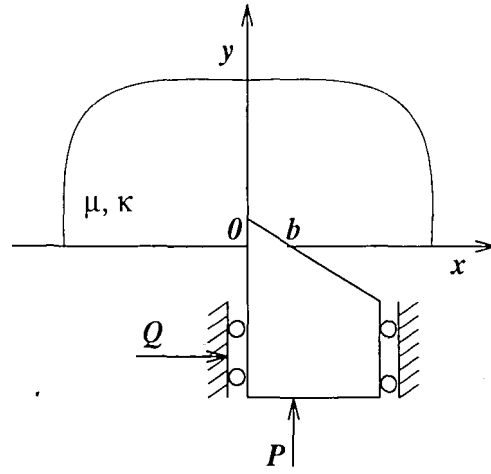


Figure 4.16: Stress distribution under a triangular punch for various values of the material non-homogeneity parameter,  $\gamma$ , in the presence of friction,  $\eta = 0.5$ ,  $\alpha = 0.5452$ ,  $\beta = -0.5452$ .

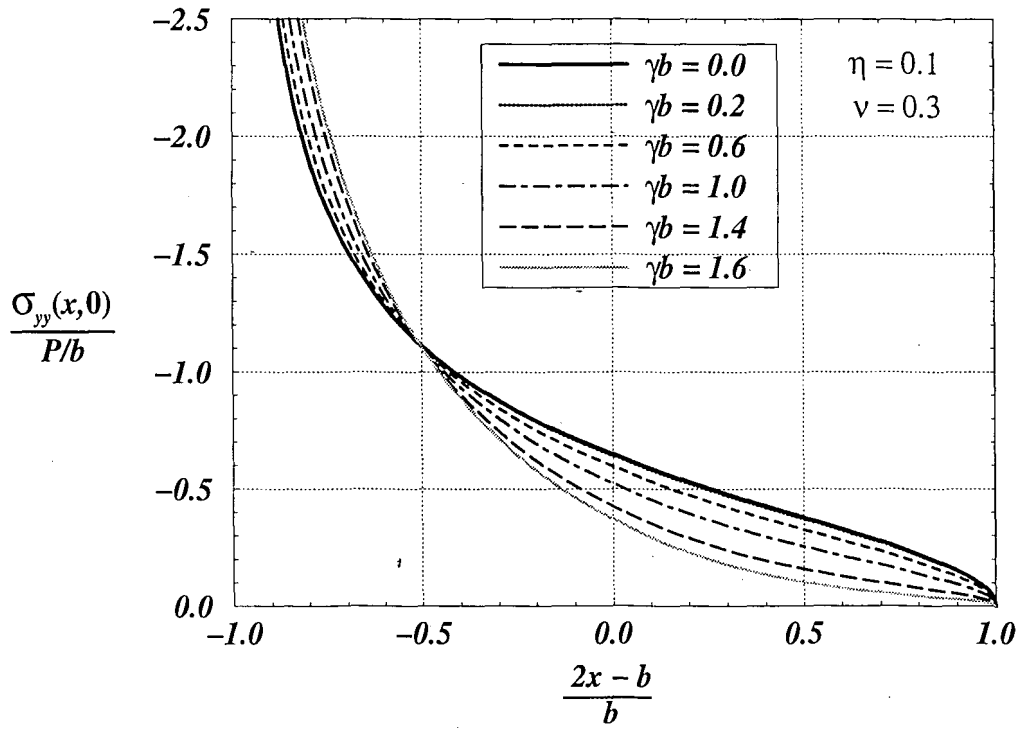
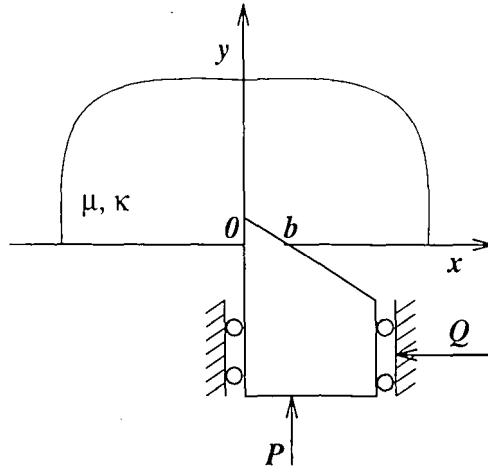


Figure 4.17: Stress distribution under a triangular punch for various values of the material non-homogeneity parameter,  $\gamma$ , in the presence of friction,  $\eta = -0.1$ ,  $\alpha = 0.4909$ ,  $\beta = -0.4909$ .

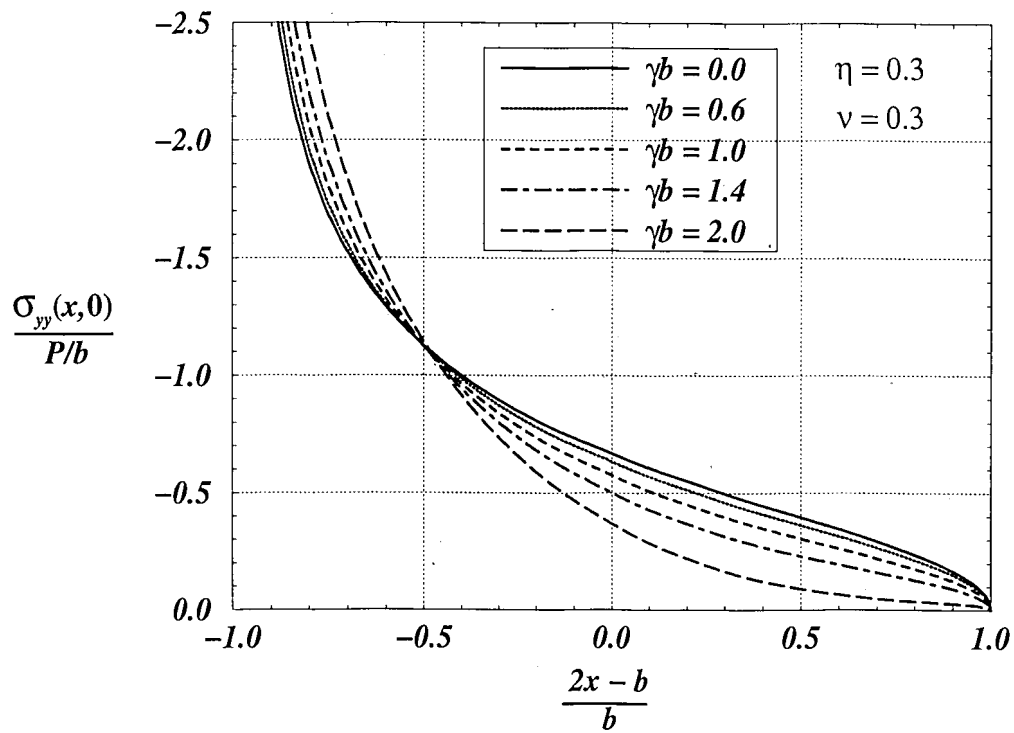
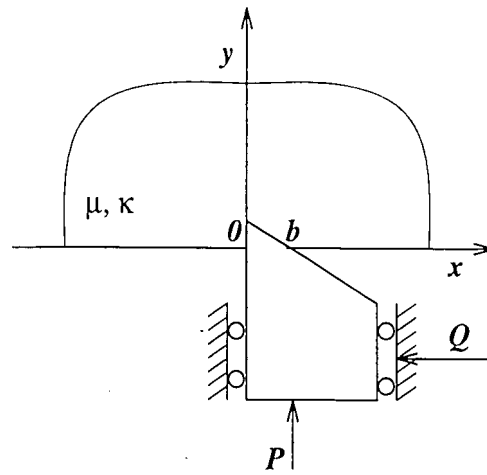


Figure 4.18: Stress distribution under a triangular punch for various values of the material non-homogeneity parameter,  $\gamma$ , in the presence of friction,  $\eta = -0.3$ ,  $\alpha = 0.4728$ ,  $\beta = -0.4728$ .

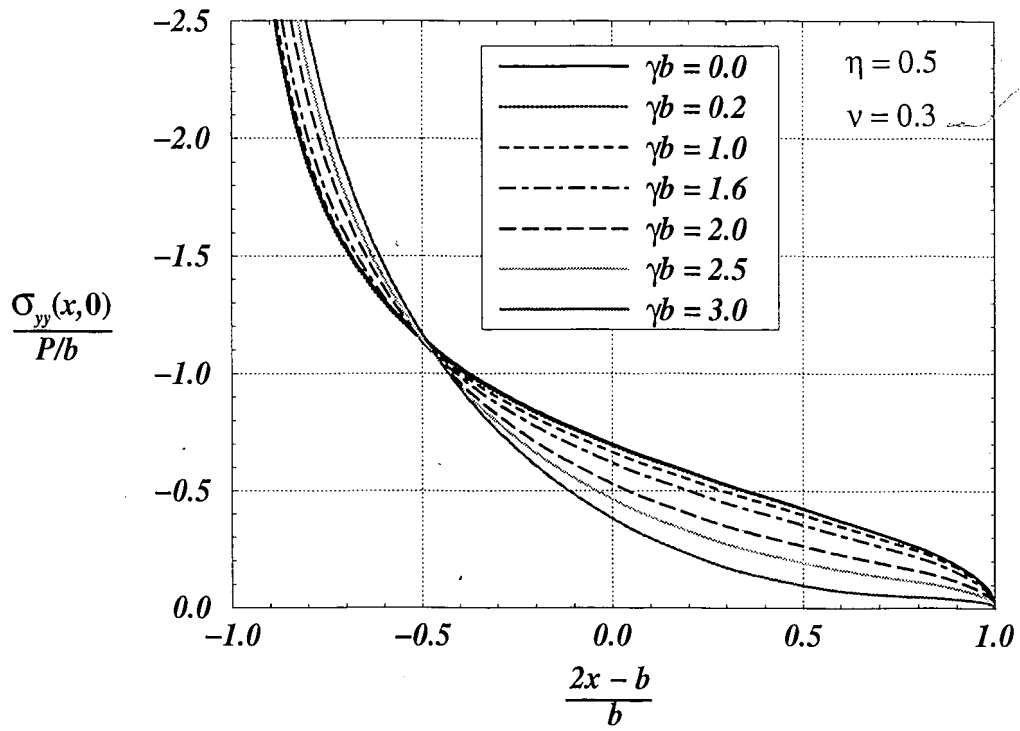
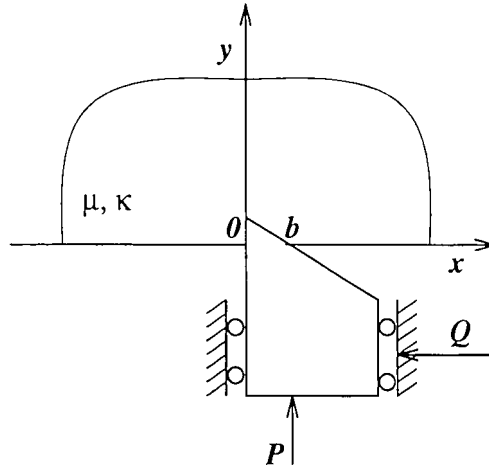


Figure 4.19: Stress distribution under a triangular punch for various values of the material non-homogeneity parameter,  $\gamma$ , in the presence of friction,  $\eta = -0.5$ ,  $\alpha = 0.4548$ ,  $\beta = -0.4548$ .

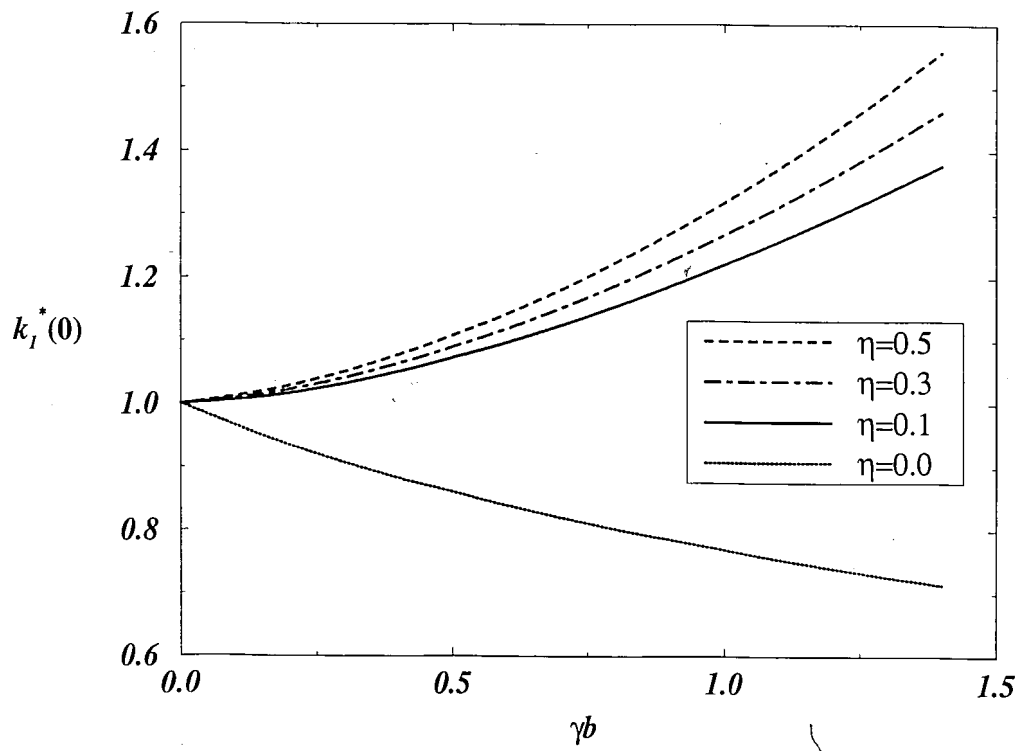
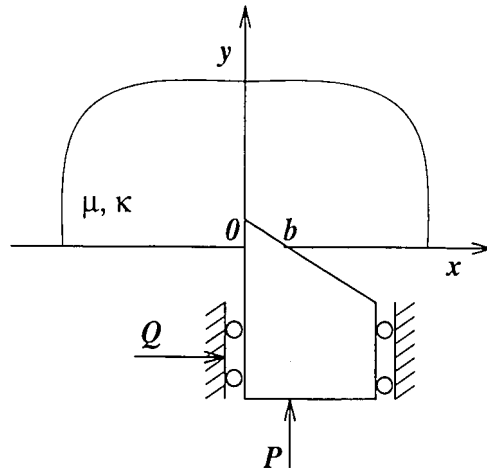


Figure 4.20: Variation of stress intensity factor for the triangular punch with the non homogeneity parameter,  $\gamma$ ,  $k_1^* = \frac{\theta_0}{2\alpha+1} \frac{k_1(0)}{Pb^{\alpha-1}}$

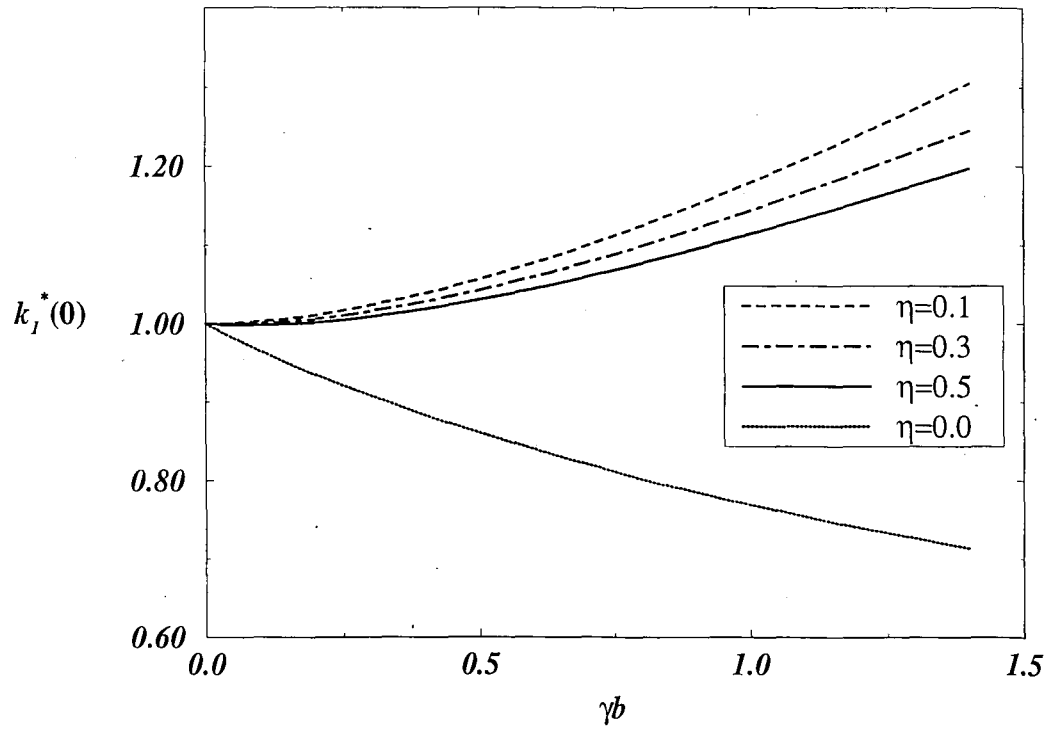
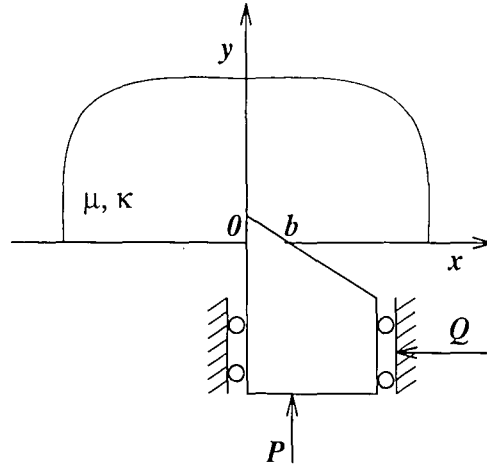


Figure 4.21: Variation of stress intensity factor for the triangular punch with the non homogeneity parameter  $\gamma$ ,  $k_I^* = \frac{\theta_0}{2\alpha+1} \frac{k_1(0)}{Pb^{\alpha-1}}$ .



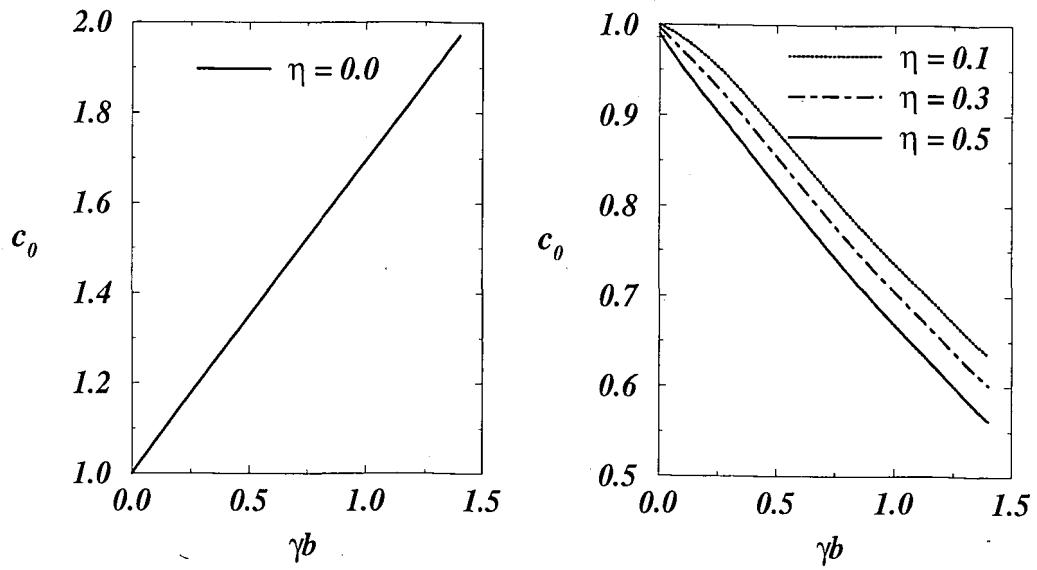
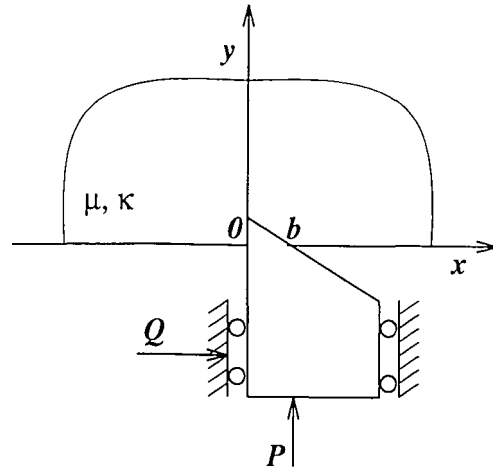


Figure 4.22: Variation of  $c_0$  for the triangular punch with the non homogeneity parameter,  $\gamma$ .

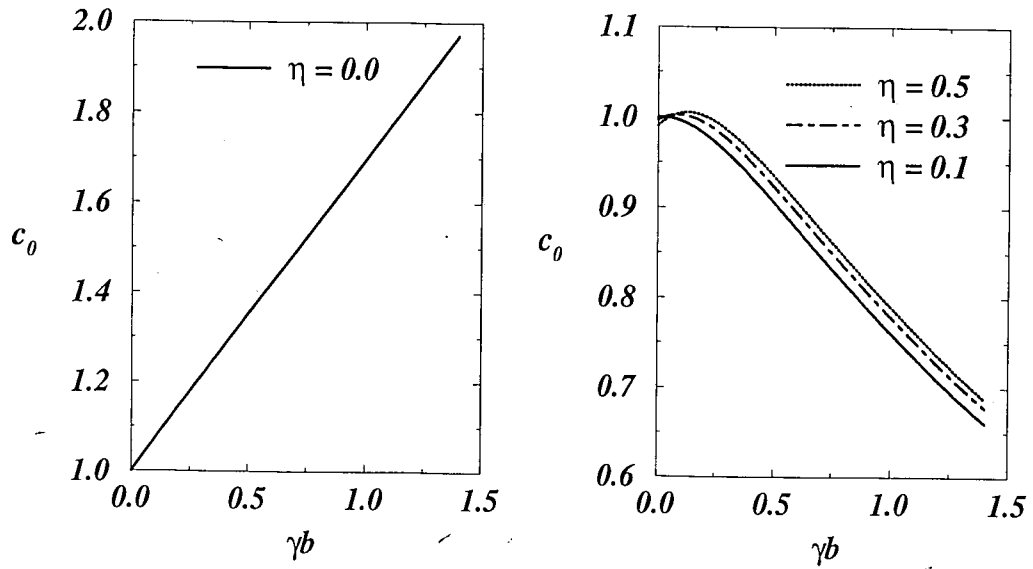
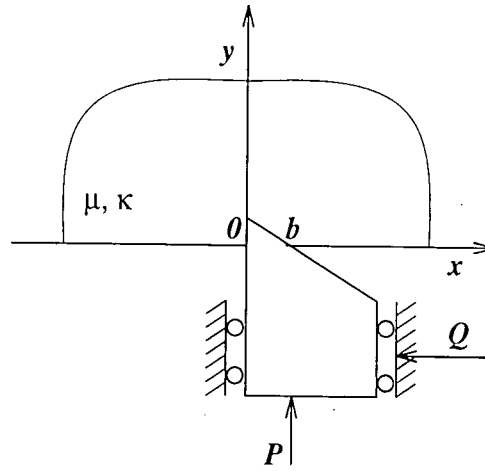


Figure 4.23: Variation of  $c_0$  for the triangular punch with the non homogeneity parameter,  $\gamma$ .

### 4.3 Semi Circular Punch

The profile for semi-circular punch is shown in Fig. 4.24. For  $b \ll R$ , the semicircular punch profile may be approximated by a parabola, where  $R$  is the radius of the circle. Therefore the displacement in  $y$  direction becomes

$$v(x, 0) = -\frac{x^2}{2R} + C.$$

giving

$$\frac{\partial}{\partial x}v(x, 0) = -\frac{x}{R}.$$

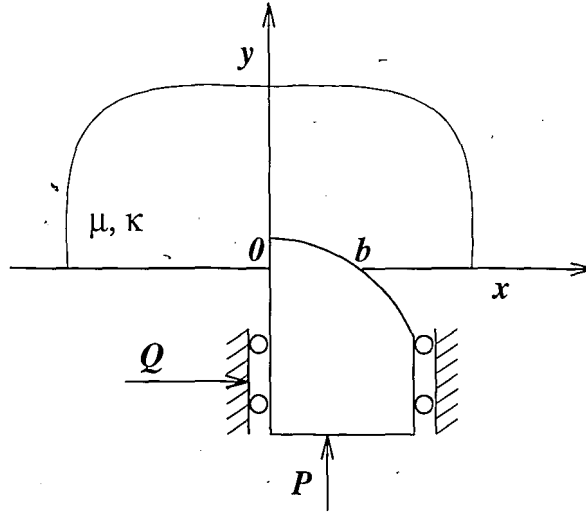


Figure 4.24: Geometry of semi-circular punch

#### 4.3.1 Solution for Homogeneous Materials

Integral equation is given by (4.3). Thus, if we define

$$\sigma_{yy}(x, 0) = -p(x), \quad \sigma_{xy}(x, 0) = -\eta p(x), \quad 0 < x < b, \quad (4.93)$$

$$\sigma_{yy}(x, 0) = \sigma_{xy}(x, 0) = 0, \quad x < 0, \quad x > b. \quad (4.94)$$

equation (4.3) becomes

$$Ap(x) + \frac{1}{\pi} \int_0^b \frac{p(t)dt}{(t-x)} = \frac{4\mu_0}{\kappa+1} \frac{\partial}{\partial x}v(x, 0), \quad 0 < x < b. \quad (4.95)$$

Again, the equilibrium equation may be expressed as

$$\int_0^b p(t)dt = P. \quad (4.96)$$

In order to solve the integral equation the limits of integration have to be normalized. Thus, setting  $d = b$ , and  $c = 0$ , equations (3.8) to (3.12) becomes

$$t = \frac{b}{2}(s+1), \quad -1 < s < 1 \quad (4.97)$$

$$x = \frac{b}{2}(r+1), \quad -1 < r < 1 \quad (4.98)$$

$$\sigma_0 = \frac{P}{b}. \quad (4.99)$$

Also, letting

$$p(t) = 2\sigma_0\phi(s) \quad (4.100)$$

one obtains

$$A\phi(r) + \frac{1}{\pi} \int_{-1}^1 \frac{\phi(s)ds}{s-r} = -\frac{\mu_0}{\kappa+1} \frac{b}{\sigma_0 R}(r+1), \quad -1 < r < 1 \quad (4.101)$$

$$\int_{-1}^1 \phi(s)ds = 1. \quad (4.102)$$

Since  $p(x)$  has an integrable singularity at  $x = 0$ , and bounded at  $x = b$ , from the physics of the problem we must require that  $\alpha$  be positive and  $\beta$  negative. Therefore in equation (3.34) and (3.35) it may be seen that we have  $N = 1$  and  $M = -1$ . From equation (3.33) the index of the problem becomes

$$\kappa_0 = -(N + M) = -(1 - 1) = 0. \quad (4.103)$$

Now assuming a solution of the form

$$\phi(s) = \frac{\mu_0}{\kappa+1} \frac{b}{\sigma_0 R} \sum_0^\infty c_n w(s) P_n^{(\alpha, \beta)}(t). \quad (4.104)$$

the solution of (4.102) may be expressed as

$$\sum_0^N c_n \left[ -\frac{1}{\sin \pi \alpha} P_n^{(-\alpha, -\beta)}(r) \right] = -(r+1). \quad (4.105)$$

Equation (4.63) gives  $N+1$  equations in  $N+1$  unknowns. Expanding right hand side of equation (4.105) into a series in Jacobi polynomials  $P_n^{(-\alpha, -\beta)}$  and observing that  $\beta = -\alpha$ , we find

$$r+1 = P_1^{(-\alpha, \alpha)}(r) + (1+\alpha)P_0^{(-\alpha, \alpha)}(r). \quad (4.106)$$

We have only two nonzero coefficients which, from (4.105) and (4.106), are obtained as follows:

$$c_0 = (1+\alpha) \sin \pi \alpha, \quad (4.107)$$

$$c_1 = \sin \pi \alpha. \quad (4.108)$$

Substituting  $\phi(s)$  into equation (4.102) and using orthogonality of Jacobi Polynomials given by equation (3.49), the unknown  $b$  can be found from

$$\frac{\mu_0}{\kappa+1} \frac{b}{\sigma_0 R} c_0 \theta_0 = P_0^{(\alpha, \beta)}(r) = 1. \quad (4.109)$$

In this case  $\alpha + \beta = 0$ , and  $\theta_0$  becomes

$$\theta_0 = \frac{2\pi\alpha}{\sin \pi \alpha}, \quad (4.110)$$

$$c_0 \theta_0 = 2\pi\alpha(1+\alpha). \quad (4.111)$$

Substituting now  $\sigma_0$  from (4.57) into (4.109) we obtain

$$b = \left( \frac{\kappa+1}{\mu_0} \frac{R}{2\pi\alpha(1+\alpha)} P \right)^{1/2}. \quad (4.112)$$

Also

$$\frac{\mu_0}{\kappa+1} \frac{b}{\sigma_0 R} = \frac{1}{c_0 \theta_0} = \frac{1}{2\pi\alpha(1+\alpha)}, \quad (4.113)$$

which follows from  $\beta = -\alpha$  and

$$P_1^{(\alpha, -\alpha)}(r) = r + \alpha.$$

Therefore, the solution is

$$\begin{aligned} p(r) &= 2\sigma_0 \phi(r), \\ &= \frac{2P}{b} \frac{1}{c_0 \theta_0} \left( \frac{1-r}{1+r} \right)^\alpha [c_0 + c_1(r + \alpha)] \\ &= \frac{P \sin \pi \alpha}{b\pi\alpha(1+\alpha)} \left( \frac{1-r}{1+r} \right)^\alpha (1+r+2\alpha). \end{aligned} \quad (4.114)$$

From equation (4.4) it then follows that

$$\sigma_{yy}(x, 0) = -\frac{2P \sin \pi \alpha}{b\pi \alpha(1 + \alpha)} \left( \frac{b-x}{x} \right)^\alpha \left( \alpha + \frac{x}{b} \right), \quad (4.115)$$

or in normalized form

$$\frac{\sigma_{yy}(x, 0)}{P/b} = -\frac{2 \sin \pi \alpha}{\pi \alpha(1 + \alpha)} \left( \frac{b-x}{x} \right)^\alpha \left( \alpha + \frac{x}{b} \right). \quad (4.116)$$

which agrees with the solution given by [31]

### Stress intensity factor

Again the stress intensity factor may be defined and evaluated as follows:

$$k_1(0) = \lim_{x \rightarrow 0} 2^\alpha x^\alpha p(x) = \frac{2^{\alpha+1} P \sin \pi \alpha b^{\alpha-1}}{\pi(1 + \alpha)}. \quad (4.117)$$

For the homogeneous case  $\alpha = 1/2$ , and (4.117) becomes

$$k_1(0) = \frac{4\sqrt{2}}{3} \frac{P}{\pi\sqrt{b}}. \quad (4.118)$$

### 4.3.2 Solution for Graded Materials

Consider the punch problem for the non-homogeneous medium where a rigid half cylinder of radius  $R$  is pressed on an elastic half plane shown in Figure (4.24). Let  $\mu$  be the shear modulus varying exponentially in  $y$  direction.

By using equations (4.4) and (4.5), equation (2.75) becomes

$$Ap(x) + \frac{1}{\pi} \int_0^b \frac{p(t)dt}{(t-x)} - \int_0^b (J_1(t, x) + \eta J_2(t, x)) p(t)dt = f(x), \quad 0 < x < b \quad (4.119)$$

where shape of the punch is approximated by a parabola as

$$v(x, 0) = -\frac{x^2}{2R} + C, \quad (4.120)$$

$$f(x) = \frac{4\mu_0}{\kappa + 1} \frac{\partial}{\partial x} v(x, 0) = -\frac{4\mu_0}{\kappa + 1} \frac{x}{R}. \quad (4.121)$$

Using equations (4.9)-(4.12) and defining

$$\gamma^* = \frac{b}{2}\gamma \quad (4.122)$$

$$J_1(t, x) = J_1^*(s, r) \quad (4.123)$$

$$J_2(t, x) = J_2^*(s, r) \quad (4.124)$$

we obtain

$$A\phi(r) + \frac{1}{\pi} \int_{-1}^1 \frac{\phi(s)ds}{s-r} - \int_{-1}^1 (J_1^*(s, r) + \eta J_2^*(s, r)) \phi(s)ds = -\frac{\mu_0}{\kappa+1} \frac{b}{R}(r+1), \quad (4.125)$$

$$\int_{-1}^1 \phi(s)ds = 1. \quad (4.126)$$

As in the homogeneous case, the index  $\kappa_0$  is zero. Thus, assuming a solution of the form (4.104) and by using collocation technique, the solution of equation (4.125) becomes

$$\sum_0^N c_n \left[ -\frac{1}{\sin \pi \alpha} P_n^{(-\alpha, -\beta)}(r_i) + h_n^1(r_i) + h_n^2(r_i) \right] = -(r_i + 1), \quad i = 1, \dots, N+1. \quad (4.127)$$

Equation (4.127) provides  $N+1$  equations for  $N+1$  unknown constants  $c_0, \dots, c_N$ ,

$$\sum_0^N c_n F_n(r_i) = -(r_i + 1), \quad i = 1, \dots, N+1, \quad (4.128)$$

$$F_n(r_i) = -\frac{1}{\sin \pi \alpha} P_n^{(-\alpha, -\beta)}(r_i) + h_n^1(r_i) + h_n^2(r_i). \quad (4.129)$$

where  $r_i$  ( $i = 1, \dots, N+1$ ) are defined by

$$P_n^{(\alpha-1, \beta+1)}(r_i) = 0. \quad (4.130)$$

By substituting  $\phi(s)$  into equation (4.126) and using orthogonality of Jacobi Polynomials given by equation (3.49), the unknown  $b$  can be evaluated as

$$b = \left( \frac{\kappa+1}{\mu_0} \frac{R}{c_0 \theta_0} P \right)^{1/2}, \quad (4.131)$$

where

$$\theta_0 = \frac{2\pi\alpha}{\sin \pi\alpha}. \quad (4.132)$$

Normalization of  $b$  gives

$$b^* = \frac{b}{\left(\frac{RP}{\mu_0}\right)^{1/2}} = \left(\frac{\kappa + 1}{c_0\theta_0}\right)^{1/2}.$$

The solution is then found to be

$$\begin{aligned} p(x) &= 2\sigma_0\phi(x), \\ &= \frac{2P}{bc_0\theta_0} \left(\frac{b-x}{x}\right)^\alpha \sum_0^N c_n P_n^{(\alpha,\beta)}(2x/b-1). \end{aligned} \quad (4.133)$$

From equation (4.4) it may now be seen that

$$\sigma_{yy}(x, 0) = -\frac{2P}{bc_0\theta_0} \left(\frac{b-x}{x}\right)^\alpha \sum_0^N c_n P_n^{(\alpha,\beta)}(2x/b-1), \quad (4.134)$$

or in normalized form

$$\frac{\sigma_{yy}(x, 0)}{P/b} = -\frac{2}{c_0\theta_0} \left(\frac{b-x}{x}\right)^\alpha \sum_0^N c_n P_n^{(\alpha,\beta)}(2x/b-1). \quad (4.135)$$

Fig. 4.24 gives the stress distribution under a semi-circular punch for various values of the material non-homogeneity parameter,  $\gamma$ , for the case of no friction. The contact stress vanishes at  $x = b$  and is unbounded at the sharp edge  $x = 0$ . When the non-homogeneity parameter is very small, the solution for non-homogeneous medium reduces to the homogeneous solution. All of the curves intersect at two points. Figures 4.26 to 4.31 give the stress distribution under a semi-circular punch various values of the material non-homogeneity parameter,  $\gamma$ , and friction coefficient,  $\eta$ .

Again,  $c_0$  plays an important role in determining the contact surface and the non-dimensional stress intensity factors. Data for  $c_0$  given in Tables 4.6 and 4.7 are plotted in Figures 4.32 and 4.33



### Stress intensity factor

The stress intensity factor may be defined and evaluated as follows

$$k_1(0) = \lim_{x \rightarrow 0} 2^\alpha x^\alpha p(x) = \frac{2^{\alpha+1} P b^{\alpha-1}}{c_0 \theta_0} \sum_0^N c_n P_n^{(\alpha, \beta)}(-1). \quad (4.136)$$

Tables 4.8 and 4.9 give the normalized stress intensity factors at the sharp end of the semi-circular punch according to the direction of application of the force  $Q$  by assuming  $\nu = 0.3$ . Note that for  $\gamma \rightarrow 0$ , as expected, the stress intensity factor ratios reduce to those of a homogeneous medium. These data given in the Tables 4.8 and 4.9 are plotted in Figures 4.34 and 4.35 respectively. Interesting thing to note here is that although in the absence of friction stress intensity factor increases with increasing  $\gamma$ , in the presence of friction stress intensity factor decreases with  $\gamma$ . Furthermore, as the direction of the application of the force  $Q$  is reversed, there is a slight change in the dependence of  $k$  on the coefficient of friction.

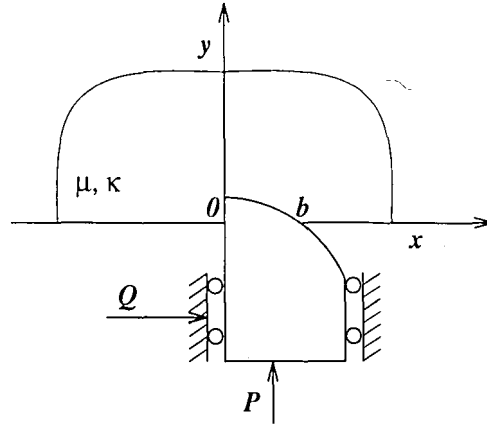


Table 4.6: The first coefficient of the Jacobi series ,  $c_0$  for semi-circular punch

	$\eta = 0.0$	$\eta = 0.1$	$\eta = 0.3$	$\eta = 0.5$
	$\alpha = +0.5$ $\beta = -0.5$	$\alpha = +0.5091$ $\beta = -0.5091$	$\alpha = +0.5272$ $\beta = -0.5272$	$\alpha = +0.5452$ $\beta = -0.5452$
$\gamma$	$c_0$	$c_0$	$c_0$	$c_0$
0.0	1.5000	1.5085	1.5216	1.5296
0.2	1.6930	1.4385	1.4279	1.4101
0.5	1.9695	1.2997	1.2835	1.2593
1.0	2.4263	1.0707	1.0577	1.0348
1.5	2.8872	0.8863	0.8766	0.8551
2.0	3.3544	0.7456	0.7374	0.7153
2.5	3.8278	0.6385	0.6301	0.6064
3.0	4.3069	0.5554	0.5462	0.5208
3.5	4.7909	0.4899	0.4796	0.4530
4.0	5.2793	0.4372	0.4260	0.3992
4.5	5.7713	0.3941	0.3823	0.3564

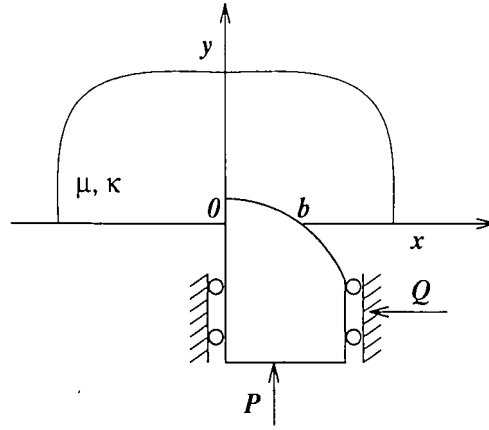


Table 4.7: The first coefficient of the Jacobi series ,  $c_0$  for semi-circular punch

	$\eta = 0.0$	$\eta = -0.1$	$\eta = -0.3$	$\eta = -0.5$
	$\alpha = +0.5$ $\beta = -0.5$	$\alpha = +0.5091$ $\beta = -0.5091$	$\alpha = +0.5272$ $\beta = -0.5272$	$\alpha = +0.5452$ $\beta = -0.5452$
$\gamma$	$c_0$	$c_0$	$c_0$	$c_0$
0.0	1.5000	1.4903	1.4674	1.4402
0.2	1.6930	1.4419	1.4381	1.4277
0.5	1.9695	1.3075	1.3072	1.2994
1.0	2.4263	1.0740	1.0685	1.0554
1.5	2.8872	0.8848	0.8740	0.8564
2.0	3.3544	0.7414	0.7276	0.7080
2.5	3.8278	0.6329	0.6178	0.5978
3.0	4.3069	0.5495	0.5341	0.5150
3.5	4.7909	0.4840	0.4692	0.4515
4.0	5.2793	0.4317	0.4178	0.4018
4.5	5.7713	0.3892	0.3764	0.3621

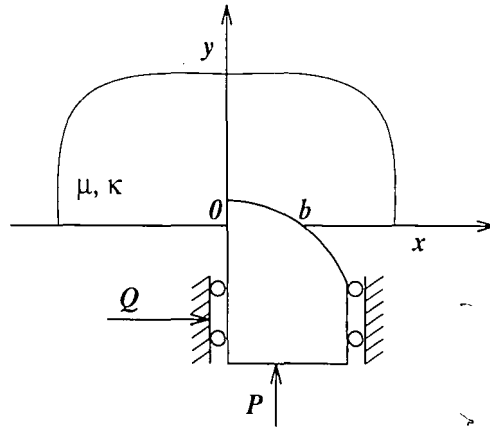


Table 4.8: Stress intensity factors for semi-circular punch,  $B(\alpha) = \frac{\pi(1+\alpha)}{2\alpha+1 \sin \pi\alpha}$

	$\eta = 0.0$	$\eta = 0.1$	$\eta = 0.3$	$\eta = 0.5$
	$\alpha = +0.5$ $\beta = -0.5$	$\alpha = +0.5091$ $\beta = -0.5091$	$\alpha = +0.5272$ $\beta = -0.5272$	$\alpha = +0.5452$ $\beta = -0.5452$
$\gamma$	$B(\alpha) \frac{k_1(0)}{P b^{\alpha-1}}$	$B(\alpha) \frac{k_1(0)}{P b^{\alpha-1}}$	$B(\alpha) \frac{k_1(0)}{P b^{\alpha-1}}$	$B(\alpha) \frac{k_1(0)}{P b^{\alpha-1}}$
0.0	1.0000	1.0000	1.0000	1.0000
0.2	1.0701	0.9402	0.9240	0.9072
0.5	1.1632	0.8507	0.8379	0.8238
1.0	1.3032	0.7258	0.7291	0.7301
1.5	1.4312	0.6377	0.6570	0.6734
2.0	1.5506	0.5780	0.6108	0.6407
2.5	1.6633	0.5374	0.5820	0.6232
3.0	1.7704	0.5098	0.5644	0.6148
3.5	1.8726	0.4908	0.5540	0.6112
4.0	1.9706	0.4777	0.5480	0.6092
4.5	2.0649	0.4687	0.5441	0.6069

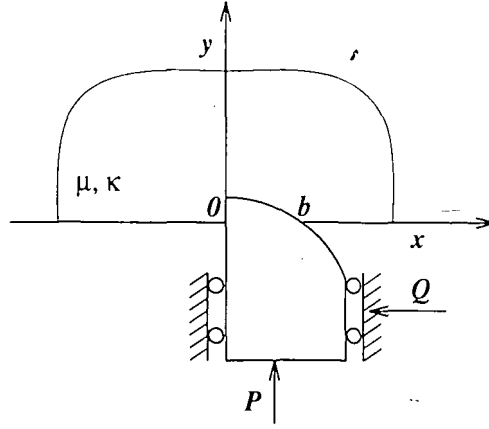


Table 4.9: Stress intensity factors for semi-circular punch,  $B(\alpha) = \frac{\pi(1+\alpha)}{2^{\alpha+1}\sin \pi\alpha}$

	$\eta = 0.0$	$\eta = -0.1$	$\eta = -0.3$	$\eta = -0.5$
	$\alpha = +0.5$ $\beta = -0.5$	$\alpha = +0.4909$ $\beta = -0.4909$	$\alpha = +0.4728$ $\beta = -0.4728$	$\alpha = +0.4548$ $\beta = -0.4548$
$\gamma$	$B(\alpha) \frac{k_1(0)}{Pb^{\alpha-1}}$	$B(\alpha) \frac{k_1(0)}{Pb^{\alpha-1}}$	$B(\alpha) \frac{k_1(0)}{Pb^{\alpha-1}}$	$B(\alpha) \frac{k_1(0)}{Pb^{\alpha-1}}$
0.0	1.0000	1.0000	1.0000	1.0000
0.2	1.0701	0.9559	0.9713	0.9865
0.5	1.1632	0.8627	0.8743	0.8858
1.0	1.3032	0.7216	0.7176	0.7151
1.5	1.4312	0.6187	0.6024	0.5903
2.0	1.5506	0.5477	0.5237	0.5072
2.5	1.6633	0.4988	0.4707	0.4531
3.0	1.7707	0.4649	0.4350	0.4178
3.5	1.8726	0.4413	0.4109	0.3943
4.0	1.9706	0.4250	0.3946	0.3780
4.5	2.0649	0.4139	0.3835	0.3658

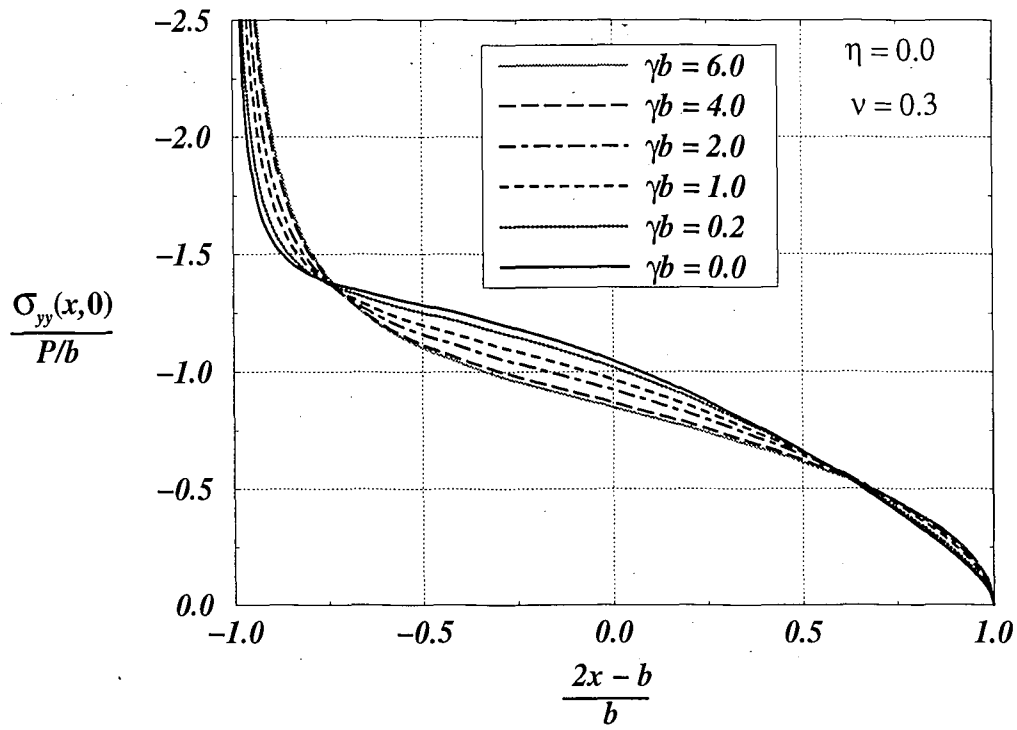
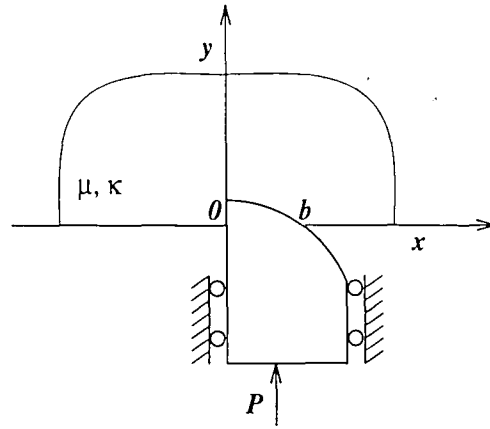


Figure 4.25: Stress distribution under a semi-circular punch for various values of the material non-homogeneity parameter,  $\gamma$ , when friction is not present,  $\alpha = 0.5$ ,  $\beta = -0.5$

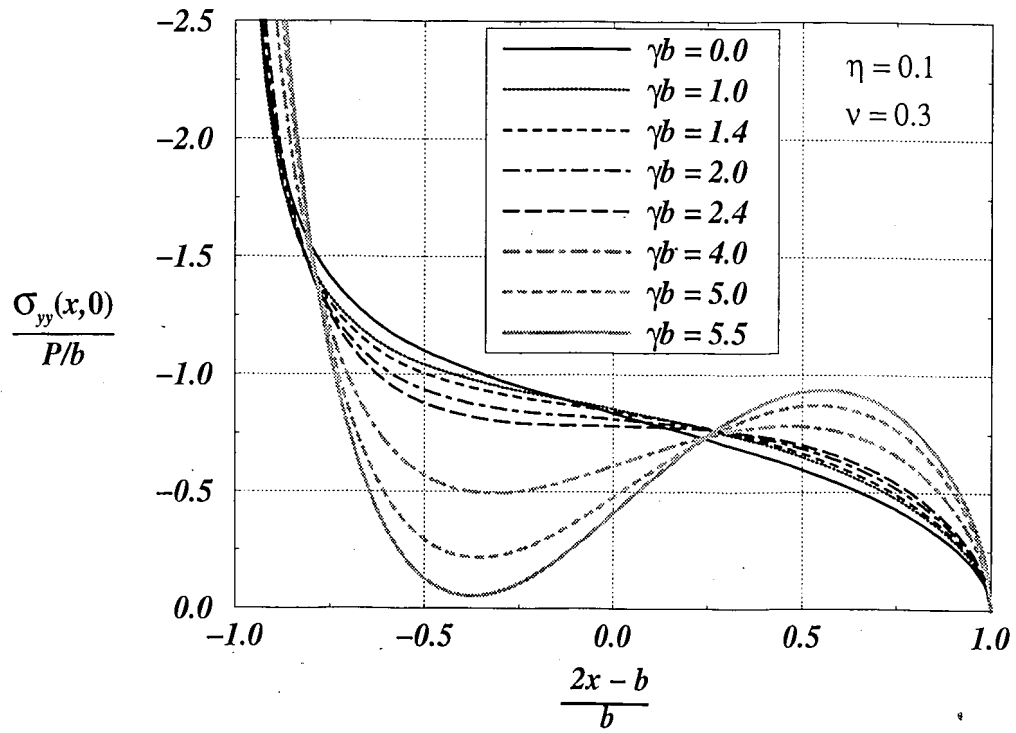
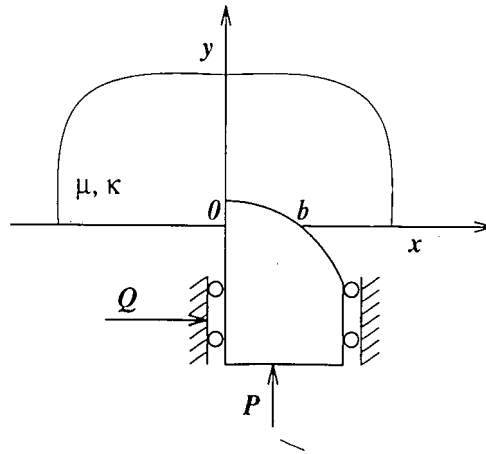


Figure 4.26: Stress distribution under a semi-circular punch for various values of the material non-homogeneity parameter,  $\gamma$ , in the presence of friction,  $\eta = 0.1$ ,  $\alpha = 0.5091$ ,  $\beta = -0.5091$ .

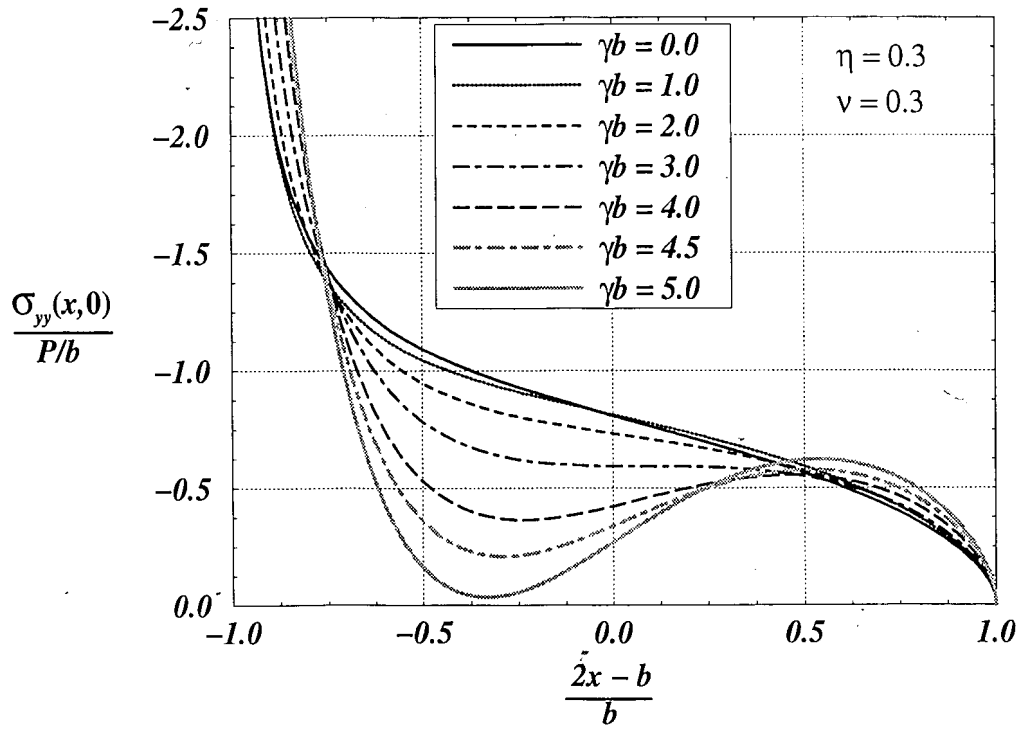
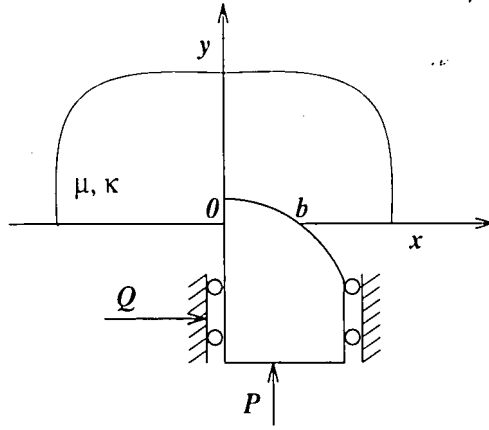


Figure 4.27: Stress distribution under a semi-circular punch for various values of the material non-homogeneity parameter,  $\gamma$ , in the presence of friction,  $\eta = 0.3$ ,  $\alpha = 0.5272$ ,  $\beta = -0.5272$ .



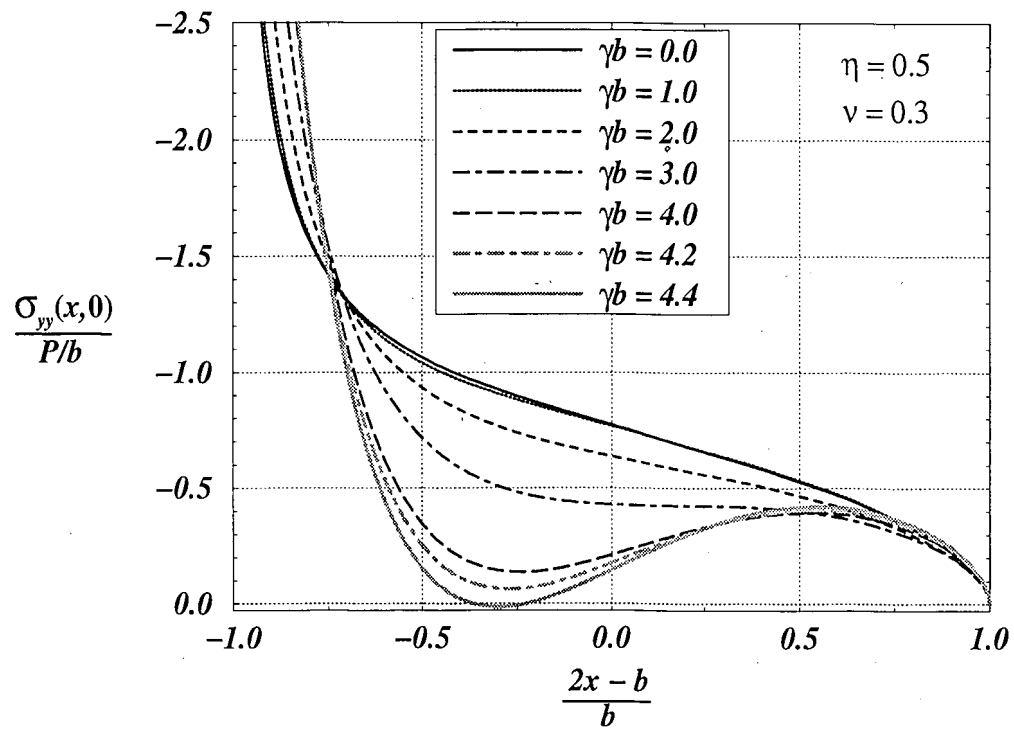
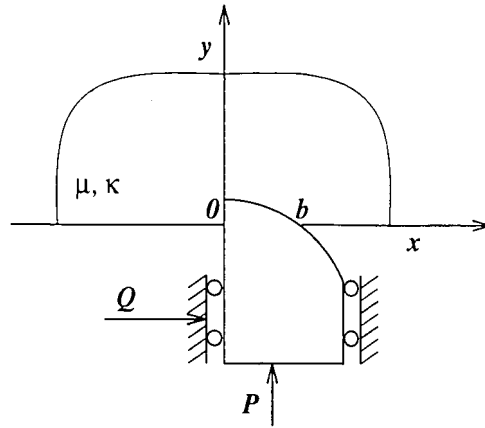


Figure 4.28: Stress distribution under a semi-circular punch for various values of the material non-homogeneity parameter,  $\gamma$ , in the presence of friction,  $\eta = 0.5$ ,  $\alpha = 0.5452$ ,  $\beta = -0.5452$ .

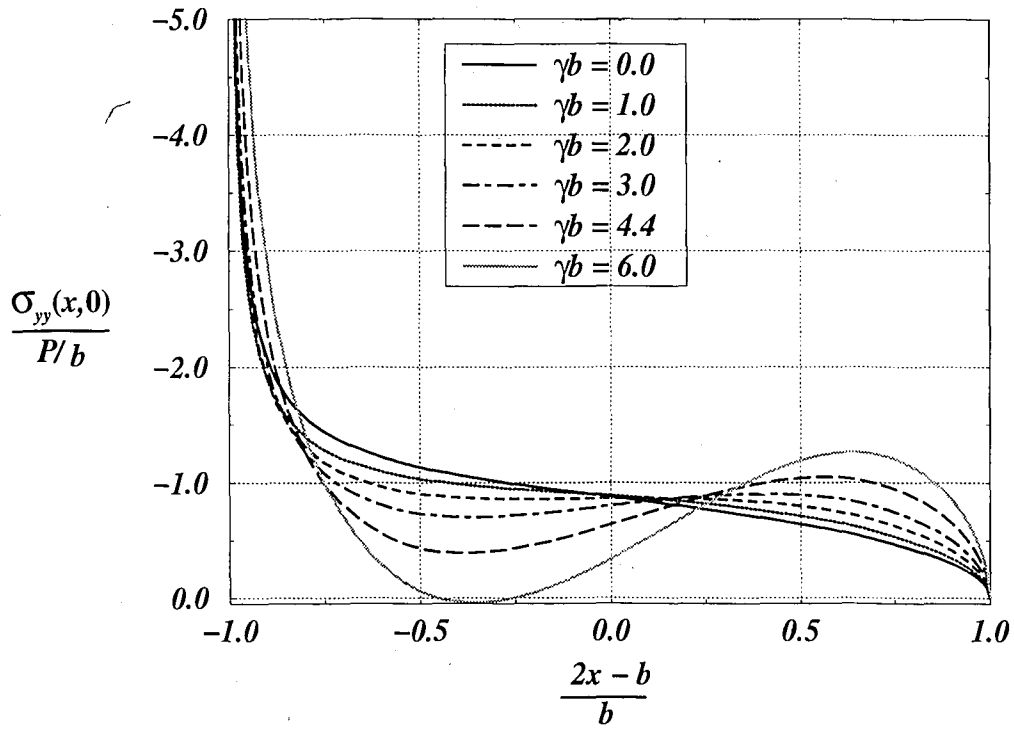
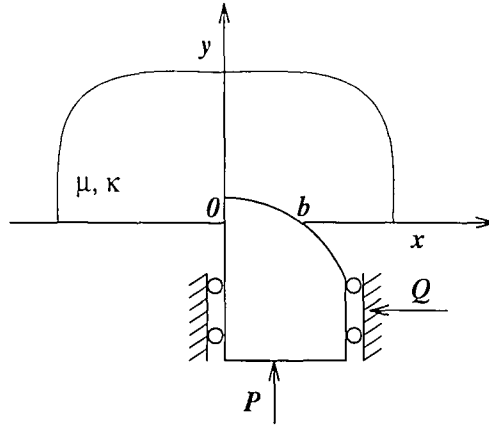


Figure 4.29: Stress distribution under a semi-circular punch for various values of the material non-homogeneity parameter,  $\gamma$ , in the presence of friction,  $\eta \cong -0.1$ ,  $\alpha = 0.4909$ ,  $\beta = -0.4909$ .

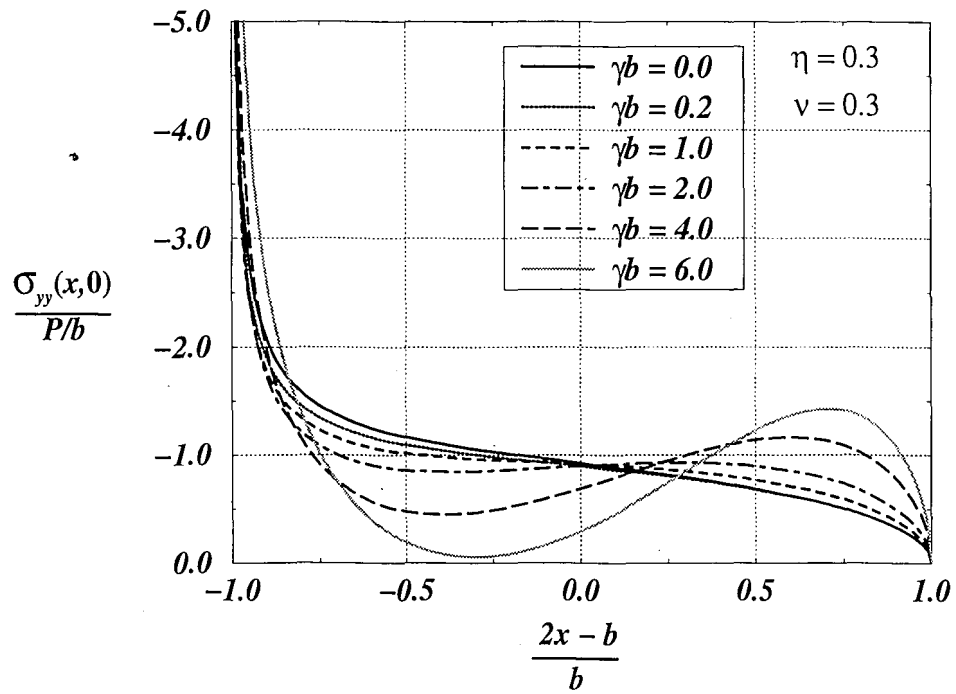
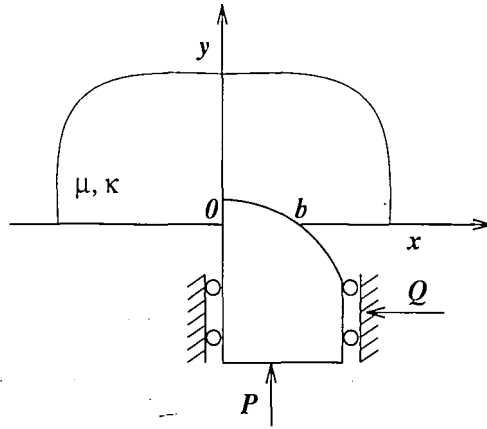


Figure 4.30: Stress distribution under a semi-circular punch for various values of the material non-homogeneity parameter,  $\gamma$ , in the presence of friction,  $\eta = -0.3$ ,  $\alpha = 0.4728$ ,  $\beta = -0.4728$ .

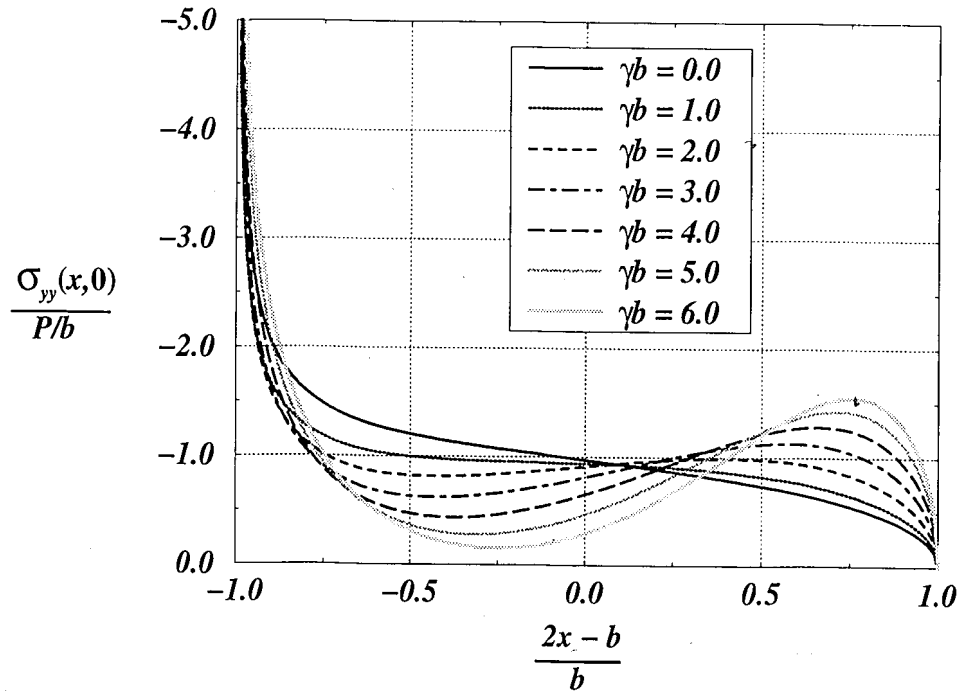
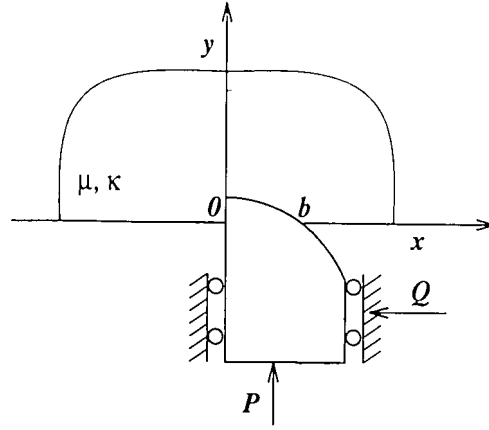


Figure 4.31: Stress distribution under a semi-circular punch for various values of the material non-homogeneity parameter,  $\gamma$ , in the presence of friction,  $\eta = -0.5$ ,  $\alpha = 0.4548$ ,  $\beta = -0.4548$ .

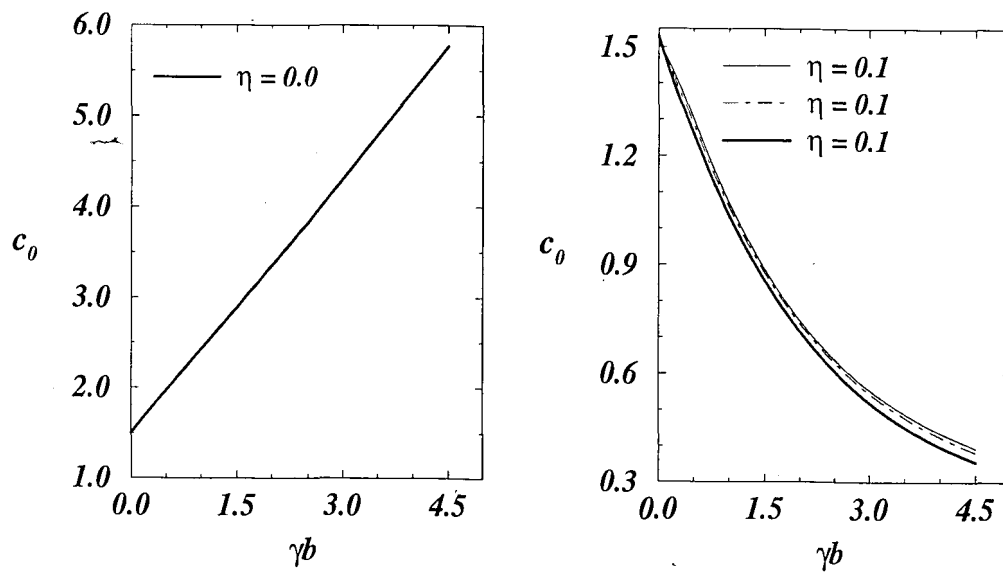
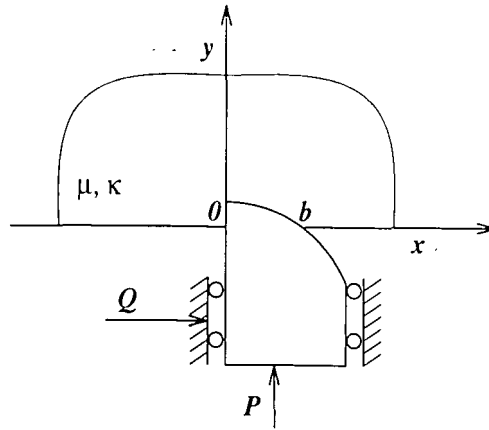


Figure 4.32: Variation of  $c_0$  for the semi-circular punch with the non homogeneity parameter,  $\gamma$ .

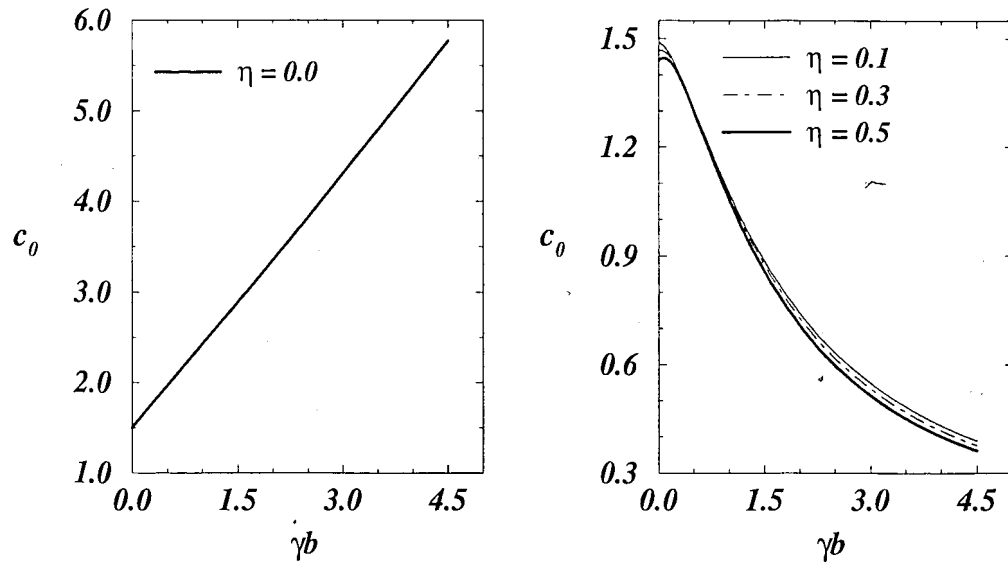
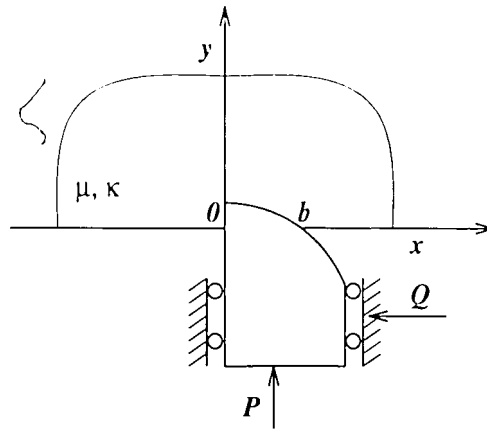


Figure 4.33: Variation of  $c_0$  for the semi-circular punch with the non homogeneity parameter,  $\gamma$ .

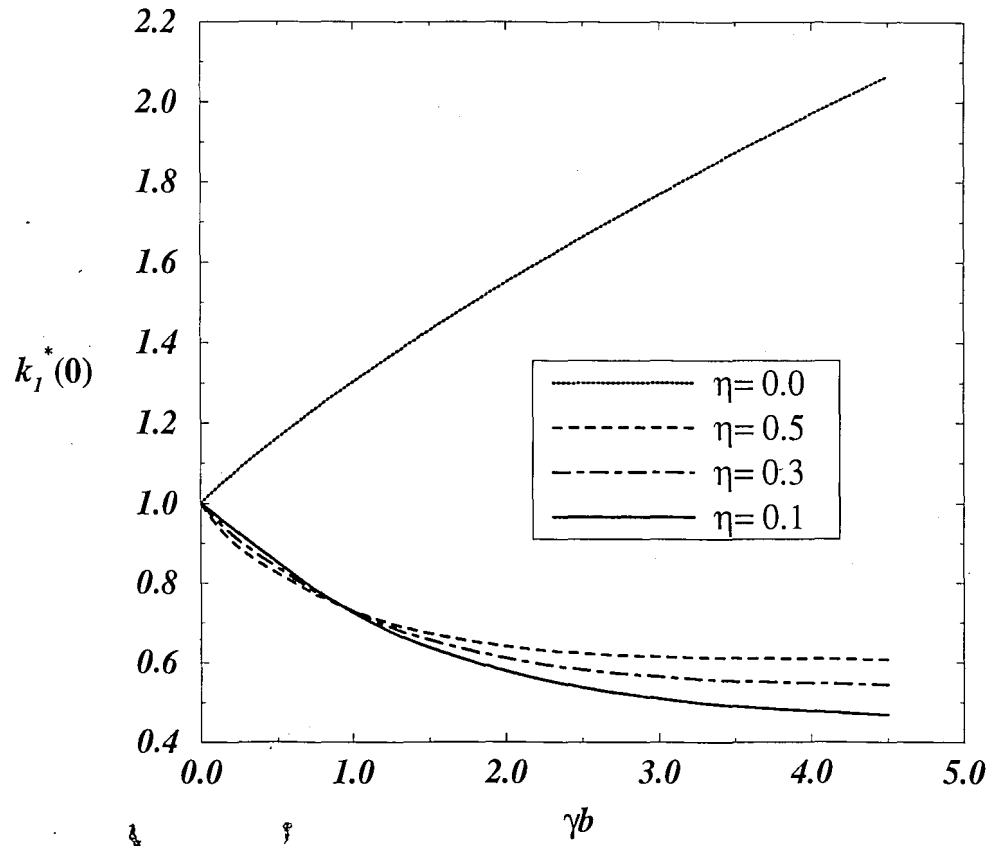
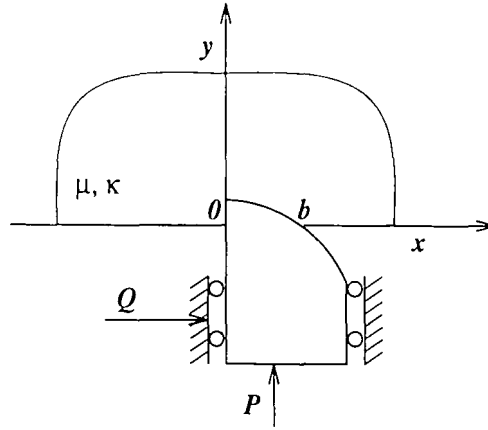


Figure 4.34: Variation of stress intensity factor with the non homogeneity parameter,

$$\gamma, k_I^*(0) = \frac{\pi(1+\alpha)}{2^{\alpha+1}\sin\pi\alpha} \frac{k_1(0)}{Pb^{\alpha-1}}$$

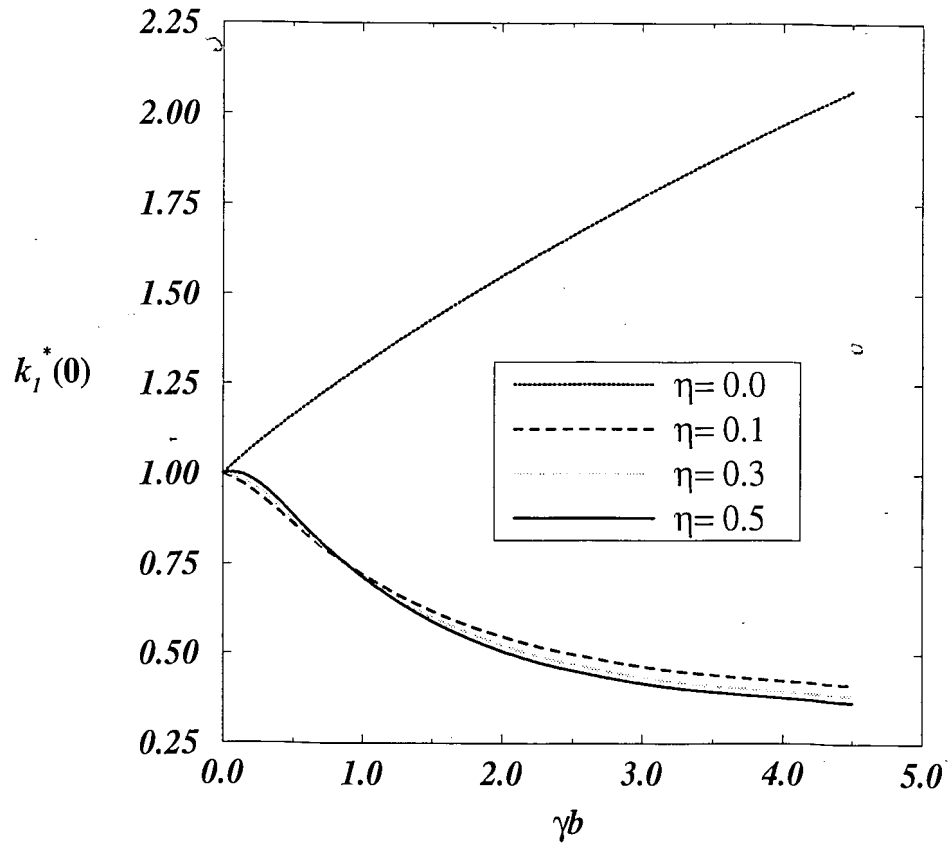
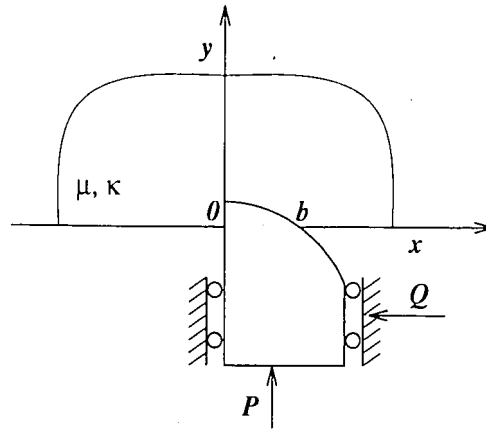


Figure 4.35: Variation of stress intensity factor with the non homogeneity parameter,

$$\gamma, k_1^*(0) = \frac{\pi(1+\alpha)}{2^{\alpha+1}\sin\pi\alpha} \frac{k_1(0)}{Pb^{\alpha-1}}$$



## 4.4 Cylindrical Punch

The cylindrical punch problem is described in Fig. 4.36. Again, for small values of  $b/R$  and  $a/R$  we can approximate the surface of the cylindrical punch by a parabola. Therefore, the displacement in  $y$  direction becomes

$$v(x, 0) = -\frac{x^2}{2R} + C. \quad (4.137)$$

or

$$\frac{\partial}{\partial x} v(x, 0) = -\frac{x}{R}. \quad (4.138)$$

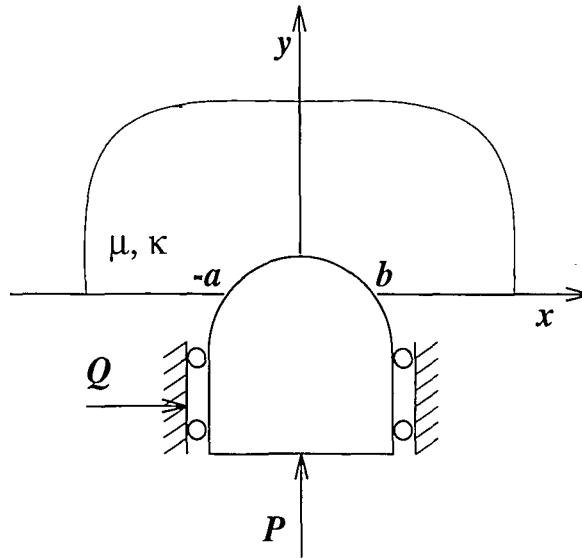


Figure 4.36: Geometry of cylindrical punch

### 4.4.1 Solution for Homogeneous Materials

Integral equation is again obtained from (4.3) by substituting

$$\sigma_{yy}(x, 0) = -p(x), \quad \sigma_{xy}(x, 0) = -\eta p(x), \quad -a < x < b, \quad (4.139)$$

$$\sigma_{yy}(x, 0) = \sigma_{xy}(x, 0) = 0, \quad x < -a, \quad x > b. \quad (4.140)$$

Equation (4.3) then becomes

$$Ap(x) + \frac{1}{\pi} \int_{-a}^b \frac{p(t)dt}{(t-x)} = \frac{4\mu_0}{\kappa+1} \frac{\partial}{\partial x} v(x,0), \quad -a < x < b \quad (4.141)$$

where, for small values of  $b/R$  and  $a/R$  we have (Figure 4.36)

$$\frac{\partial}{\partial x} v(x,0) = -\frac{x}{R} \quad (4.142)$$

and the equilibrium equation becomes

$$\int_{-a}^b p(t)dt = P \quad (4.143)$$

In order to solve the integral equation the limits of integration have to be normalized.

Now setting  $d = b$ , and  $c = -a$ , equations (3.8) to (3.12) become

$$t = \frac{b+a}{2}s + \frac{b-a}{2}, \quad -1 < s < 1 \quad (4.144)$$

$$x = \frac{b+a}{2}r + \frac{b-a}{2}, \quad -1 < r < 1 \quad (4.145)$$

$$\sigma_0 = \frac{P}{b+a}. \quad (4.146)$$

Also letting

$$p(t) = 2\sigma_0\phi(s), \quad (4.147)$$

one obtains

$$A\phi(r) + \frac{1}{\pi} \int_{-1}^1 \frac{\phi(s)ds}{s-r} = f(r), \quad -1 < r < 1, \quad (4.148)$$

$$\int_{-1}^1 \phi(s)ds = 1, \quad (4.149)$$

where

$$f(r) = -\frac{\mu_0}{\kappa+1} \frac{1}{\sigma_0 R} [(b+a)r + (b-a)]. \quad (4.150)$$

Now defining

$$b' = \frac{b}{R}, \quad (4.151)$$

$$a' = \frac{a}{R}, \quad (4.152)$$

from (4.150) it follows that

$$f(r) = -\frac{\mu_0}{\kappa+1} \frac{1}{\sigma_0} [(b' + a')r + (b' - a')] = -\frac{\mu_0}{(\kappa+1)\sigma_0} f^*(r). \quad (4.153)$$

Since  $p(x)$  is bounded both at  $x = -a$ , and  $x = b$ , from the physics of the problem we must require that both  $\alpha$  and  $\beta$  be positive. Therefore, in equation (3.34) and (3.35)  $N = 1$  and  $M = 0$ . The index of the problem is then found to be

$$\kappa_0 = -(N + M) = -(1 + 0) = -1. \quad (4.154)$$

Now assuming a solution of the form

$$\phi(s) = \frac{\mu_0}{\kappa+1} \frac{1}{\sigma_0} \sum_0^\infty c_n w(s) P_n^{(\alpha, \beta)}(t). \quad (4.155)$$

equation (4.148) may be expressed as

$$\sum_0^N c_n \left[ -\frac{2}{\sin \pi \alpha} P_{n+1}^{(-\alpha, -\beta)}(r) \right] = -[(b' + a')r + (b' - a')]. \quad (4.156)$$

In this case, note that (4.156) starts with a constant times  $c_0 P_1^{(-\alpha, -\beta)}(r)$ . Therefore in (3.51)  $c_{-1} = 0$ . Observing that  $P_0^{(\alpha, \beta)} = 1$ , the first equation ( $k = 0$ ) in (3.51) has to be set to zero

$$F_0^* = 0. \quad (4.157)$$

Substituting  $F_0^*$ ,  $d_{0n}^1$ ,  $d_{0n}^2$ , from (3.54), (3.52) and (3.53), we obtain the consistency condition as follows.

$$\int_{-1}^1 f^*(r) \frac{dr}{w(r)} = 0. \quad (4.158)$$

By substituting for  $f^*(r)$  from (4.153) and (4.156) it follows that

$$\int_{-1}^1 [(b' + a')r + (b' - a')] \frac{dr}{w(r)} = 0. \quad (4.159)$$

Expanding  $f^*(r)$  into a series of Jacobi polynomials  $P_n^{(-\alpha, -\beta)}$  where  $-\beta = \alpha - 1$  we find

$$(b' + a')r + (b' - a') = 2(b' + a')P_1^{(-\alpha, \alpha-1)}(r) + 2[\alpha(b' + a') - a']P_0^{(-\alpha, \alpha-1)}(r). \quad (4.160)$$

By substituting now from (4.160) into (4.159) we obtain

$$\alpha(b' + a') - a' = 0. \quad (4.161)$$

Comparing the coefficients of (4.156) and (4.160) it is seen that

$$c_0 = (b' + a') \sin \pi \alpha. \quad (4.162)$$

Equation (4.161) is the consistency condition and relates  $b$  to  $a$ , namely

$$b' = \frac{1 - \alpha}{\alpha} a'. \quad (4.163)$$

Substituting  $\phi(s)$  into equation (4.149) and using orthogonality of Jacobi Polynomials given by equation (3.48), we find

$$\frac{\mu_0}{\kappa + 1} \frac{1}{\sigma_0} c_0 \theta_0 = P_0^{(\alpha, \beta)}(r) = 1. \quad (4.164)$$

where in this case  $(\alpha + \beta = 1)$ , and  $\theta_0$  becomes

$$\theta_0 = \frac{2\pi\alpha(1 - \alpha)}{\sin \pi \alpha}. \quad (4.165)$$

Substituting  $\sigma_0$  from (4.57) into (4.149) we have

$$(b' + a')^2 = \frac{P}{\mu_0 R} \frac{\kappa + 1}{2\pi\alpha(1 - \alpha)}. \quad (4.166)$$

Solving (4.163) together with (4.166) it may be shown that

$$a' = \left( \frac{P}{\mu_0 R} \frac{\alpha(\kappa + 1)}{2\pi(1 - \alpha)} \right)^{1/2}, \quad (4.167)$$

$$b' = \left( \frac{P}{\mu_0 R} \frac{(1 - \alpha)(\kappa + 1)}{2\pi\alpha} \right)^{1/2}. \quad (4.168)$$

We also have

$$\frac{\mu_0}{\kappa + 1} \frac{1}{\sigma_0} = \frac{1}{c_0 \theta_0}. \quad (4.169)$$

Thus, the solution is found to be

$$\begin{aligned} p(x) &= 2\sigma_0 \phi_0 \\ &= \frac{P \sin \pi \alpha}{(b + a)\pi\alpha(1 - \alpha)} \left( 1 - \frac{2x - b + a}{b + a} \right)^\alpha \left( \frac{2x - b + a}{b + a} + 1 \right)^\beta \end{aligned} \quad (4.170)$$

From equation (4.4), it now follows that

$$\sigma_{yy}(x, 0) = -\frac{P \sin \pi \alpha}{(b+a)\pi \alpha(1-\alpha)} \left(1 - \frac{2x-b+a}{b+a}\right)^\alpha \left(\frac{2x-b+a}{b+a} + 1\right)^\beta \quad (4.171)$$

or in normalized form

$$\frac{\sigma_{yy}(x, 0)}{P/(b+a)} = -\frac{\sin \pi \alpha}{\pi \alpha(1-\alpha)} \left(1 - \frac{2x-b+a}{b+a}\right)^\alpha \left(\frac{2x-b+a}{b+a} + 1\right)^\beta. \quad (4.172)$$

#### 4.4.2 Solution for Graded Materials

Consider the punch problem for the non-homogeneous medium where a rigid half cylinder of radius  $R$  is pressed on an elastic half plane (Fig 4.36). The integral equation of the problem is obtained from (4.3), by substituting

$$\sigma_{yy}(x, 0) = -p(x), \quad \sigma_{xy}(x, 0) = -\eta p(x), \quad -a < x < b \quad (4.173)$$

$$\sigma_{yy}(x, 0) = \sigma_{xy}(x, 0) = 0, \quad x < -a, \quad x > b \quad (4.174)$$

Equation (4.3) would then becomes

$$Ap(x) + \frac{1}{\pi} \int_{-a}^b \frac{p(t)dt}{(t-x)} - \int_{-a}^b (J_1(t, x) + \eta J_2(t, x)) p(t)dt = f(x), \quad -a < x < b \quad (4.175)$$

where for a cylindrical punch profile the input function is given by

$$f(x) = \frac{4\mu_0}{\kappa+1} \frac{\partial}{\partial x} v(x, 0) = -\frac{4\mu_0}{\kappa+1} \frac{x}{R}. \quad (4.176)$$

Using equations (4.9) - (4.12) and defining

$$\gamma^* = \frac{b+a}{2} \gamma, \quad (4.177)$$

$$J_1(t, x) = J_1^*(s, r), \quad (4.178)$$

$$J_2(t, x) = J_2^*(s, r). \quad (4.179)$$

one obtains

$$A\phi(r) + \frac{1}{\pi} \int_{-1}^1 \frac{\phi(s)ds}{s-r} - \int_{-1}^1 (J_1^*(s,r) + \eta J_2^*(s,r)) \phi(s)ds = f(r), \quad (4.180)$$

$$\int_{-1}^1 \phi(s)ds = 1, \quad (4.181)$$

where  $f(r)$  is given in equation (4.176).

Using the same physical reasoning as in homogeneous case,  $\kappa_0$  is found to be  $-1$ . Assuming a solution of the form (4.155), equation (4.180) may be reduced to

$$\sum_0^N c_n \left[ -\frac{1}{\sin \pi \alpha} P_{n+1}^{(-\alpha, -\beta)}(r) + h_n^1(r) + h_n^2(r) \right] = -[(b' + a')r + (b' - a')]. \quad (4.182)$$

To solve the functional equation (4.182), collocation points may be chosen as

$$P_{n+1}^{(\alpha-1, \beta-1)}(r_i) = 0, \quad i = 1, \dots, N+1. \quad (4.183)$$

Since the problem under consideration has no symmetry, after collocation (4.182) gives  $N+1$  equations. Thus, together with (4.149) we obtain  $N+2$  equations for the  $N+3$  unknown constants  $c_0, \dots, c_N, a$  and  $b$ . The additional equation is obtained from consistency condition which is derived below.

In this case, note that (4.156) starts with a constant times  $c_0 P_1^{(-\alpha, -\beta)}(r)$ . Therefore in (3.51)  $c_{-1} = 0$ . Observing that  $P_0^{(\alpha, \beta)} = 1$ , the first equation ( $k=0$ ) in (3.51) has to be set to zero

$$F_0^* - \sum_{k=0}^N (d_{0n}^1 + d_{0n}^2) c_n = 0. \quad (4.184)$$

substituting  $F_0^*, d_{0n}^1, d_{0n}^2$ , from (3.54), (3.52) and (3.53) we obtain

$$\int_{-1}^1 f^*(r) \frac{dr}{w(r)} - \int_{-1}^1 \frac{dr}{w(r)} \sum_0^\infty c_n [h_n^1(r) + h_n^2(r)] = 0. \quad (4.185)$$

or

$$\int_{-1}^1 \frac{dr}{w(r)} \left[ f^*(r) - \int_{-1}^1 [J_1^*(s,r) + J_2^*(s,r)] P_n^{(\alpha, \beta)}(s) w(s) ds \right] = 0, \quad (4.186)$$

which is the consistency condition of the integral equation. Equation (4.182) provides  $N+1$  equations for  $N+3$  unknowns. In solving (4.182) it can be formally assumed that  $c_{-1} = 0$ .

Substituting  $\phi(s)$  into equation (4.181) and using orthogonality of Jacobi Polynomials given by equation (3.48), we find

$$\frac{\mu_0}{\kappa + 1} \frac{1}{\sigma_0} c_0 \theta_0 = P_0^{(\alpha, \beta)}(r) = 1. \quad (4.187)$$

where  $\theta_0$  is given in equation (4.165).

The system of equations is nonlinear in  $(c_0, \dots, c_N, a', b')$  therefore it is necessary to adopt an iterative scheme. First we guess  $a'$  which makes the system linear and, therefore, we can solve for  $(c_0, \dots, c_N, b')$ . Using this calculated results, we can find  $a'$  from (4.187) and compare the calculated and guessed values. The problem is then solved by following a standard iterative scheme. The contact stress may then be expressed as

$$\begin{aligned} p(x) &= 2\sigma_0 \phi(x), \\ &= \frac{2P}{(b+a)c_0\theta_0} w(x) \sum_0^N c_n P_n^{(\alpha, \beta)} \left( \frac{2x-b+a}{b+a} \right), \end{aligned} \quad (4.188)$$

where

$$w(x) = \left( 1 - \frac{2x-b+a}{b+a} \right)^\alpha \left( \frac{2x-b+a}{b+a} + 1 \right)^\beta. \quad (4.189)$$

From equation (4.4) and (4.188) it follows that

$$\sigma_{yy}(x, 0) = -\frac{2P}{(b+a)c_0\theta_0} w(x) \sum_0^N c_n P_n^{(\alpha, \beta)} \left( \frac{2x-b+a}{b+a} \right), \quad (4.190)$$

or, in normalized form

$$\frac{\sigma_{yy}(x, 0)}{P/(b+a)} = -\frac{2}{c_0\theta_0} w(x) \sum_0^N c_n P_n^{(\alpha, \beta)} \left( \frac{2x-b+a}{b+a} \right). \quad (4.191)$$

Stress distribution under a cylindrical punch for various values of the material non-homogeneity parameter,  $\gamma$ , and friction coefficient,  $\eta$  is given in figures Fig4.37 to Fig 4.40.

In the punch problem for the non-homogeneous medium, the location of the end points of the contact region  $a^*$  and  $b^*$  can not be obtained in closed form. The problem is solved by assuming a value for  $a^*$  and by obtaining the coefficients  $c_0, \dots, c_N$

and  $b^*$  from the numerical solution of the integral equation and the consistency condition. Since the problem is highly nonlinear in  $b^*$ , the solution requires the application of an iterative technique. The assumed constant  $a$  is then related to the resultant force  $P$  by using the equilibrium condition (4.181). The normalized values of  $a$  and  $b$  in a punch problem for a homogeneous medium in the presence of friction is given in Fig.4.41. Note that for  $\eta = 0$ ,  $a = b$ , and the effect of  $\eta$  on  $a$  and  $b$  does not seem to be very significant. Figure 4.42 shows the variation of  $a$  and  $b$  as a function of the non-homogeneity parameter  $\gamma$  and friction coefficient  $\eta$ . It may be seen that, in the non-homogeneous medium the influence of  $\gamma$  and  $\eta$  on  $a$  and  $b$  is much more significant than that of the homogeneous medium.



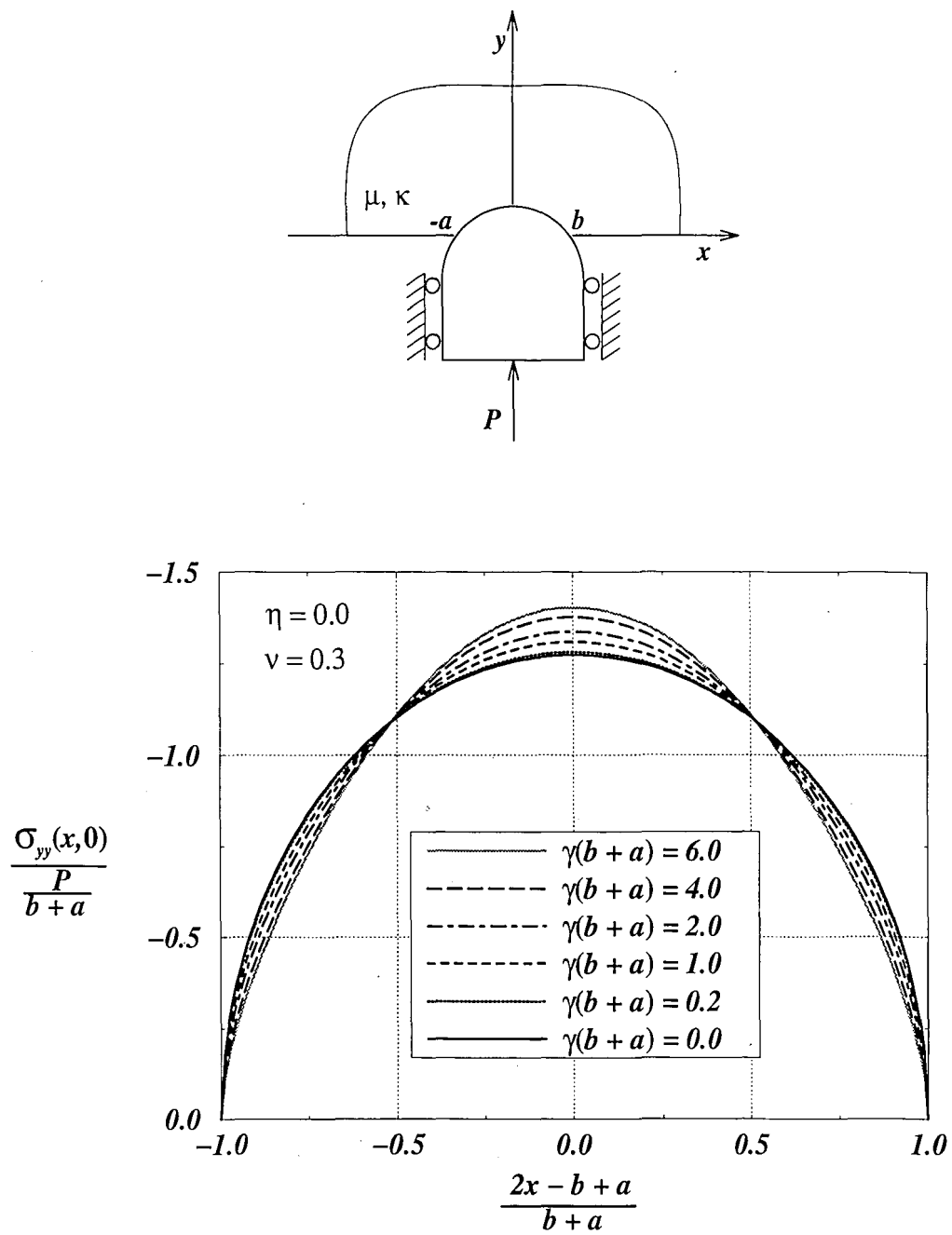


Figure 4.37: Stress distribution under a cylindrical punch for various values of the material non-homogeneity parameter,  $\gamma$ , when friction is not present,  $\alpha = 0.5$ ,  $\beta = 0.5$

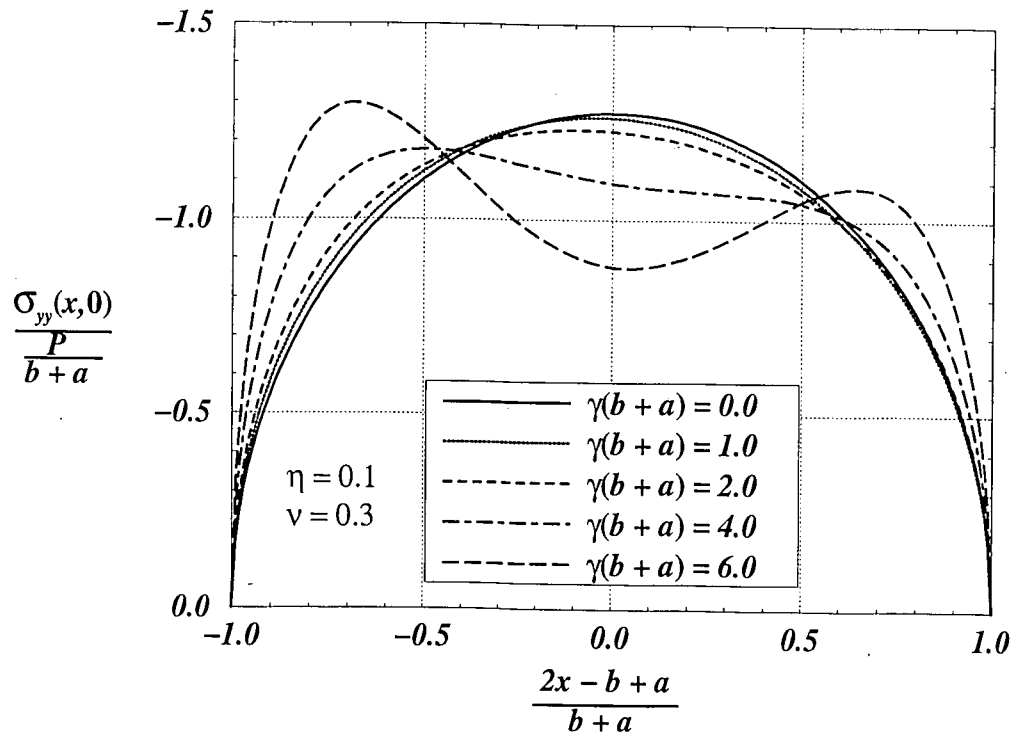
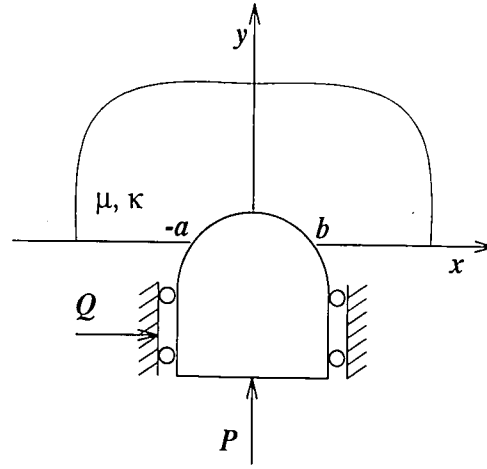


Figure 4.38: Stress distribution under a cylindrical punch for various values of the material non-homogeneity parameter,  $\gamma$ , in the presence of friction,  $\eta = 0.1$ ,  $\alpha = 0.5091$ ,  $\beta = 0.4909$ .

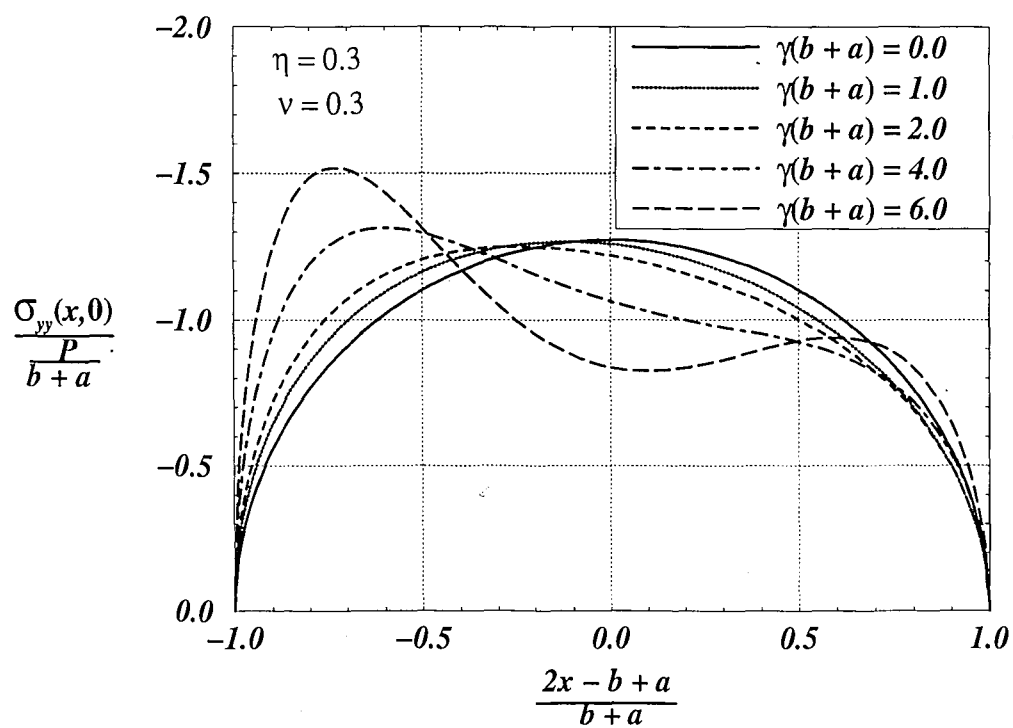
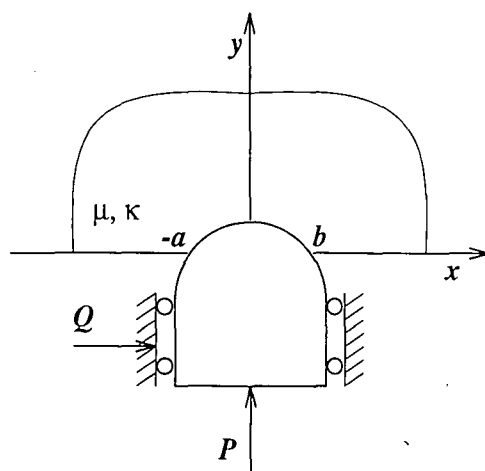


Figure 4.39: Stress distribution under a cylindrical punch for various values of the material non-homogeneity parameter,  $\gamma$ , in the presence of friction,  $\eta = 0.3$ ,  $\alpha = 0.5272$ ,  $\beta = 0.4728$ .

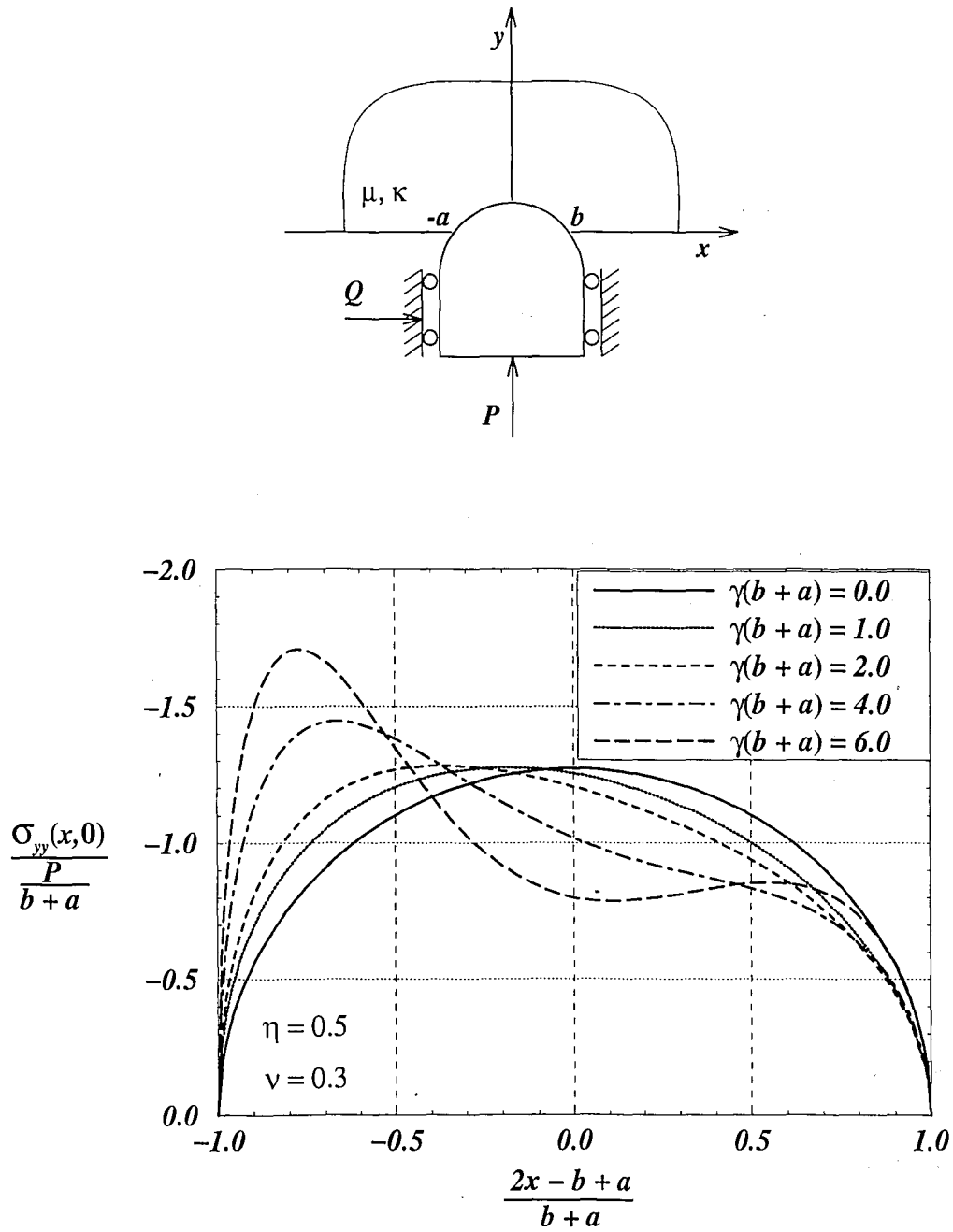


Figure 4.40: Stress distribution under a cylindrical punch for various values of the material non-homogeneity parameter,  $\gamma$ , in the presence of friction,  $\eta = 0.5$ ,  $\alpha = 0.5452$ ,  $\beta = 0.4548$ .

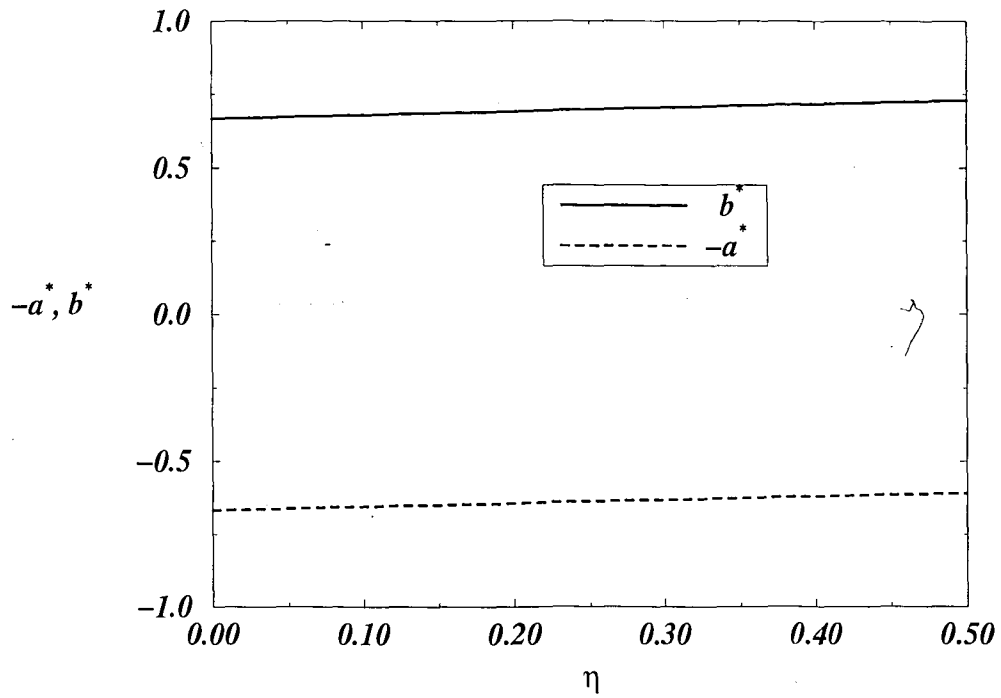
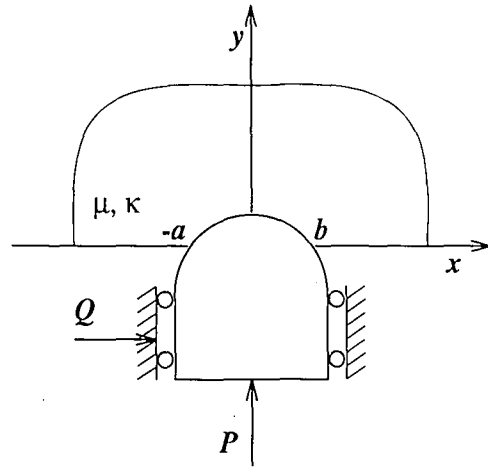


Figure 4.41: Variation of the end points of the contact region for a cylindrical punch on a homogeneous medium with respect to the coefficient of friction,  $\eta$ ,  
 $a^* = \frac{a}{R} \left( \frac{P}{\mu R} \right)^{1/2}$ ,  $b^* = \frac{b}{R} \left( \frac{P}{\mu R} \right)^{1/2}$ .

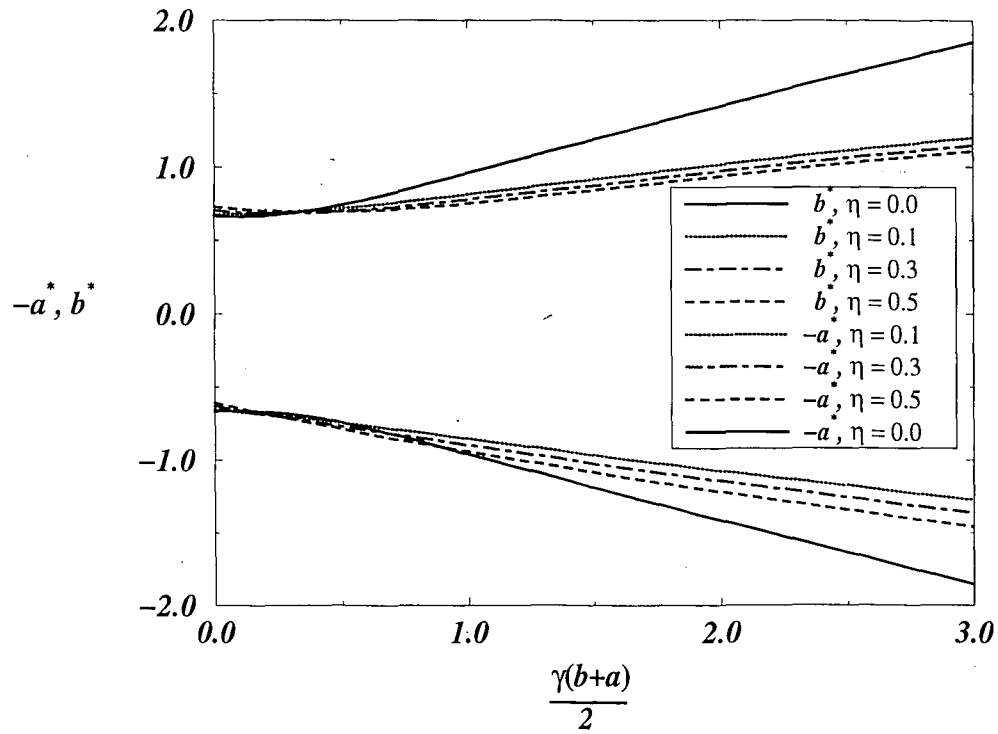
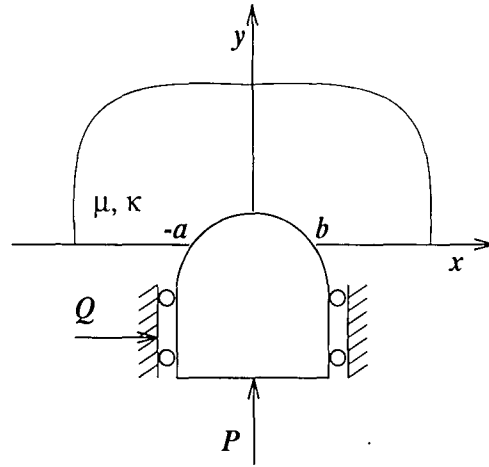


Figure 4.42: Variation of the end points of the contact region for a cylindrical punch with respect to nonhomogeneity parameter,  $\gamma$  for various values of the coefficient of friction,  $\eta$ ,  $a^* = \frac{a}{R} \left( \frac{P}{\mu R} \right)^{1/2}$ ,  $b^* = \frac{b}{R} \left( \frac{P}{\mu R} \right)^{1/2}$ .

## Chapter 5

### Conclusions and Future Work

In this study, the contact stresses between an elastic rigid punch and a nonhomogeneous elastic half space in the presence of friction has been investigated. Also, stress intensity factors whenever applicable has been calculated. The main parameters used in this study was the non-homogeneity parameter,  $\gamma$ , and the coefficient of friction,  $\eta$ . The effect of these parameters for different cases of punch profile can be summarized as follows:

1) For the flat punch, contact stresses are unbounded at the ends. For frictional contact, the magnitude of the contact stresses decrease as  $\gamma$  increases. However as  $\eta$  increases, stresses increase quite significantly at the edge  $x = -a$ , for the punch shown in Fig 4.1. On the other hand stresses decrease at the edge  $x = a$  with increasing  $\eta$ . For sufficiently large values of  $\eta$  the contact stresses become positive and separation would take place. This phenomenon will be investigated in a future study.

2) For the triangular punch, a peculiar behavior has been observed in the contact stress distribution. Stress curves intersect at one point and change their trend, near the sharp corner for both frictional and frictionless punch. But the trend is opposite in each case. The contact surface is determined by  $b$  which is a linear function of the applied force  $P$ . Stress intensity factors are nondimensionalized with respect to the first coefficient,  $c_0$  of the Jacobi polynomial series expansion. This constant is needed to calculate  $b$  and is tabulated in Table 4.4 and 4.5.  $c_0$  has a great influence

on the distribution of the stress intensity factor. Although in the frictionless punch  $c_0$  increases with increasing  $\gamma$ , in the frictional case it decreases. There is also a critical value of  $\gamma = \gamma_{critical}$  above which the contact stresses become positive.  $\gamma_{critical}$  decreases as  $\eta$  increases. Also, if the direction of application of the tangential force is reversed,  $\gamma_{critical}$  increases.

3) For the semi-circular punch, contact stresses are unbounded at the sharp end. In this case the length of the contact surface,  $b$  is a parabolic function of the applied force  $P$ . If there is more friction  $\gamma_{critical}$  decreases, however  $\gamma_{critical}$  is much greater than that of triangular punch. Stress intensity factors at the sharp end is nondimensionalized as in the triangular punch case and the effect of the  $c_0$  has been investigated for various values of  $\gamma b$  and  $\eta$ . There is a slight change in  $c_0$  with a change in  $\eta$ .

4) For the cylindrical punch the contact is smooth at both ends of the contact region, hence stresses are zero at the ends. In the frictionless contact, stress distribution is symmetric. However, for frictional contact it is slanted through the application point of the applied tangential force,  $Q$  and becomes more slanted with increasing the friction coefficient  $\eta$ .

An important potential application of the graded material would be wear control. Usually load transfer components are coated with a ceramic layer to increase wear resistance. A graded layer bonded to a half plane could be studied as future research. In the case of separation, another type of model should be used to investigate the problem.

Also, contacting solids in load transfer components(e.g., gears) can be coated by graded elastic layers to increase wear resistance. The contact stresses and the size of the contact zone could again be studied as future research.



# Bibliography

- [1] Hertz, H., *Gesammelte Werke von Heinrich Hertz*, Voll, Leipzig, 1895, pp.155-195.
- [2] Love, A. E. H., *A Treatise on the Mathematical Theory of Elasticity*, Cambridge University Press, 1927.
- [3] Harding, J. W., and Sneddon, I. N., "The Elastic Stresses Produced by the Indentation of the Plane Surface of a Semi-infinite Elastic Solid by a Rigid Punch", *Proceedings of the Cambridge Philosophical Society*, Vol. 41, 1945, pp. 16-26.
- [4] Sneddon, I. N., "Boussinesq's Problem for a Flat -ended Cylinder", *Proceedings of the Cambridge Philosophical Society*, Vol. 42, 1946, pp. 29-39.
- [5] Galin, L. A., *Contact Problems on the Theory of Elasticity*, North Carolina State Translation Series, Raleigh, N. C., 1961.
- [6] Sneddon, I. N., and Hill, R., *Progress in Solid Mechanics*, Vol. 1, North-Holland Publishing Company, Amsterdam, 1960, pp. 410-413.
- [7] Muskhelishvili, N. I., *Some basic Problems of the Mathematical Theory of Elasticity*. Noordhoff, Groningen, The Netherlands(1963).
- [8] Ufliand, Ia S., *Survey of Articles on the Application of Integral Transforms in the Theory of Elasticity*. North Carolina State Translation Series, Raleigh, N. C., 1965

- [9] Sneddon, I. N., *Fourier Transforms*, McGraw-Hill, 1951.
- [10] Wu, T. S., and Chiu, Y. P., "On the Contact Problems of Layered Elastic Bodies", *Quarterly Journal of Applied Mathematics*, Vol. 25, 1967, pp. 233-242.
- [11] Pao, Y. C., Wu, T. S., and Chiu, Y. P., "Bounds on the Maximum Contact Stress of an Indented Elastic Layer", *Journal of Applied Mechanics*, Vol. 38, Transactions of the ASME, 1971, pp. 608-614.
- [12] Kasmalkar, M. B., M. S. Thesis, Lehigh University, 1993
- [13] Ratwani, M., and Erdogan, F., "On the Plane Contact Problem for a Frictionless Elastic Layer", *Journal of Solids and Structures*, Vol. 9, 1973, pp. 921-936.
- [14] Civelek, M. B., and Erdogan, F., "The Axisymmetric Double Contact Problem for a Frictionless Elastic Layer", *International Journal of Solids and Structures*, Vol. 10, 1974, pp. 639-659.
- [15] Oden, J. T. and Martins, J. A. C., "Models and Computational Methods for Dynamic Friction Phenomena", *Comput. Meth. appl. Mech. Engng*, Vol. 52, 1985, pp. 527-634.
- [16] Tabor, D., "Friction-the Present State of Our Understanding", *J. Lubr. Technol.*, Vol. 103, 1981, pp.169-179.
- [17] Chan, S. K., Tuba, I. S., "A Finite Element Method for Contact Problems of Solid Bodies-Part I. Theory and Validation", *Int. J. Mech. Sci.*, Vol. 13, 1971, pp. 519-530.
- [18] Tsuta T, and Yamaji S., *Finite Element Analysis of Contact Problems. Theory and Practice in Finite Element Structural Analysis*. University of Tokyo Press, Japan, 1973.
- [19] Ohte, S., "Finite Element Analysis of Elastic Contact Problems", *Bull. JSME*, Vol. 16, 1973, pp.797-804.

- [20] Lindeman, R. A., "Finite Element Computer Program for the Solution of Non-linear Axisymmetric Contact Problem with Interference Fits", *Rep. TR-3148*, Naval Weapons Lab., Virginia, 1974.
- [21] Korenev, B. G., *Dokl. Akad. Nauk SSSR*, Vol. 112(5), 1957 (in Russian).
- [22] Mossakovski, V. I., "The Fundamental Mixed Problem of the Theory of Elasticity for a Half Space with a Circular line of Separation of the Boundary Conditions. *PMM*, Vol 18(2), 1954.
- [23] Popov, G. Ia., "On a Remarkable Property of Jacoby Polynomials" *Ukr. Matem. Zh.*, Vol 20(4), 1968.
- [24] Mushiku M. and Teodosiu, "Solution of an Elastic Static Plane Problem for Nonhomogeneous Isotropic Bodies by means of the Theory of Complex Variables" *PMM*, Vol 30(2), 1966.
- [25] Popov, G. Ia., "On the Method of Orthogonal Polynomials in Contact Problems of the Theory of Elasticity" *PMM*, Vol 33(3), 1969.
- [26] Bakırtaş, I., "The Problem of a Rigid Punch on a Non-homogeneous Elastic Half Space", *Int. J. Engng. Sci.*, Vol 18, 1980, pp. 597-610.
- [27] Bakırtaş, I., *Solution of Certain Elasticity Problems for a Medium with Varying Modulus of Elasticity*. Ph. D. Dissertation, Istanbul, Istanbul Technical University(1977) (in Turkish).
- [28] Muskhelishvili, N. L., *Singular Integral equations*, P. Noordhoff, Groningen, The Netherlands, 1953.
- [29] Erdogan, F., and Gupta, G. D., "On the Numerical Solution of Singular Integral Equations", *Quarterly of Applied Mathematics*, Vol. 29. 1972, pp. 525-534.
- [30] Kaya, A.C., and Erdogan, F., "On the Solution of Integral Equation with a Generalized Cauchy Kernel", *Quarterly of Applied Mathematics*, Vol. xiv, pp. 455-469, 1987

- [31] Erdogan, F., Gupta, G. D., and Cook, T. S., "Numerical Solution of Singular Integral Equations," *Method of Analysis and Solution of Crack Problems*, G.C. Sih (ed.), Noordhoff Int. Publ., Leyden(1973) 368-425.
- [32] Tricomi, F.G., *Integral Equations*, Interscience, New York (1957)
- [33] Szegő, G., *Orthogonal Polynomials*, Colloquium Publications, 23, Am. Math. Soc.(1939)
- [34] Abramowitz, M. and Stegun, I. A., *Handbook of Mathematical Functions*, National Bureau of Standards, Applied Mathematics Series, 1964.
- [35] Stroud, A. H. and Secrest, D., *Gaussian Quadrature Formulas*. Prentice-Hall, New York, 1966

# Appendix A

## Asymptotic Analysis of Kernels

In the derivation of the integral equations, an important step is to find the asymptotic values of the infinite integrals (3.19) and (3.20). There are two reasons why we asymptotically expand the infinite integrals as  $\alpha \rightarrow \infty$ . First the singular behavior of the integral equation comes from the leading order term in the large  $\alpha$  expansion of the kernel in integrands (3.21) and (3.22). The second reason is that the subsequent terms in the expansion facilitate computational efficiency when we numerically solve the singular integral equation (3.18).

A straightforward asymptotic analysis of the integrands of the infinite integrals would start with the asymptotic expansion of the roots (2.20) and (2.22). We start by analyzing the roots of the characteristic equation asymptotically. Defining a new variable

$$r = \frac{\gamma}{2\alpha}, \quad (\text{A.1})$$

from

$$\begin{aligned} n_2 &= -\frac{\gamma}{2} - \frac{1}{2}\sqrt{\gamma^2 + 4\alpha^2 + 4i\alpha\gamma\delta}, \\ &= |\alpha|N_2, \end{aligned} \quad (\text{A.2})$$

$$\delta = \sqrt{\frac{3-\kappa}{\kappa+1}} \quad (\text{A.3})$$

we find

$$N_2 = -r - \sqrt{r^2 + 1 + 2i\delta r} \quad (\text{A.4})$$

The Other root  $n_4$  from (2.22) is

$$n_4 = -\frac{\gamma}{2} - \frac{1}{2}\sqrt{\gamma^2 + 4\alpha^2 - 4i\alpha\gamma\delta} = \overline{n_2}. \quad (\text{A.5})$$

Substituting (A.2) into (2.25)

$$A_2 = i\frac{\alpha}{|\alpha|}\frac{A_3}{A_4}, \quad (\text{A.6})$$

where

$$A_3 = 1 + i(\kappa + 1)\delta r, \quad (\text{A.7})$$

$$A_4 = N_2 + (3 - \kappa)r, \quad (\text{A.8})$$

$Z_1$  becomes

$$\begin{aligned} Z_1 &= i\alpha(3 - \kappa)A_2 + (\kappa + 1)n_2, \\ &= |\alpha|Z_3, \end{aligned} \quad (\text{A.9})$$

$$Z_3 = \frac{-(3 - \kappa)A_3 + (\kappa + 1)N_2A_4}{A_4}. \quad (\text{A.10})$$

Similarly,  $Z_2$  becomes

$$\begin{aligned} Z_2 &= n_2A_2 + i\alpha, \\ &= i\alpha Z_4. \end{aligned} \quad (\text{A.11})$$

where

$$Z_4 = \frac{N_2A_3 + A_4}{A_4}. \quad (\text{A.12})$$

From (2.34)

$$\begin{aligned} \Delta_0 &= -(Z_1\overline{Z_2} + \overline{Z_1}Z_2), \\ &= -\frac{i\alpha|\alpha|}{(|A_4|)^2}\Delta_1, \end{aligned} \quad (\text{A.13})$$

where

$$\Delta_1 = \overline{Z_3}Z_4 - Z_3\overline{Z_4}. \quad (\text{A.14})$$

Observing that as  $\alpha \rightarrow \infty$   $n_2$  and  $n_4$  behaves like  $-\alpha + O\left(\frac{1}{\alpha}\right)$ , (2.43)- (2.46) become

$$H_{11}(\alpha, y) = \frac{-i\alpha(\kappa-1)}{\Delta_0} (\bar{Z}_2 \vee Z_2) e^{-|\alpha|y}, \quad (\text{A.15})$$

$$H_{21}(\alpha, y) = \frac{-i\alpha(\kappa-1)}{\Delta_0} (A_2 \vee Z_2(\alpha) \sim \bar{A}_2 Z_2(\alpha)) e^{-|\alpha|y}, \quad (\text{A.16})$$

$$H_{21}(\alpha, y) = \frac{i\alpha}{\Delta_0} (Z_1 - \bar{Z}_1) e^{-|\alpha|y}, \quad (\text{A.17})$$

$$H_{22}(\alpha, y) = \frac{i\alpha}{\Delta_0} (-A_2 \bar{Z}_1(\alpha) \vee \bar{A}_2 Z_1(\alpha)) e^{-|\alpha|y}. \quad (\text{A.18})$$

Substituting the asymptotic expansions of Equations (A.4), (A.7), (A.8), (A.10), (A.12) and (A.14) as  $r \rightarrow 0$  i.e.  $\alpha \rightarrow \infty$  into (A.15)-(A.18), we have

$$H_{11}(\alpha, y) = i \frac{\alpha}{|\alpha|} \psi_{11}(\alpha) e^{-|\alpha|y}, \quad (\text{A.19})$$

$$H_{21}(\alpha, y) = h_{21}(\alpha) e^{-|\alpha|y}, \quad (\text{A.20})$$

$$H_{12}(\alpha, y) = h_{12}(\alpha) e^{-|\alpha|y}, \quad (\text{A.21})$$

$$H_{22}(\alpha, y) = i \frac{\alpha}{|\alpha|} \psi_{22}(\alpha) e^{-|\alpha|y}, \quad (\text{A.22})$$

where

$$h_{11}(\alpha) = \sum_{k=1}^{13} \beta_k \frac{\gamma^n}{2^n \alpha^n}, \quad (\text{A.23})$$

$$h_{21}(\alpha) = \sum_{k=1}^{13} \beta_k \frac{\gamma^n}{2^n \alpha^n}, \quad (\text{A.24})$$

$$h_{12}(\alpha) = \sum_{k=1}^{13} \beta_k \frac{\gamma^n}{2^n \alpha^n}, \quad (\text{A.25})$$

$$h_{22}(\alpha) = \sum_{k=1}^{13} \beta_k \frac{\gamma^n}{2^n \alpha^n}, \quad (\text{A.26})$$

$$\begin{aligned}
a_0 &= -\frac{\kappa + 1}{4}, \\
a_1 &= \frac{5 + \kappa}{4}, \\
a_2 &= -\frac{5}{2}, \\
a_3 &= 2, \\
a_4 &= -\frac{5\kappa - 8}{2(\kappa + 1)}, \\
a_5 &= \frac{2(-3 + \kappa)}{\kappa + 1}, \\
a_6 &= -\frac{5\kappa^2 - 36\kappa + 57}{2(\kappa + 1)^2}, \\
a_7 &= \frac{2(-3 + \kappa)(\kappa - 7)}{(\kappa + 1)^2}, \\
a_8 &= -\frac{5\kappa^3 - 84\kappa^2 + 375\kappa - 493}{2(\kappa + 1)^3}, \\
a_9 &= +\frac{2(-3 + \kappa)(\kappa^2 - 18\kappa + 61)}{(\kappa + 1)^3}, \\
a_{10} &= -\frac{5\kappa^4 - 152\kappa^3 + 1318\kappa^2 - 4324\kappa + 4783}{2(\kappa + 1)^4}, \\
a_{11} &= +\frac{\kappa^4 - 40\kappa^3 + 446\kappa^2 - 1844\kappa + 2531}{2(\kappa + 1)^4}, \\
a_{12} &= -\frac{5\kappa^5 - 240\kappa^4 + 3410\kappa^3 - 20130\kappa^2 + 52395\kappa - 49790}{2(\kappa + 1)^5}, \\
a_{13} &= +\frac{(-6 + 2\kappa)(\kappa^4 - 52\kappa^3 + 734\kappa^2 - 3748\kappa + 6217)r^{13}}{(\kappa + 1)^5}, \\
b_0 &= -\frac{\kappa - 1}{4}, \\
b_1 &= -\frac{(\kappa + 1)}{4}, \\
b_2 &= +1, \\
b_3 &= -\frac{1}{2}, \\
b_4 &= +\frac{-3 + \kappa}{\kappa + 1},
\end{aligned}$$



$$\begin{aligned}
b_5 &= -\frac{\kappa - 4}{2\kappa + 2}, \\
b_6 &= \frac{(-3 + \kappa)(\kappa - 7)}{(\kappa + 1)^2}, \\
b_7 &= -\frac{\kappa^2 - 12\kappa + 29}{2(\kappa + 1)^2}, \\
b_8 &= \frac{(-3 + \kappa)(\kappa^2 - 18\kappa + 61)}{(\kappa + 1)^3}, \\
b_9 &= -\frac{\kappa^3 - 24\kappa^2 + 147\kappa - 257}{2(\kappa + 1)^3}, \\
b_{10} &= +\frac{(-3 + \kappa)(\kappa - 7)(\kappa^2 - 26\kappa + 85)}{(\kappa + 1)^4}, \\
b_{11} &= -\frac{\kappa^4 - 40\kappa^3 + 446\kappa^2 - 1844\kappa + 2531}{2(\kappa + 1)^4}, \\
b_{12} &= +\frac{(-3 + \kappa)(\kappa^4 - 52\kappa^3 + 734\kappa^2 - 3748\kappa + 6217)}{(\kappa + 1)^5}, \\
b_{13} &= -\frac{\kappa^5 - 60\kappa^4 + 1050\kappa^3 - 7530\kappa^2 + 23535\kappa - 26610}{2(\kappa + 1)^5}, \\
c_0 &= -\frac{\kappa - 1}{4}, \\
c_1 &= +\frac{(\kappa + 1)}{4}, \\
c_2 &= -1, \\
c_3 &= +\frac{1}{2}, \\
c_4 &= -\frac{-3 + \kappa}{\kappa + 1}, \\
c_5 &= +\frac{\kappa - 4}{2(\kappa + 1)}, \\
c_6 &= -\frac{(\kappa - 7)(-3 + \kappa)}{(\kappa + 1)^2}, \\
c_7 &= +\frac{\kappa^2 - 12\kappa + 29}{2(\kappa + 1)^2}, \\
c_8 &= -\frac{(-3 + \kappa)(\kappa^2 - 18\kappa + 61)}{(\kappa + 1)^3},
\end{aligned}$$

$$\begin{aligned}
c_9 &= +\frac{\kappa^3 - 24\kappa^2 + 147\kappa - 257}{2(\kappa + 1)^3}, \\
c_{10} &= -\frac{(\kappa - 7)(-3 + \kappa)(\kappa^2 - 26\kappa + 85)}{(\kappa + 1)^4}, \\
c_{11} &= +\frac{\kappa^4 - 40\kappa^3 + 446\kappa^2 - 1844\kappa + 2531}{2(\kappa + 1)^4}, \\
c_{12} &= -\frac{(-3 + \kappa)\kappa^4 - 52\kappa^3 + 734\kappa^2 - 3748\kappa + 6217}{(\kappa + 1)^5}, \\
c_{13} &= +\frac{\kappa^5 - 60\kappa^4 + 1050\kappa^3 - 7530\kappa^2 + 23535\kappa - 26610}{2(\kappa + 1)^5}, \\
d_0 &= -\frac{\kappa + 1}{4}, \\
d_1 &= +\frac{\kappa + 1}{4}, \\
d_2 &= -1, \\
d_3 &= +\frac{1}{2}, \\
d_4 &= -\frac{-3 + \kappa}{\kappa + 1}, \\
d_5 &= +\frac{\kappa - 4}{2\kappa + 2}, \\
d_6 &= -\frac{(-3 + \kappa)(\kappa - 7)}{(\kappa + 1)^2}, \\
d_7 &= +\frac{\kappa^2 - 12\kappa + 29}{2(\kappa + 1)^2}, \\
d_8 &= -\frac{(-3 + \kappa)(\kappa^2 - 18\kappa + 61)}{(\kappa + 1)^3}, \\
d_9 &= +\frac{\kappa^3 - 24\kappa^2 + 147\kappa - 257}{2(\kappa + 1)^3}, \\
d_{10} &= -\frac{(-3 + \kappa)(\kappa - 7)(\kappa^2 - 26\kappa + 85)}{(\kappa + 1)^4}, \\
d_{11} &= +\frac{\kappa^4 - 40\kappa^3 + 446\kappa^2 - 1844\kappa + 2531}{2(\kappa + 1)^4}, \\
d_{12} &= -\frac{(-3 + \kappa)(\kappa^4 - 52\kappa^3 + 734\kappa^2 - 3748\kappa + 6217)}{(\kappa + 1)^5},
\end{aligned}$$

$$d_{13} = + \frac{\kappa^5 - 60 \kappa^4 + 1050 \kappa^3 - 7530 \kappa^2 + 23535 \kappa - 26610}{2 (\kappa + 1)^5}.$$

When  $\alpha$  tends to infinity  $h_{11}$ ,  $h_{21}$ ,  $h_{12}$ ,  $h_{22}$  behaves like

$$h_{11} = -\frac{\kappa+1}{4} + O\left(\frac{1}{\alpha}\right), \quad (\text{A.27})$$

$$h_{21} = +\frac{\kappa-1}{4} + O\left(\frac{1}{\alpha}\right), \quad (\text{A.28})$$

$$h_{12} = -\frac{\kappa-1}{4} + O\left(\frac{1}{\alpha}\right), \quad (\text{A.29})$$

$$h_{22} = -\frac{\kappa+1}{4} + O\left(\frac{1}{\alpha}\right). \quad (\text{A.30})$$

Therefore asymptotic behavior of  $H_{11}$ ,  $H_{21}$ ,  $H_{12}$ ,  $H_{22}$  becomes

$$H_{11}(\alpha, y) = i \frac{\alpha}{|\alpha|} e^{-\alpha y} \left( -\frac{\kappa+1}{4} + \frac{(5+\kappa)\gamma}{8\alpha} + O\left(\frac{1}{\alpha^2}\right) \right), \quad (\text{A.31})$$

$$H_{21}(\alpha, y) = e^{-\alpha y} \left( \frac{\kappa-1}{4} + \frac{(\kappa+1)\gamma}{8\alpha} + O\left(\frac{1}{\alpha^2}\right) \right), \quad (\text{A.32})$$

$$H_{12}(\alpha, y) = e^{-\alpha y} \left( -\frac{\kappa-1}{4} + \frac{(\kappa+1)\gamma}{8\alpha} + O\left(\frac{1}{\alpha^2}\right) \right), \quad (\text{A.33})$$

$$H_{22}(\alpha, y) = i \frac{\alpha}{|\alpha|} e^{-\alpha y} \left( -\frac{\kappa+1}{4} + \frac{(\kappa+1)\gamma}{8\alpha} + O\left(\frac{1}{\alpha^2}\right) \right). \quad (\text{A.34})$$

## Appendix B

# Numerical Evaluation of Fredholm Kernels

In solving equations such as (3.18), the accuracy is very highly dependent on the correct evaluation of the Fredholm kernels  $h_n^1(r)$  and  $h_n^2(r)$  given by equations (3.46) and (3.47). By adding and subtracting the asymptotic values of the integrands these functions may be expressed as

$$h_n^1(r) = \int_{-1}^1 w(s) P_n^{(\alpha, \beta)}(s) ds \int_0^\infty \left[ \Phi_1^*(\zeta) - \frac{5 + \kappa}{8} \frac{|s - r|}{s - r} \frac{\gamma^*}{\zeta} \right] \sin \zeta |s - r| d\zeta \\ + \frac{5 + \kappa}{8} \int_{-1}^1 w(s) P_n^{(\alpha, \beta)}(s) ds \frac{|s - r|}{s - r} \gamma^* \int_0^\infty \frac{\sin \zeta |s - r|}{\zeta} d\zeta, \quad (\text{B.1})$$

$$= \int_{-1}^1 \int_0^\infty \left[ \Phi_1^*(\zeta) - \frac{5 + \kappa}{8} \frac{|s - r|}{s - r} \frac{\gamma^*}{\zeta} \right] \sin \zeta |s - r| d\zeta \quad (\text{B.2})$$

$$+ \frac{\pi}{2} \gamma^* \frac{5 + \kappa}{8} \int_{-1}^1 \frac{|s - r|}{s - r} \frac{\pi}{2} w(s) P_n^{(\alpha, \beta)}(s) ds, \quad (\text{B.3})$$

$$h_n^2(r) = \int_{-1}^1 w(s) P_n^{(\alpha, \beta)}(s) ds \int_0^\infty \left[ \Phi_2^*(\zeta) \cos \zeta (s - r) + \frac{\kappa + 1}{8} \gamma^* \ln |s - r| \right] d\zeta \quad (\text{B.4})$$

$$- \int_{-1}^1 \frac{\kappa + 1}{8} \gamma^* \ln |s - r| w(s) P_n^{(\alpha, \beta)}(s) ds. \quad (\text{B.5})$$

The Fredholm and kernels are evaluated by using the following Gaussian Quadrature formula:

$$\int_{-1}^1 G(t, x) (1 - t)^\alpha (1 + t)^\beta dt \cong \sum_1^n W_k G(x, t_k), \quad -1 < \Re(\alpha, \beta) < 1, \quad (\text{B.6})$$

where  $t_k$  and  $x_k$  are determined from [31]

$$\begin{aligned}
P_n^{(\alpha,\beta)}(t_k) &= 0, \\
P_{n-\kappa}^{(\alpha+\kappa,\beta+\kappa)}(x_k) &= 0, \quad \text{for } \kappa = \pm 1, \\
P_n^{(\alpha+1,\beta-1)}(x_k) &= 0, \quad \text{for } \kappa = 0, \quad -1 < \alpha < 0, \quad 0 < \beta < 1, \\
P_n^{(\alpha-1,\beta+1)}(x_k) &= 0. \quad \text{for } \kappa = 0, \quad 0 < \alpha < 1, \quad -1 < \beta < 0,
\end{aligned} \tag{B.7}$$

and the weighting constants are given by

$$W_k = - \frac{(2n + \alpha + \beta + 2)\Gamma(n + \alpha + 1)\Gamma(n + \beta + 1)2^{(\alpha+\beta)}}{(n + 1)!(n + \alpha + \beta + 1)\Gamma(n + \alpha + \beta + 1)P_{n+1}^{(\alpha,\beta)}(t_k)\frac{d}{dt}P_n^{(\alpha,\beta)}(t_k)}. \tag{B.8}$$

For a list of Gaussian quadrature formulas see Abramowitz and Stegun [34] and also Stroud and Secrest [35]. This procedure reduces the problem to a system of linear algebraic equations where in our case  $G(x, t_k)$  are the Jacobi Polynomials.

## B.1 The Infinite Integral

The Fredholm kernels contain integrals with infinite upper limit. Evaluation of the infinite integrals to a high degree of accuracy is essential.

We shall treat the integrands with sine and cosine terms separately. Integration of  $J_1$  and  $J_2$  is done by separating the integration limits, i.e.

$$J_1(s, r) = \left( \int_0^A + \int_A^\infty \right) \Phi_1(\alpha) \sin \alpha(s - r) d\alpha, \tag{B.9}$$

$$J_2(s, r) = \left( \int_0^A + \int_A^\infty \right) \Phi_2(\alpha) \cos \alpha(s - r) d\alpha. \tag{B.10}$$

First integrals in  $J_1$  and  $J_2$  are bounded and are evaluated numerically. However, the second integrals are evaluated using the 13 term approximation in the asymptotic expansion.

For the 0 to A part, integration is done by using a Gaussian quadrature. We can choose A so that  $(\frac{\gamma}{2A})^{12}$  is small to any degree we want. For a particular

nonhomogeneity constant, there is a point where any further increase in  $A$  will only serve to tax the numerical effort. If  $A$  becomes larger in 0 to  $A$  integral, there will be more computing effort to calculate this integral. If the desired error is of order  $10^{-12}$ , the integration limit,  $A$ , may be taken as  $5\gamma$ .

The second integrals consist of

$$L_1^*(s, r) = \int_A^\infty (\Phi_1^*(\zeta) - c_1) \sin \zeta(s - r) d\zeta, \quad (\text{B.11})$$

$$L_2^*(s, r) = \int_A^\infty (\Phi_2^*(\zeta) - d_1) \cos \zeta(s - r) d\zeta, \quad (\text{B.12})$$

where  $c_1$  and  $d_1$  is given in equations (A.27) and (A.27). For the  $A$  to infinity part, the integrands  $\Phi_1^*(\zeta)$  and  $\Phi_2^*(\zeta)$  are asymptotically expanded for  $\zeta \rightarrow \infty$  as follows:

$$\begin{aligned} \Phi_1^*(\zeta) &= \sum_1^\infty \frac{c_n}{\zeta^n} \sin \zeta(s - r), \\ \Phi_2^*(\zeta) &= \sum_1^\infty \frac{d_n}{\zeta^n} \cos \zeta(s - r). \end{aligned}$$

where  $c_n$  and  $d_n$  are given in equations (A.27) and (A.27). Thus

$$L_1^*(s, r) = \sum_2^\infty c_n \int_A^\infty \frac{\sin \zeta(s - r)}{\zeta^n} d\zeta, \quad (\text{B.13})$$

$$L_2^*(s, r) = \sum_2^\infty d_n \int_A^\infty \frac{\cos \zeta(s - r)}{\zeta^n} d\zeta. \quad (\text{B.14})$$

Calculation of the integrals can be done by integrating by parts until one obtains the necessary recursion formulas. Note that

$$Si(x) = \int_0^x \frac{\sin(t)}{t} dt = \left( \int_0^\infty - \int_x^\infty \right) \frac{\sin(t)}{t} dt = \frac{\pi}{2} \frac{|t|}{t} - \int_x^\infty \frac{\sin(t)}{t} dt, \quad (\text{B.15})$$

$$Ci(x) = \int_0^x \frac{\cos(t)}{t} dt = \gamma_0 + \log|x| - \int_0^{|x|} \frac{1 - \cos t}{t} dt. \quad (\text{B.16})$$

where

$$\gamma_0 = 0.57721566490.$$

Therefore

$$\int_x^\infty \frac{\sin(t)}{t} dt = \frac{\pi}{2} \frac{|t|}{t} - Si(x), \quad (\text{B.17})$$

$$\begin{aligned}
\int_x^\infty \frac{\cos(t)}{t} dt &= \left( \int_0^\infty - \int_0^x \right) \frac{\cos(t)}{t} dt \\
&= -\gamma_0 - \log|x| + \int_0^{|x|} \frac{1 - \cos t}{t} dt.
\end{aligned} \tag{B.18}$$

$A$  to  $\infty$  part of the integrals reduce to calculating the following integrals which have closed form expressions.

$$\begin{aligned}
\int_A^\infty \frac{\cos \zeta(s-r)}{\zeta^{2n-1}} d\zeta &= \cos(A|s-r|) \sum_{j=1}^{n-1} \frac{(-1)^{j+1} (|s-r|)^{2j-2} (2n-2j-1)!}{A^{2n-2j} (2n-2)!} \\
&+ \sin(A|s-r|) \sum_{j=1}^{n-1} \frac{(-1)^j (|s-r|)^{2j-1} (2n-2j-2)!}{A^{2n-2j-1} (2n-2)!} \\
&+ \frac{(-1)^n (|s-r|)^{2n-2} \text{Ci}(A|s-r|)}{(2n-2)!},
\end{aligned} \tag{B.19}$$

$$\begin{aligned}
\int_A^\infty \frac{\sin \zeta(s-r)}{\zeta^{2n}} d\zeta &= \cos(A|s-r|) \sum_{j=1}^{n-1} \frac{(-1)^{j+1} (|s-r|)^{2j-1} (2n-2j-1)!}{A^{2n-2j} (2n-1)!} \\
&+ \sin(A|s-r|) \sum_{j=1}^n \frac{(-1)^{j+1} (|s-r|)^{2j-2} (2n-2j)!}{A^{2n-2j+1} (2n-1)!} \\
&+ \frac{(-1)^n (|s-r|)^{2n-1} \text{Ci}(A|s-r|)}{(2n-1)!},
\end{aligned} \tag{B.20}$$

$$\begin{aligned}
\int_A^\infty \frac{\cos \zeta(s-r)}{\zeta^{2n}} d\zeta &= \cos(A|s-r|) \sum_{j=1}^n \frac{(-1)^{j+1} (|s-r|)^{2j-2} (2n-2j)!}{A^{2n-2j+1} (2n-1)!} \\
&+ \sin(A|s-r|) \sum_{j=1}^{n-1} \frac{(-1)^j (|s-r|)^{2j-1} (2n-2j-1)!}{A^{2n-2j} (2n-1)!} \\
&+ \frac{(-1)^{n+1} (|s-r|)^{2n-1} \left( \text{Si}(A|s-r|) - \frac{\pi}{2} \right)}{(2n-1)!},
\end{aligned} \tag{B.21}$$

$$\begin{aligned}
\int_A^\infty \frac{\sin \zeta(s-r)}{\zeta^{2n-1}} d\zeta &= \cos(A|s-r|) \sum_{j=1}^{n-1} \frac{(-1)^{j+1} (|s-r|)^{2j-1} (2n-2j-2)!}{A^{2n-2j-1} (2n-2)!} \\
&+ \sin(A|s-r|) \sum_{j=1}^{n-1} \frac{(-1)^{j+1} (|s-r|)^{2j-2} (2n-2j-1)!}{A^{2n-2j} (2n-2)!} \\
&+ \frac{(-1)^n (|s-r|)^{2n-2} \left( Si(A|s-r|) - \frac{\pi}{2} \right)}{(2n-2)!}. \tag{B.22}
\end{aligned}$$



## Appendix C

### Calculation of Logarithmic Kernels

We want to calculate the following integral

$$I_n(x) = \int_{-1}^1 \ln(|t - x|) (1 - t)^\alpha (1 + t)^\beta P_n^{(\alpha, \beta)}(t) dt \quad (\text{C.1})$$

where  $P_n^{(\alpha, \beta)}(t)$  are defined by the Rodrigues formula

$$P_n^{(\alpha, \beta)}(t) = \frac{(-1)^n}{2^n n!} (1 - t)^{-\alpha} (1 + t)^{-\beta} \frac{d^n}{dt^n} [(1 - t)^{\alpha+n} (1 + t)^{\beta+n}] \quad (\text{C.2})$$

#### C.1 Calculation of the Logarithmic Kernel when

$$n = 0$$

The integral

$$\int_{-1}^1 \ln(|t - x|) (1 - t)^\alpha (1 + t)^\beta dt \quad (\text{C.3})$$

does not have a closed form solution. It has to be evaluated numerically. Gaussian Quadrature is used to evaluate this integral.

It has to be pointed out that when  $t \rightarrow x$ , the integrand shows irregular behavior. This leads to convergence problems. Therefore it is necessary to take more Gaussian points in the vicinity of the collocation points. This can be done effectively by

splitting the range of integral  $(-1, 1)$  into sub-intervals  $(-1, x-\epsilon)$ ,  $(x-\epsilon, x)$ ,  $(x, x+\epsilon)$ ,  $(x+\epsilon, 1)$  where  $\epsilon$  is a small value(say 0.01). This generates more points close to the collocation point and evaluation of the integral is highly accurate.

## C.2 Calculation of the Logarithmic Kernel when $n > 0$

We want to calculate the following integral

$$I_n = \int_{-1}^1 \ln(|t-x|) (1-t)^\alpha (1+t)^\beta P_n^{(\alpha,\beta)}(t) dt. \quad (C.4)$$

First observe that,

$$\begin{aligned} & (1-t)^\alpha (1+t)^\beta P_n^{(\alpha,\beta)}(t) \\ &= \frac{(-1)^n}{2^n n!} \frac{d^n}{dt^n} \left[ (1-t)^{\alpha+n} (1+t)^{\beta+n} \right], \\ &= -\frac{(-1)^{n-1}}{2^n 2^{n-1} (n-1)!} \frac{d}{dt} \frac{d^{n-1}}{dt^{n-1}} \left[ (1-t)^{\alpha+1+(n-1)} (1+t)^{\beta+1+(n-1)} \right], \\ &= -\frac{1}{2n} \frac{d}{dt} \left[ \frac{(-1)^{n-1}}{2^{n-1} (n-1)!} \frac{d^{n-1}}{dt^{n-1}} \left[ (1-t)^{\alpha+1+(n-1)} (1+t)^{\beta+1+(n-1)} \right] \right], \\ &= -\frac{1}{2n} \frac{d}{dt} \left[ (1-t)^{\alpha+1} (1+t)^{\beta+1} P_{n-1}^{(\alpha+1,\beta+1)}(t) \right]. \end{aligned} \quad (C.5)$$

We also have the relationship

$$\begin{aligned} & \frac{1}{\pi} \int_{-1}^1 \frac{P_n^{(\alpha,\beta)}(t) (1-t)^\alpha (1+t)^\beta}{t-x} dt = \cot \pi \alpha P_n^{(\alpha,\beta)}(x) (1-x)^\alpha (1+x)^\beta \\ & - \frac{n! \Gamma(-\alpha - \beta + 2n - 2\kappa + 1) \Gamma(\alpha + \beta + n + 1) P_{n-\kappa}^{(-\alpha, -\beta)}(x)}{\sin \pi \alpha \Gamma(n - \kappa + 1) \Gamma(-\alpha - \beta + n - \kappa + 1)}, \end{aligned} \quad (C.6)$$

where  $\kappa = -(\alpha + \beta)$ . Integrating by parts, we obtain the solution of  $I_n(x)$  as follows:

$$\int_{-1}^1 \ln(|t-x|) (1-t)^\alpha (1+t)^\beta P_n^{(\alpha,\beta)}(t) dt$$

$$\begin{aligned}
&= -\frac{1}{2n} \int_{-1}^1 \ln(|t-x|) \frac{d}{dt} \left[ (1-t)^{\alpha+1} (1+t)^{\beta+1} P_{n-1}^{(\alpha+1, \beta+1)}(t) \right] dt \\
&= -\frac{1}{2n} \ln|x-t| (1-x)^{\alpha+1} (1+x)^{\beta+1} P_{n-1}^{(\alpha+1, \beta+1)} \\
&\quad + \frac{1}{2n} \int_{-1}^1 \frac{(1-x)^{\alpha+1} (1+x)^{\beta+1} P_{n-1}^{(\alpha+1, \beta+1)}}{x-t} dx \\
&= \frac{\pi}{2n} \frac{1}{\pi} \int_{-1}^1 \frac{P_{n-1}^{(\alpha+1, \beta+1)}(t) (1-t)^{\alpha+1} (1+t)^{\beta+1}}{t-x} dt \tag{C.7}
\end{aligned}$$

Therefore,

$$\begin{aligned}
&\int_{-1}^1 \ln(|t-x|) (1-t)^\alpha (1+t)^\beta P_n^{(\alpha, \beta)}(t) dt = \\
&\quad \frac{\pi}{2n} \left[ \cot \pi(\alpha+1) P_{n-1}^{(\alpha+1, \beta+1)}(x) (1-x)^{\alpha+1} (1+x)^{\beta+1} \right] \\
&\quad - \frac{\pi}{2n} \left[ \frac{2^{-\kappa_1}}{\sin \pi(\alpha+1)} P_{n-\kappa_1-1}^{(-\alpha-1, -\beta-1)}(x) \right]. \tag{C.8}
\end{aligned}$$

Observing that

$$\cot \pi(\alpha+1) = \cot \pi\alpha \tag{C.9}$$

$$\sin \pi(\alpha+1) = -\sin \pi\alpha \tag{C.10}$$

and substituting

$$\kappa_1 = -(\alpha+1+\beta+1) = -(\alpha+\beta+2), \tag{C.11}$$

(C.4) becomes

$$\begin{aligned}
I_n &= \frac{\pi}{2n} \cot \pi\alpha P_{n-1}^{(\alpha+1, \beta+1)}(x) (1-x)^{\alpha+1} (1+x)^{\beta+1} \\
&\quad + \frac{2^{\alpha+\beta+1}}{n \sin \pi\alpha} P_{n+\alpha+\beta+1}^{(-\alpha-1, -\beta-1)}(x) \tag{C.12}
\end{aligned}$$

In his paper Popov [23] gave the solution using complex integration. His result is

$$\int_{-1}^1 \ln(|t-x|) (1-t)^\alpha (1+t)^\beta P_n^{(\alpha, \beta)}(t) dt =$$

$$\begin{aligned} & \frac{2^{\alpha+\beta+1}\Gamma(1+\alpha)\Gamma(1+\beta+n)}{n\Gamma(\alpha+\beta+n+2)}F\left(n, -1-\alpha-\beta-n, -\alpha, \frac{(1-x)}{2}\right) \\ & + \frac{\Gamma(1+\alpha+n)\pi\cot\pi\alpha}{2^{-\beta}\Gamma(\alpha+2)n!(1-x)^{-\alpha-1}}F\left(-\beta-n, 1+\alpha+\beta+n, 2+\alpha, \frac{(1-x)}{2}\right) \end{aligned} \quad (\text{C.13})$$

By using the formulas

$$F\left(1+\alpha+\beta+n, -n, 1+\alpha, \frac{(1-x)}{2}\right) = \frac{n!}{(1+\alpha)_n}P_n^{(\alpha,\beta)}(t), \quad (\text{C.14})$$

$$F(A, B, C, z) = (1-z)^{C-A-B}F(C-A, C-B, C, z), \quad (\text{C.15})$$

where

$$(1+\alpha)_n = \frac{\Gamma(1+\alpha+n)}{\Gamma(1+\alpha)}, \quad (\text{C.16})$$

and replacing

$$\begin{aligned} n & \rightarrow m + \alpha' + \beta' + 1, \\ \alpha & \rightarrow -\alpha' - 1, \\ \beta & \rightarrow -\beta' - 1, \end{aligned}$$

the equation (C.14) reads

$$\begin{aligned} & F(m, -1-\alpha'-\beta'-m, -\alpha', (1-x)/2) \\ & = \frac{\Gamma(-\alpha')\Gamma(n+\alpha'+\beta'+2)}{\Gamma(n+\beta'+1)}P_{n+\alpha'+\beta'+1}^{(-\alpha'-1, -\beta'-1)}(t). \end{aligned} \quad (\text{C.17})$$

Now, replacing  $\alpha, \beta, n$  in equation (C.14) by

$$\begin{aligned} n & \rightarrow m - 1, \\ \alpha & \rightarrow \alpha' + 1, \\ \beta & \rightarrow \beta' + 1, \end{aligned}$$

equation (C.14) becomes

$$\begin{aligned} & F(\alpha' + \beta' + n + 2, -n + 1, \alpha' + 2, (1-x)/2) \\ & = \frac{\Gamma(n)\Gamma(\alpha' + 2)}{\Gamma(n + \alpha' + 1)}P_{n-1}^{(\alpha'+1, \beta'+1)}(t). \end{aligned} \quad (\text{C.18})$$

Similarly, replacing  $\alpha, \beta$  and  $\gamma$  in equation (C.15) by

$$\begin{aligned}\alpha' &= \alpha' + \beta' + n + 2 \\ \beta' &= 1 - n \\ \gamma &= \alpha' + 2\end{aligned}$$

we find

$$\begin{aligned}& F(\alpha' + \beta' + n + 2, -n + 1, \alpha' + 2, (1 - x)/2) \\&= \left(\frac{1+x}{2}\right)^{-\beta'-1} F\left(-\beta' - n, \alpha' + n + 1, \alpha' + 2, \frac{1-x}{2}\right) \\&= \frac{\Gamma(n)\Gamma(\alpha' + 2)}{\Gamma(n + \alpha' + 1)} P_{n-1}^{(\alpha'+1, \beta'+1)}(t).\end{aligned}\tag{C.19}$$

Therefore

$$\begin{aligned}& F(-\beta' - n, \alpha' + n + 1, \alpha' + 2, (1 - x)/2) \\&= \frac{2^{-\beta}}{2} \frac{1}{(1+x)^{(1+\beta)}} \frac{\Gamma(n)\Gamma(\alpha' + 2)}{\Gamma(n + \alpha' + 1)} P_{n-1}^{(\alpha'+1, \beta'+1)}(t).\end{aligned}\tag{C.20}$$

Substituting equations (C.18) and (C.20) and simplifying we may find the same result as given by (C.13).

## Vita

Mehmet Ali Güler was born in İskenderun, Hatay, Turkey on the 16th of April, 1968. He is the youngest son of Cemil Güler and Nezahat Güler.

After graduating from İskenderun High School in 1984, he had started his undergraduate study in the Department of Mechanical Engineering at Gaziantep campus of Middle East Technical University, Ankara, Turkey and obtained his B.S. degree in 1990. He joined Lehigh University in 1994.

**END OF  
TITLE**